

# POLITECNICO DI TORINO

**Master's Degree course in  
Management Engineering**

Master's Degree Final Thesis

## **Assessing the Economic Feasibility and Sustainability of Solar-Powered Charging Stations for Electric Scooter Rental Services**



**Supervisor**

Prof. Andrea Tuni

*signature of the supervisors*

.....

**Candidate**

Juan Ignacio Spagnolo

*candidate's signature*

.....

**A.A. 2024/2025**

Abstract	3
1. Introduction	4
2. Literature review	7
2.1 Renewable Energy Integration in Urban Infrastructure	7
2.2 Urban Mobility and Electric Scooters	8
2.3 Optimization Techniques for Infrastructure Placement	9
2.4 Case Studies and Best Practices in Urban Charging Networks	11
2.4.1 Dubai	12
2.4.2 United States	12
2.4.3 Italy	12
2.5 Research Gap	13
3. Methodology	13
4. Conceptual Model	15
4.1 Objective of the Conceptual Model	15
4.2 System Variables	15
4.2.1 Decision Variables	15
4.2.2 Reference Variables	16
4.2.3 State Variables	16
4.2.4 Auxiliary Variables	16
4.3 Entities and Attributes	17
4.4 Resources	18
4.5 IDEF0 Diagram	18
4.6 Flow Charts	21
4.7 Activities	24
4.8 Parameters	24
4.9 Exogenous and Endogenous Events	24
4.10 Process	25
4.11 Assumptions	26
5. Data Model and Quantification	28
5.1 Survey Development	28
5.2 Survey results	29

Commuting behavior and frequency	29
Customer's willingness to pay	34
Finding a scooter	36
5.3 Random Variables	37
6. Operational Model	38
6.1 Development of Different Blocks	38
6.1.1 Block 1: Pedestrian arrival and scooter matching	39
6.1.1.1 Pedestrian Agent	39
6.1.1.2 Scooter Agent	43
6.1.2 Utility function	44
6.1.3 Block 2: Pedestrian's travel	46
6.1.4 Block 3: Solar Powered Charging	50
6.1.5 Block 4: Scooter Charging by Chargers	52
6.2 Reference Variables Definition	56
6.3 Stress Test	59
7. Verification & Validation: Number of Runs	62
8. Experimentation Process	64
8.1 Analyzed Alternatives	64
8.2 Experimentation Procedure	68
8.3 Experiment Conditions	70
9. Results	71
9.1 Analysis of Results	71
9.1.1 Zero resource case vs. Solar-powered charging station without incentive case	71
9.1.2 Solar-powered charging station allocation: Random vs Metaheuristic	74
9.1.3 Number of solar-powered charging stations versus population density	78
9.1.4 Optimal number of docks per solar-powered charging stations	84
9.1.5 Optimal discount to offer in order to maximize the solution	91
9.2 Interpretation of Results	95
9. Conclusions and Recommendations	100
9.1 Challenges, Debugging and Limitations	100
9.2 Final Conclusions and Recommendations	102
BIBLIOGRAPHY	105
APPENDIX	109

# Abstract

Urbanization and environmental challenges have increased the need for innovative solutions to adapt urban mobility to new and ever-changing needs while promoting sustainability. This thesis explores the integration of solar-powered charging stations into electric scooter rental networks as a dual strategy for reducing greenhouse gas emissions and improving the economic feasibility of micro-mobility services. Through a simulation-based approach using AnyLogic, this study evaluates various configurations of charging infrastructure, user incentive strategies, and optimization techniques to identify the most effective solutions without the need for real-world pilot testing.

The analysis encompasses five experimental scenarios: baseline comparisons, optimal placement strategies using metaheuristics, scaling infrastructure to population density, determining the ideal number of charging docks, and evaluating the impact of user discounts. Results demonstrate that strategic placement of solar-powered charging stations can significantly enhance system efficiency, reducing conventional energy consumption by up to 90% and increasing renewable energy usage on average to 356 kWh every 6 months. Furthermore, offering discounts of 40% to customers returning scooters to solar-powered charging stations emerged as a viable strategy to encourage user adoption by 77% with only a 7,9% profitability decrease, when paired with the sale of excess solar energy to the grid.

This research contributes to academic literature by bridging gaps between simulation-based evaluation methodologies and renewable energy-powered micro-mobility solutions, revealing insights into user behavior and sustainable infrastructure development. Practically, it provides a roadmap for e-scooter operators to implement cost-effective and environmentally friendly systems. However, limitations such as computational constraints and a limited scope highlight areas for future research. This work puts into evidence the transformative potential of integrating renewable energy into urban mobility.

# 1. Introduction

Urbanization is rapidly transforming the global landscape, creating significant challenges for cities in maintaining livability and sustainability. Currently, 56% of the global population resides in urban areas, a figure projected to rise to nearly 70% by 2050 (Boin et al., 2023). This trend is straining urban transport systems, resulting in traffic congestion, long commutes, noise pollution, and environmental degradation. Even cities with stable populations face growing pressures as transport volumes increase and outpace the capacity of existing infrastructure.

Cities are not only hubs of social interaction and innovation but also critical drivers of the global economy, generating over 80% of global GDP (Boin et al., 2023). Urban road networks, as key facilitators of economic growth and access to services, are under significant strain from high population densities and growing urban areas. These pressures contribute to cities consuming two-thirds of global energy and producing over 70% of greenhouse gas emissions (Boin et al., 2023). Such figures highlight the critical role sustainable transformations in transportation systems can play in mitigating emissions, pollution, and congestion.

Urban mobility systems are becoming increasingly complex to manage, driven by evolving trends, such as traffic volume growth and the necessary transition to low-carbon mobility.

OECD projections indicate that urban passenger transport demand will more than double by 2050 compared to 2015. Recent shifts in consumer behavior have increased challenges through the rapid growth of e-commerce and the resulting surge in last-mile delivery vehicles. As transport infrastructure becomes increasingly constrained, stakeholders must address road safety and accident prevention while adapting infrastructure to accommodate emerging modes of transport like electric vehicles, e-scooters, and e-bikes (“OECD Environmental Outlook to 2050”, 2011).

The key actor in this exponential growth in passenger transport, according to a study realized by McKinsey’s Boin et al. (2023), are passenger cars. They account for over half of transport-related emissions worldwide. In response, governments and institutions worldwide are committing to ambitious decarbonization goals. For example, the European Union aims to achieve climate neutrality by 2050 under the European Green Deal, while the United States has set a similar target of net-zero emissions by 2050 (Boin et al., 2023). Given that transportation emissions contribute approximately one-fifth of total greenhouse gas emissions and are on an exponential trajectory, technological innovation aimed at mitigating their global impact is essential for achieving climate objectives (Gates, 2021).

To adapt to these trends, cities are required to evolve and prioritize sustainability, livability and quality of life. Research emphasizes that successful cities are those that invest in transport network expansions, road infrastructure improvements, and pedestrian-friendly spaces (Doll et al., 2014). Measures such as dedicated public transport lanes, optimized bus routes, road modernization, and digital upgrades can significantly enhance the commuter experience while addressing the complex demands of urban mobility.

As vehicle flows, pedestrian volumes, and cyclist activity increase, synchronized decision-making and coordination across transport ecosystems will become essential for sustainable urban development (Doll et al., 2014).

In this context of rapid urbanization and increasing pressure on transportation systems, efficient mobility solutions like electric vehicles (EVs), including electric scooters, are emerging as a transformative option. EVs have the potential to significantly reduce greenhouse gas emissions, air pollution, and noise levels, making cities cleaner and quieter. Their lack of engine noise minimizes urban sound pollution, while their sleek design reduces visual clutter. When powered by renewable energy, EVs further enhance sustainability, supporting the transition to greener urban mobility.

Particularly, shared e-scooters address critical urban mobility challenges by offering a convenient, cost-effective alternative for short trips, particularly those between 0.5 and 4 kilometers. They help reduce traffic congestion, lower greenhouse gas emissions, and complement public transportation networks by serving as a first- and last-mile solution (Rose et al., 2020). These attributes make e-scooters a practical and scalable intervention for modern urban transport systems.

The convenience and scalability of this unmet need in urbanized society has not gone unnoticed, e-scooter rentals are one of the fastest growing worldwide consumer phenomena in the last years, currently in operation in more than 350 cities worldwide (Rose et al., 2020). The extraordinary growth of electric scooters is due to many factors, including advancements in hardware and operational strategies. Second-generation scooters, designed for increased durability, now have a lifespan of 12 to 24 months, enhanced power, and advanced smart features like sensors, further increasing their appeal and environmental sustainability (Rose et al., 2020). Additionally, innovations such as swappable batteries are revolutionizing operational efficiency, enabling users to charge batteries in exchange for credits (Pineiro, 2023). Data analytics play a pivotal role in optimizing fleet utilization, with operators leveraging insights on high-demand areas to strategically manage drop-off locations and maximize uptime. (Rose et al., 2020)

Moving away from technological aspects, pricing strategies have also evolved, with companies raising per-minute rates in both the US and Europe, alongside standard unlock fees. These adjustments have not affected users, who prioritize availability over marginal cost increases (Rose et al., 2020). Despite pressures from regulatory fees and fines, leading companies in mature markets are achieving positive margins through improved product durability, operational advancements, and strategic pricing (Rose et al., 2020). However, to achieve sustainable profitability and justify current valuations, companies must scale their models across a wider range of cities and micro mobility modes, ensuring operations are large enough to offset overhead costs. (Rose et al., 2020)



Figure 1: Presence of E-scooters in major cities (Rose et al., 2020)

The growth trajectory of the e-scooter market in the US and Europe can be envisioned in the short and long term. In the short term, the market is characterized by continued expansion in existing urban centers and new city markets. However, widespread regulatory restrictions will likely limit fleet sizes, capping the total number of e-scooters at approximately 1 million by the end of this phase, generating revenues of \$3 to \$4 billion annually at a global scale (Rose et al., 2020).

The long-term phase will be marked by the full integration of e-scooters into broader mobility systems. E-scooters will expand beyond urban cores into suburbs and smaller towns, leading to a fleet size of 4 to 5 million scooters and annual revenues of \$12 to \$15 billion (Rose et al., 2020). Europe is expected to dominate the market, with megacities contributing a significant share of the overall revenue. This phase represents the widespread adoption and sustainability of e-scooters as a transformative urban mobility solution. (Rose et al., 2020)

While electric vehicles, in particular e-scooters, appear to be a sustainable and scalable solution for urban mobility, it is crucial to consider the source of the electricity that powers them. In many countries, the majority of grid electricity still comes from non-renewable sources (Wang et al., 2021; IEA, 2019). With a projected global fleet of 4 to 5 million e-scooters, the energy consumption during peak weekday usage, equivalent to 30,653% of full battery capacity, could result in substantial greenhouse gas emissions. Considering an average emission factor of 475 gCO<sub>2</sub>/kWh in energy production, this market would contribute approximately 1.5 metric tons of CO<sub>2</sub>e annually on a global scale (Wang et al., 2021; IEA, 2019). A crucial question arises for the electric scooter rental industry: how can these services become more environmentally friendly while simultaneously reducing overhead costs and boosting profitability? This thesis sheds light on how leveraging green energy solutions could revolutionize the industry. It seeks to demonstrate the potential of renewable energy to not only minimize the environmental footprint of shared e-scooters but also to create a more cost-effective and sustainable operational model.

Specifically, this thesis will look at the possibility of integrating solar-powered charging stations into cities that already have electric scooter rental services present. This idea stems from Pinheiro (2023), who showcases a pilot project in Regensburg, Germany, where Zeus Scooters introduced solar-powered wireless charging stations, called "Zolar" stations, at strategic multimodal transfer points. These stations not only optimize operations by reducing the need for manual battery-swapping but also align with the company's

commitment to sustainability. Such infrastructure enhances scooter availability, environmental responsibility and reduces operational costs, offering a glimpse into how renewable energy solutions can reshape micro mobility.

To evaluate the economic and sustainability feasibility of this solution, this study employs a simulation-based approach developed in AnyLogic. This platform provides several key advantages for modeling complex, dynamic systems, involving interactions between people, IoT-enabled electric scooters, charging stations, GPS systems, and solar-powered chargers. AnyLogic not only facilitates the modeling of such dynamic systems through its Java-based interface but also supports the seamless integration of external data sources. Moreover, it enables the construction of a dynamic and visually intuitive interface, allowing for real-time monitoring and analysis of simulation outcomes.

The ability to develop and test a plethora of scenarios for implementing solar-powered charging stations within a virtual environment offers significant benefits. It allows for the exploration of multiple configurations and strategies without the high costs and logistical challenges of real-life pilot testing. The solution developed in this thesis aims to provide value for e-scooter rental companies looking to adopt more sustainable practices, demonstrating the potential of solar energy to drive environmentally and economically viable results. In conclusion, the research question to be answered is: Are solar-powered charging stations an economically feasible way for Electric Scooter Rental Services to increase profitability while becoming more sustainable?

## 2. Literature review

Urban mobility has undergone a significant transformation in recent years, with electric scooters emerging as a key micro-mobility solution. This section explores the state of the literature regarding the key aspects of electric scooters within urban transportation systems, examining their impact on travel behavior, safety, and environmental sustainability. By analyzing the overlap with bike-sharing and EV systems and identifying gaps in current research, this review sets the foundation for understanding how renewable energy-powered infrastructure, such as solar charging stations, can be integrated to enhance their utility and sustainability.

### 2.1 Renewable Energy Integration in Urban Infrastructure

The integration of renewable energy into urban infrastructure represents a rapidly expanding field of research, reflecting both significant opportunities and critical challenges for sustainable cities. Perea-Moreno et al. (2018) emphasize that this area has gained considerable attention over recent decades, fueled by growing urban populations and the pressing need to address climate change. Among the technologies facilitating the transformation of cities into energy-efficient hubs, solar energy stands out for its scalability, adaptability, and suitability for dense urban environments (IRENA, 2016; IRENA, 2020).

According to Ulpiani et al. (2023), solar panels are increasingly utilized as decentralized energy sources that align with the vision of climate-neutral cities. Their integration into existing urban structures, such as rooftops, parking lots, and street lighting, demonstrates their potential to enhance urban energy systems. Notably, several pilot projects are exploring the use of solar energy to power electric vehicle (EV) charging

infrastructure, underlining its critical role in advancing sustainable urban mobility (Ulpiani et al, 2023). However, despite these promising developments, significant challenges remain in scaling renewable energy systems to meet the demands of emerging urban transport networks.

Ulpiani et al. (2023) further highlights the importance of leveraging digital tools and fostering collaborations among stakeholders to address regulatory and operational barriers. Optimizing renewable energy technologies for urban mobility requires balancing energy efficiency, accessibility, and cost-effectiveness. Researchers also point to the necessity of innovative system designs, such as microgrids and advanced energy storage solutions, to ensure an uninterrupted energy supply and resilience to fluctuations in urban energy demand.

Legislative changes have also contributed to making renewable energy projects more viable. For example, as of July 1, 2022, new regulations in EU, allow micro-producers to generate more electricity than they consume annually without incurring overproduction charges from grid operators (Hemetsberger et al., 2023). This policy incentivizes the installation of larger solar-powered systems and addresses one of solar energy's major drawbacks, intermittency. It addresses it by enabling excess energy to be fed back into the grid during periods of low consumption.

Such regulatory advancements open new areas for research, including in the context of solar-powered EV charging stations. By feeding surplus energy back into the grid when not actively charging scooters, these stations could create a secondary revenue stream for electric scooter rental companies. This approach not only increases the economic viability of renewable energy projects but also promotes the natural "greenification" of the electric grid.

## 2.2 Urban Mobility and Electric Scooters

Shared bikes were arguably the most prevalent micro mobility service in urban areas before the arrival of electric scooters (Want et al., 2021b). Since shared bikes and electric scooters cater to the same demographic, cities with established bike sharing systems are likely to provide a favorable environment for electric scooters. This has naturally led to research in the two systems to have common ground (Curl and Fitt, 2020; McKenzie, 2019; Zhu et al., 2020). McKenzie (2019) explored the spatial and temporal usage patterns of e-scooters and compared them to bike-sharing systems within a major urban center, identifying when and where e-scooters are utilized. Furthermore, Lazarus et al. (2020) revealed that e-scooters are used more frequently in lower-density communities compared to other shared modes.

E-scooters have emerged as a promising solution to alleviate traffic congestion and reduce greenhouse gas emissions. Research in this area primarily addresses travel behavior (Bai and Jiao, 2020; Caspi et al., 2020; Jiao and Bai, 2020; Severengiz et al., 2020), safety (Che et al., 2020; Dhillon et al., 2020; Sikka et al., 2019; Yang et al., 2020), and environmental impacts (Hollingsworth et al., 2019).

### **Travel behavior**

Some studies have investigated e-scooter riding patterns and the factors influencing usage. Bai and Jiao (2020) utilized a negative binomial regression model and GIS hotspot spatial analysis to examine e-scooter usage characteristics in U.S. cities, identifying correlations with ridership and urban features. Moreover,

Caspi et al. (2020) used spatial regression models to explore travel behavior, analyzing land-use characteristics, built environment, and demographics. However, a research gap has been identified for travel behaviour in the context of the willingness of users to deviate from intended destinations to accommodate for fixed infrastructure. This should be further explored in order to obtain a comprehensive understanding of how users would interact with eventual solar powered charging stations whose position is fixed.

### **Safety**

Safety concerns for both riders and pedestrians have been widely documented, as the rapid expansion of e-scooter services has led to an increase in crashes and fatalities. Misuse, such as parking on sidewalks or unsafe riding practices, threatens pedestrian safety. Fang et al. (2018) and Gossling (2020) examined the primary causes of e-scooter-related injuries, identifying falls and collisions as leading factors. Nevertheless, safety regarding e-scooter rental services remains a hot topic given the lack of proper safety equipment like helmets and protection; regulatory entities are constantly looking for ways to ensure their safe use (European commission, 2020). For example, these regulations have already put in place a speed limit of 20 km/h in Europe.

### **Environmental impacts**

There is still little research conducted on the environmental effects of e-scooters. Severengiz et al. (2020) conducted a life cycle assessment in Berlin, comparing the ecological impacts of e-scooters with private cars, public transport, biking, and walking. Hollingsworth et al. (2019) used Monte Carlo simulations to estimate the life cycle global warming potential of shared e-scooters. Additionally, Want et al. (2021b) discussed the significant impact of energy efficiency in e-scooters, warning that around 30% of energy consumption is consumed during the overall idle periods of e-scooters.

Given the reduced number of research papers regarding the impact of electric scooter rental services, there is a necessity to expand the evaluation of the energy consumption and associated greenhouse gases emissions of this solution. Then to develop a way to mitigate the environmental impact, in doing this, implementing solar powered charging stations may contribute to the production of clean energy for scooter consumption.

## **2.3 Optimization Techniques for Infrastructure Placement**

When analyzing methodologies for the placement of solar-powered charging stations, the scarcity of studies focused on electric scooters necessitates drawing parallels from research on EV charging stations. Several methodologies have been proposed, leveraging mathematical optimization, heuristic algorithms, and geographic analysis to optimize charging station placement.

Calvo-Jurado et al. (2024) explore the use of Voronoi diagrams to strategically identify potential sites for electric vehicle (EV) charging stations, aiming to enhance intercity travel infrastructure. This study addresses challenges such as the scarcity of fast-charging stations and competition among providers, while considering user behavior and land-use regulations. Their approach relies on geometric analysis to optimize locations that are distant from competitors yet accessible from main roads. A case study in Catalonia, Spain, validates their methodology, incorporating factors like traffic density, average EV ranges, and regional planning guidelines.

Dorigo and Stützle (2003) present Ant Colony Optimization (ACO) as a compelling metaheuristic for infrastructure placement problems. Applying this concept to solar-powered charging stations, ACO's artificial pheromones and probabilistic decision-making offer a decentralized and adaptive approach to site selection. This is particularly valuable in dynamic environments where traffic patterns, energy demands, and solar energy availability fluctuate over time. Advanced variants such as the Ant Colony System (ACS) and MAX-MIN Ant System (MMAS) improve upon traditional ACO implementations by balancing exploration and exploitation more effectively, reducing the risk of getting stuck in local optima.

Franco et al. (2024) develop a mixed-integer linear programming (MILP) approach to optimize the deployment of electric vehicle charging stations. Their methodology considers grid constraints, spatial distribution of demand, and economic feasibility to ensure an efficient network. Their study incorporates real-world energy consumption data and shows optimization techniques can enhance the scalability and reliability of charging networks.

Another study by Xylia and Silveira (2018) examines the spatial distribution of EV chargers using a combination of geographic information systems (GIS) and MILP. Their framework uses energy grid capacity, land-use constraints, and projected EV adoption rates to propose optimal locations for new charging stations. The research highlights the importance of a data-driven approach in balancing accessibility, cost, and sustainability in infrastructure planning.

Sadeghian et al. (2022) present an optimization model that integrates renewable energy resources into EV charging networks. By leveraging a stochastic programming approach, their study accounts for uncertainties in solar energy generation, demand fluctuations, and grid constraints. Their findings show the importance in building resilient and efficiency of solar-powered charging stations.

Source	Goal/Objective	Methodology	EV Type (Scooter, Bike, etc.)	Solar-Powered Charging	Other Relevant Dimensions
Calvo-Jurado et al. (2024)	Optimize EV station placement for intercity travel	Voronoi Diagrams	Cars	No	Competition, Land-use regulations
Dorigo & Stützle (2003)	Optimize infrastructure placement efficiently	Ant Colony Optimization	General	Yes	Decentralized decision-making, adaptability
Franco et al. (2024)	Optimize three-phase EV charging deployment	MILP	Cars	Yes	Grid constraints, scalability
Xylia & Silveira (2018)	Optimize spatial distribution of charging stations	GIS + MILP	Cars	No	Land-use constraints, adoption trends
Sadeghian et al. (2022)	Integrate renewables into EV charging networks	Stochastic Programming	Cars	Yes	Energy storage, demand response
This Work	Optimize solar-powered charging for e-scooters	Hybrid approach (e.g., ACO + MILP)	Scooters	Yes	Demand forecasting, multimodal transport

*Table 1: Summary of Optimization Techniques for Infrastructure Placement*

This review highlights the gap in the literature concerning the placement of solar-powered charging stations for electric scooters. Existing studies focus primarily on EVs, neglecting the unique challenges of micromobility infrastructure. By integrating methodologies such as ACO and MILP with demand forecasting and multimodal transport considerations, this work seeks to develop a comprehensive optimization framework tailored to e-scooter charging networks.

## 2.4 Case Studies and Best Practices in Urban Charging Networks

Studying successful implementations of renewable energy in urban infrastructure offers valuable insights. This section explores notable case studies to identify key success factors, focusing on how these examples can inspire the integration of solar-powered charging stations for e-scooter rental services. By examining different contexts, we can understand the challenges faced, strategies adopted, and outcomes achieved in implementing renewable energy systems.

### 2.4.1 Dubai

The Dubai Electricity and Water Authority (DEWA) launched the EV Green Charger initiative in 2015 to support sustainable transportation through an extensive network of electric vehicle (EV) charging stations. By January 2022, this initiative had expanded to include over 325 stations with more than 560 charge points, catering to 5,107 EVs. Since its inception, DEWA's charging network has provided over 8,800 megawatt-hours (MWh) of electricity, enabling EVs to travel approximately 58 million kilometers while reducing refueling costs by 73%.

To enhance user experience, DEWA offers features such as automatic account creation for EV owners registered with Dubai's Roads and Transport Authority (RTA), enabling quick charging access within an hour. Additional services include account setup via DEWA's website, smart app, or interactive voice response system. Registered users benefit from a personalized EV Green Charger Dashboard to manage their accounts, while guest users can access charging facilities through a streamlined system. This initiative supports Dubai's Green Mobility Initiative 2030 and demonstrates a successful model for integrating renewable energy with urban transport infrastructure (Salian, N., 2022).

### 2.4.2 United States

In the United States, drop-down streetlight and utility pole charging technology has been deployed in cities like Los Angeles and Melrose, Massachusetts. This innovation, incentivized by programs such as the Bureau of Street Lighting and National Grid pilots, offers a cost-effective and practical solution for urban EV infrastructure. According to the Center for Law, Energy & the Environment (CLEE), this approach leverages existing infrastructure, reducing installation costs by avoiding expensive trenching and sidewalk modifications. Chargers are mounted on elevated streetlights or utility poles, addressing vandalism concerns while enhancing pedestrian safety. Retractable charging cables that descend only when activated via a payment system further optimize usability and minimize visual impact.

This technology is particularly suited for dense urban areas with limited ground space. Its rapid deployment potential and integration with public utilities make it an innovative model for expanding urban charging networks (Center for Law, Energy & the Environment, 2024).

### 2.4.3 Italy

The Photovoltaic Village in Alessandria, Italy, is an example of the integration of solar energy at an urban scale. This project rejuvenated a residential community by incorporating photovoltaic (PV) systems into multi-story buildings and public spaces. The PV installations provide 163 kW of power, meeting 100% of electricity consumption for common areas and up to 70% for apartments. Annual energy production ranges between 674–830 kWh/kWp, showcasing the potential for renewable energy to meet urban residential needs.

The project was a collaborative effort involving public and private stakeholders, with public funds covering approximately 70% of the photovoltaic installation costs. Additional features include green areas, water ponds, and bioclimatic zones designed to foster community interaction and environmental sustainability. This initiative underscores the importance of stakeholder collaboration, funding mechanisms, and integrated urban design in successfully implementing renewable energy solutions (Formolli et al., 2022).

## 2.5 Research Gap

This literature review has explored the current state of research on urban mobility, renewable energy integration, simulation frameworks, and optimization techniques. Studies on e-scooters highlight their potential to reduce traffic and emissions but reveal gaps in understanding user behavior around fixed infrastructure. Research on renewable energy emphasizes the scalability of solar energy but notes challenges in efficiency and cost-effectiveness, while simulation and optimization methods provide robust tools for evaluating systems such as these.

Case studies from Dubai, the United States, and Italy illustrate best practices in integrating renewable energy into urban infrastructure, ranging from user-friendly EV networks to innovative solar-powered solutions. Despite these advancements, significant gaps remain in assessing the feasibility and strategic placement of solar-powered charging stations for e-scooter rentals which could differ from electric vehicles. The work in this thesis is novel since it will take various research areas that have not yet been put together, combining an evaluation of e-scooter user behavior, the integration of renewable energy infrastructure into urban landscapes for electric scooters, to develop a tool that can evaluate in virtually any scenario a clear implementation strategy for deploying solar-powered charging stations for e-scooters. By addressing these areas, the thesis aims to contribute directly to sustainability goals, tackle global warming concerns, enhance economic viability, and improve user convenience.

## 3. Methodology

The methodology of modeling and simulation (M&S) has evolved into a cornerstone of research across various disciplines, offering structured approaches to analyze and optimize complex systems. As discussed by Yin and McKay (2018), M&S encompasses a comprehensive cycle, including model design, development, and iterative processes of verification and validation, to ensure its applicability and reliability in solving real-world problems. These stages facilitate the accurate representation of both real-life dynamic systems, making M&S a versatile research tool.

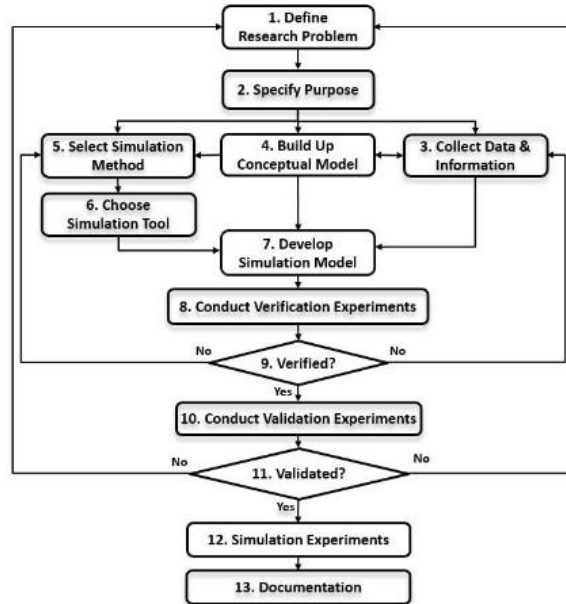


Figure 2: Modeling and simulation procedure (Yin & McKay, 2018)

The foundational stages of modeling involve defining the system under study, as Shannon (1983) outlined, by creating a conceptual model to abstractly represent the key interactions and behaviors within the system. This is followed by data collection and preparation, which are critical for grounding the simulation in empirical evidence or synthetic datasets when real data is unavailable. The selection of a suitable simulation methodology is integral to capturing the system's nuances. Discrete-event simulation (DES), as introduced by Klingstam and Gullander (1999), is commonly employed for systems with well-defined processes and queues, while agent-based simulation (ABS), discussed by Macal and North (2007), excels in modeling decentralized systems where emergent behaviors arise from individual agent interactions.

Subsequent phases involve constructing the simulation model within a selected software tool, such as AnyLogic or Arena, which ensures flexibility and scalability depending on the research's complexity. As highlighted by Sargent (2013), verification and validation are iterative and intertwined phases essential for model credibility. Verification ensures that the model operates as intended, adhering to its conceptual framework, while validation aligns simulation outcomes with real-world behaviors and results. Techniques such as sensitivity analysis, and stress condition testing are frequently employed to enhance model robustness.

Finally, the experimentation phase allows researchers to test various scenarios, optimize parameters, and derive actionable insights. Yin and McKay (2018) emphasize the importance of documenting the process to ensure transparency and replicability. Such rigor in the M&S methodology fosters confidence in its findings and facilitates its application in disciplines ranging from industrial engineering to organizational systems.

In the following chapters, this thesis will utilize the M&S methodology alongside a model developed in Anylogic to evaluate the sustainability and economic viability of implementing solar-powered charging stations in a virtual city. The model has been programmed in order to simulate 4 main agents (Pedestrians,

Scooters, Chargers and Charging stations) and how they interact with each other. To model pedestrian behavior a survey has been constructed and will be at the core of agent decision making. The simulation will be run to extract certain indicators like energy consumption, charging station utilization and economic benefits, among others. Nevertheless, before developing the model we first had to lay down the conceptual model.

## 4. Conceptual Model

### 4.1 Objective of the Conceptual Model

The objective of the conceptual model is to define the various elements involved in the process of electric scooter usage within the urban environment under study. This model establishes the necessary foundation to simulate its operations and, through different variations, aims to fulfill the ultimate purpose of making recommendations regarding the implementation and optimization of solar-powered charging stations for electric scooters.

### 4.2 System Variables

#### 4.2.1 Decision Variables

Decision variables are the elements in a model that can be controlled or adjusted to influence outcomes and achieve desired objectives. These variables directly impact the performance of the system being modeled, and adjusting them allows for exploration of different scenarios to identify local or global optimal solutions. In essence, decision variables are the levers that guide a model's behavior and help to evaluate the effects of different strategies on achieving set goals. Here are the decision variables that will be utilized in this model:

Main Agent:

- Number of scooters (present in the map during the whole simulation run). The optimal relationship between the number of scooters and the number of people in the simulation will be determined through the stress test.
- Number of solar powered charging stations (present in the map during the whole simulation run). For the base case scenario, there will be no charging stations, following this analysis the number of charging stations required will be determined.
- Number of docks at solar powered charging stations (present in the map during the whole simulation run).
- Maximum X coordinate, set to a maximum of 2000 m in the X coordinate.
- Maximum Y coordinate, set to a maximum of 2000 m in the Y coordinate.
- Solar powered charging station placement method: random versus metaheuristic.

Pedestrian Agent:

- Discount offered to pedestrians for deviating from their route and leaving the electric scooter in a solar powered charging station. For the base case scenario, there will be no discount, following this

analysis the required discount will be determined. This discount will be measured as a percentage of the trip cost.

#### 4.2.2 Reference Variables

Reference variables are values in a model that define specific characteristics of the system but are not controlled or adjusted during the simulation (Yin and McKay, 2018). They provide essential context and constraints, and allow for the evaluation of the outcome of the model. Reference variables are continuous during the simulation run and the experimenter can evaluate them constantly, however for the extraction of meaningful results the measurement of the reference variables is only done at the end. In conclusion, they are the values measured, here are the reference variables analyzed in this model:

##### Energy

- Conventional energy consumption of the entire system (kWh)
- Solar power energy production of the entire system (kWh)
- Solar power energy consumption of the entire system (kWh)

##### Pedestrian behaviour

- Number of agents traveling to final destination
- Number of agents traveling to charging station
- Total revenue generated (€)

##### Economic viability

- Energy cost (€)
- Investment cost (€)
- Simulation hotspots

#### 4.2.3 State Variables

State variables represent the dynamic conditions within a model that evolve over time based on interactions and events (Yin and McKay, 2018). State variables are essential for capturing the model's progression and allowing for responsive decision-making based on the system's real-time conditions. Here are the state variables that will be monitored in this model (modeled as intergers):

- Number of scooters being utilized
- Number of scooters available
- Number of scooters low on battery (below 30%)
- Number of scooters outside the system being charged
- Number of charging docks available
- Number of charging docks utilized
- Solar power being generated (kWh)

#### 4.2.4 Auxiliary Variables

Auxiliary variables are intermediate variables used to support calculations within a model (Yin and McKay, 2018). They often derive values from other variables and help streamline complex formulas or enhance

readability without directly affecting the system's state. Here are the auxiliary variables that will be utilized in the model:

- Price to unlock an electric scooter (€)
- Price per minute to ride an electric scooter (€)
- Duration of each ride (min)
- Frequently traveled locations (It is assumed that in natural pedestrian behavior some destinations will be more visited than others. This leads to the creation of an auxiliary variable that stores which locations these are and where they are located on the map)

### 4.3 Entities and Attributes

- **Main**
  - Number of pedestrians present in the virtual city. The number of pedestrians in the simulation will be established at 200 and then will be stress tested for robustness with other values.
  - Average cost for electricity is imported from the QERY database and will be utilized to calculate the average cost for conventional electricity. (*Consumer Electricity Prices for Households in Europe*, 2024)
- **Pedestrians**
  - The speed at which the pedestrians will walk is to be established at 1.42 m/s. (*Google Maps Community*, 2021)
  - The maximum time agents will be willing to walk to a scooter is to be established from the data gathered from the survey.
  - $t$  - is the factor that establishes the utility a pedestrian receives from every minute that they don't have to walk to their final destination, this value was deduced from the survey.
- **Scooters**
  - The average rate at which the scooter consumes energy under normal conditions is 0.0000225 kWh/m. (Barslund, 2024)
  - Speed of the scooter is limited by EU commission therefore each ride will have their own unique speed that cannot surpass this value. (*Overview of Policy Relating to E-scooters in European Countries*, 2020)
  - Battery size for this type of scooter is 0.45 kWh. (Barslund, 2024)
  - An ID is defined for every scooter to identify it.
- **Solar powered charging stations**
  - Hourly solar radiation information will be fed into the system to simulate real world weather. (European Commission, n.d.)
  - Each simulation run will commence at a different part of the year, so to randomize weather patterns and avoid biases.
  - Panel wattage is the energy output these solar panels will generate given the solar radiation 100 W/m<sup>2</sup>. (*Amazon.com: Patio, Lawn & Garden*, n.d.)
  - The efficiency factor is defined as the maximum amount of solar energy that the solar panel can convert into electrical energy. It is defined at 30%. (*Amazon.com: Patio, Lawn & Garden*, n.d.)
  - An ID is defined for every charging station and dock to identify it.
- **Charger**

- The speed at which the charger can travel is defined as the average traveling speed of a van inside an urban area. See section 3.11 on assumptions.
- The charger will utilize a 42V and 2 Amps standard charger.
- The maximum number of scooters that may be picked up at once by a charger is established at 8. See section 3.11 on assumptions.

## 4.4 Resources

The resources will provide a service to the entities. They have specific capacities and characteristics that limit the other entities in performing their activities. For example, pedestrians can't ride scooters if none are available. The resources to be used in the model are listed below:

- Scooters
- Docks at the solar powered charging stations
- Chargers
- Solar irradiance

## 4.5 IDEF0 Diagram

The following IDEF0 diagram presents different levels of detail to facilitate understanding of the various "Processes" under study in this simulation. At the highest level, "Global Process" offers a general overview of the transportation process within the urban electric scooter system. Entities representing pedestrians appear on the left, each evaluating the need for transportation. On the right, pedestrians are returned to either general city locations (final destinations) or specific charging stations, based on agent's utility, and destination proximity. Some agents may exit the system without completing their journey if a scooter is unavailable within their tolerance for proximity.

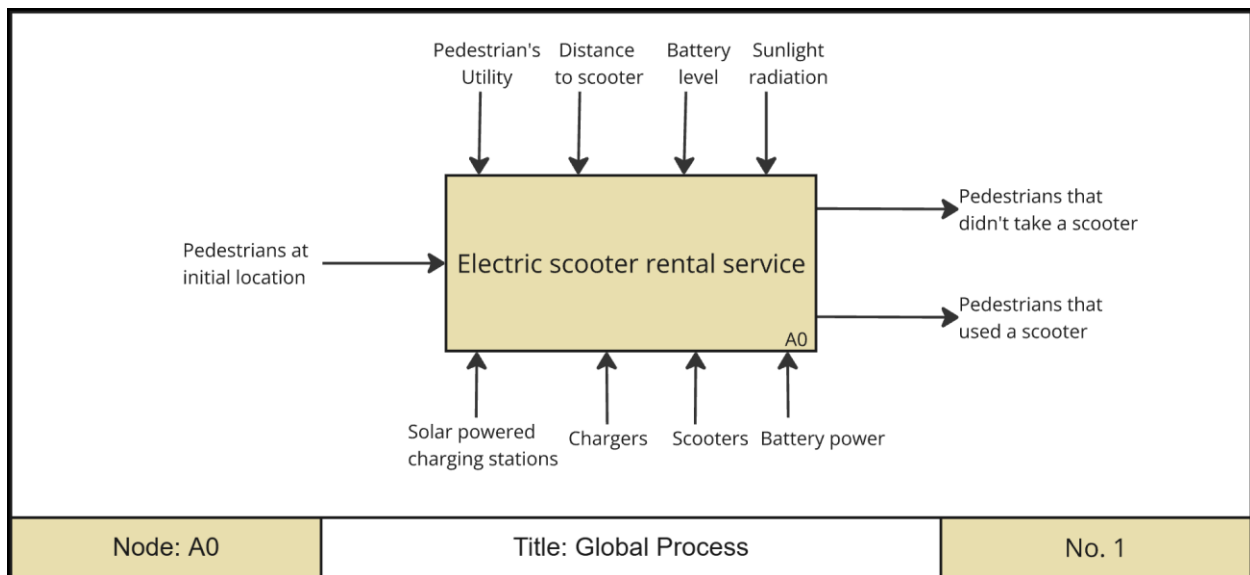


Figure 3: IDEF0 Node: A0, No. 1

The block in Figure 3 can be divided into two main macro activities: "Charging" and "Riding." As can be seen in figure 4.

In the Charging phase, the scooters serve as resources undergoing transformation. This process is governed by specific constraints, such as available sunlight or battery level, and relies on either a solar-powered charging dock or an external charger as resources. Once this activity completes and the scooter has gained sufficient charge, it is ready for the Riding phase.

During Riding, a pedestrian agent takes the scooter and uses its battery to travel toward their final destination, depleting its charge as they go.

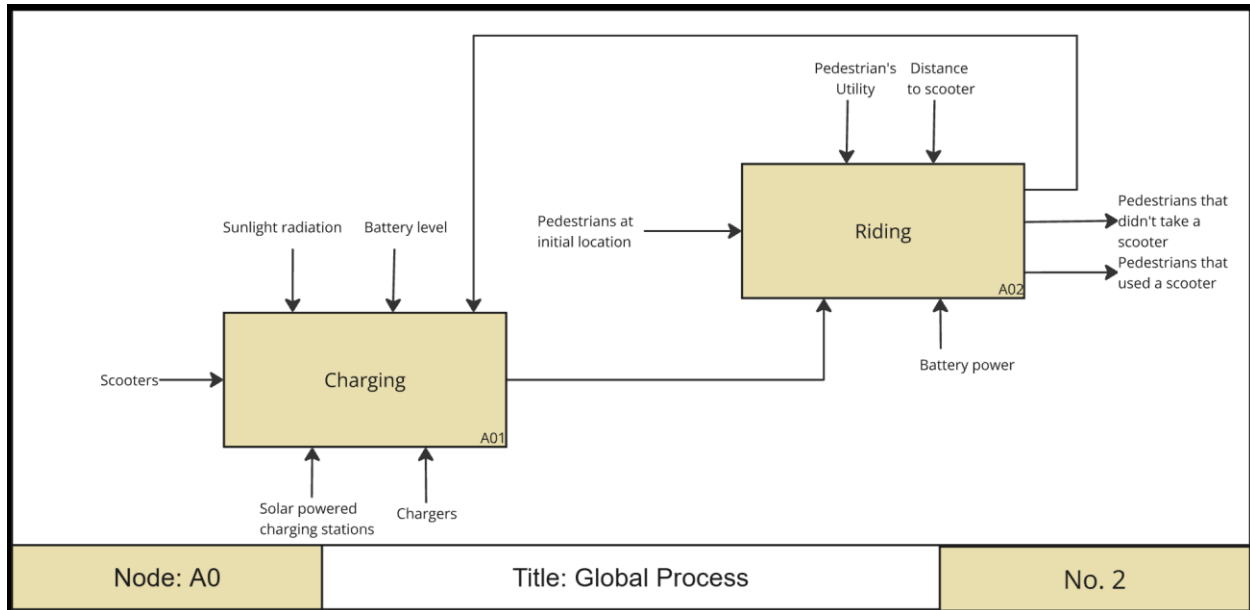


Figure 4: IDEF0 Node: A0, No. 2

Each macro activity can be further detailed, as shown in figure 5, by dividing the charging activity into two primary branches: charging via a solar-powered charging dock and charging via an external charger.

The solar-powered charging dock is the simpler of the two methods, as it requires only the presence of a charging dock as a resource, with sunlight being the primary condition for charging. In contrast, charging via an external charger involves a sequence of more complex steps. This begins with the charger picking up a low-battery scooter, filtered by proximity, battery level, and available space in the van. Once the scooter is collected, the charger uses conventional energy to recharge it, a process determined by the scooter's initial battery level and the charging rate. Finally, the charged scooters are dropped off in high-demand locations to optimize availability.

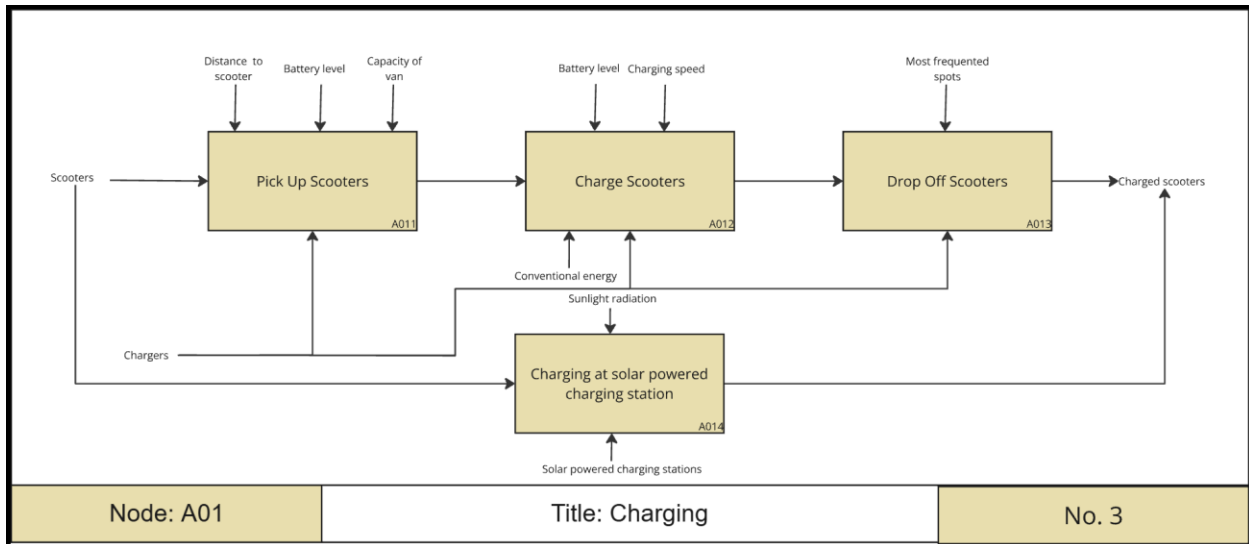


Figure 5: IDEF0 Node: A01, No. 3

In examining the activities within the riding macro activity, three primary sub-activities emerge. First, a pedestrian selects and picks up a scooter based on filtered conditions, such as distance to the scooter and its battery level. This initial action results in one of two outcomes: either the pedestrian picks up the scooter and begins their ride, or they decide against taking it and exits the system. Once the agent begins the ride, the utility of two options is calculated: riding directly to their destination or stopping at the nearest charging station and continuing on foot. This utility calculation determines the ride path taken. Upon arrival, the agent completes the ride by dropping off the scooter at the determined location, making it available for the next user in the system.

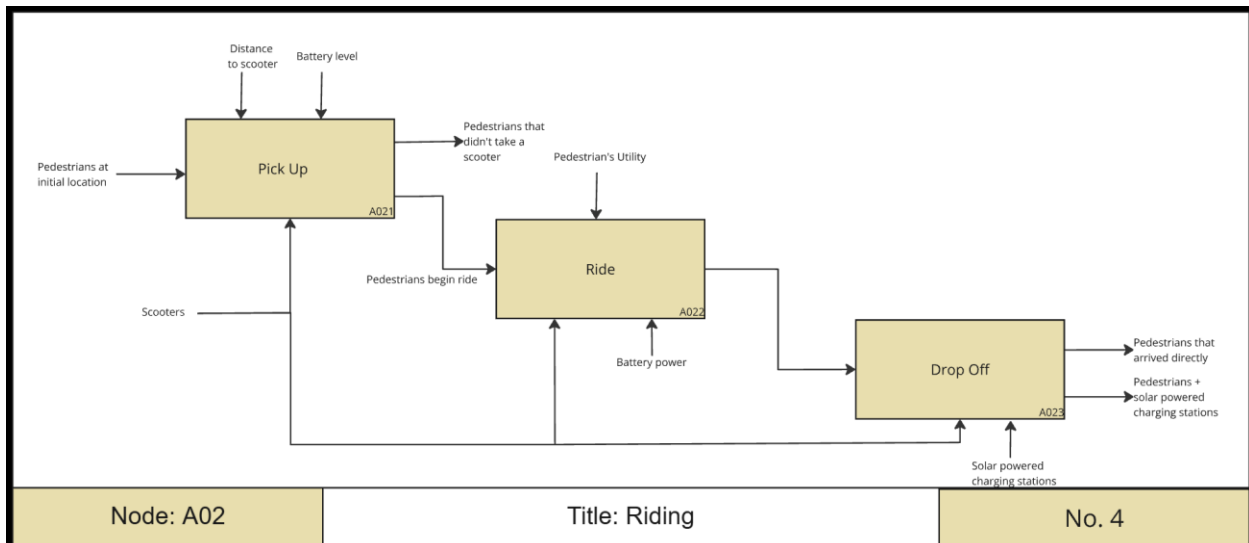


Figure 6: IDEF0 Node: A02, No. 4

## 4.6 Flow Charts

In this section, two flowcharts have been developed to illustrate the core logic driving the model. Figure 7 details the charging process, highlighting the main decision points that determine the agents' actions, including scooter availability, battery level, and van capacity. These factors act as key decision gates, guiding the flow of activity for agents in this part of the model, as seen in the earlier IDEF0 diagrams.

Figure 8 outlines the riding logic, which is more complex. Initially, pedestrians identify the nearest scooter and check if it is in the correct direction (between their current location and their final destination), the exact logic for pickup scooter refer to section 6.1.1. If the scooter does not meet this criterion, they continue evaluating the next closest scooter until they find one that does. It also verifies other criteria as if the scooter is available, if it has the minimum battery level to arrive at the final destination. Once a suitable scooter is identified, they assess if it is within their maximum acceptable walking distance. If no scooter is within this limit, they exit the system, choosing an alternative mode of transport, as there are no viable options to proceed.

If a scooter within the acceptable distance is found, the pedestrian walks to it. Upon arrival, if the scooter is unavailable, they assess nearby alternatives. If no other scooter is accessible, they exit the system. Otherwise, once the scooter is secured, they decide whether to ride directly to their final destination or to a solar-powered charging station, depending on which option offers higher utility.

If they choose the final destination, the process is straightforward. However, if they opt for a charging station, one last decision is required: upon arrival, if no charging dock is available, they continue to their final destination on the scooter. If a dock is available, they drop off the scooter and proceed on foot for the remainder of their journey. For the selection of the charging station agents will travel with the pre-determined logic that they will always choose the charging station closest to their final destination.

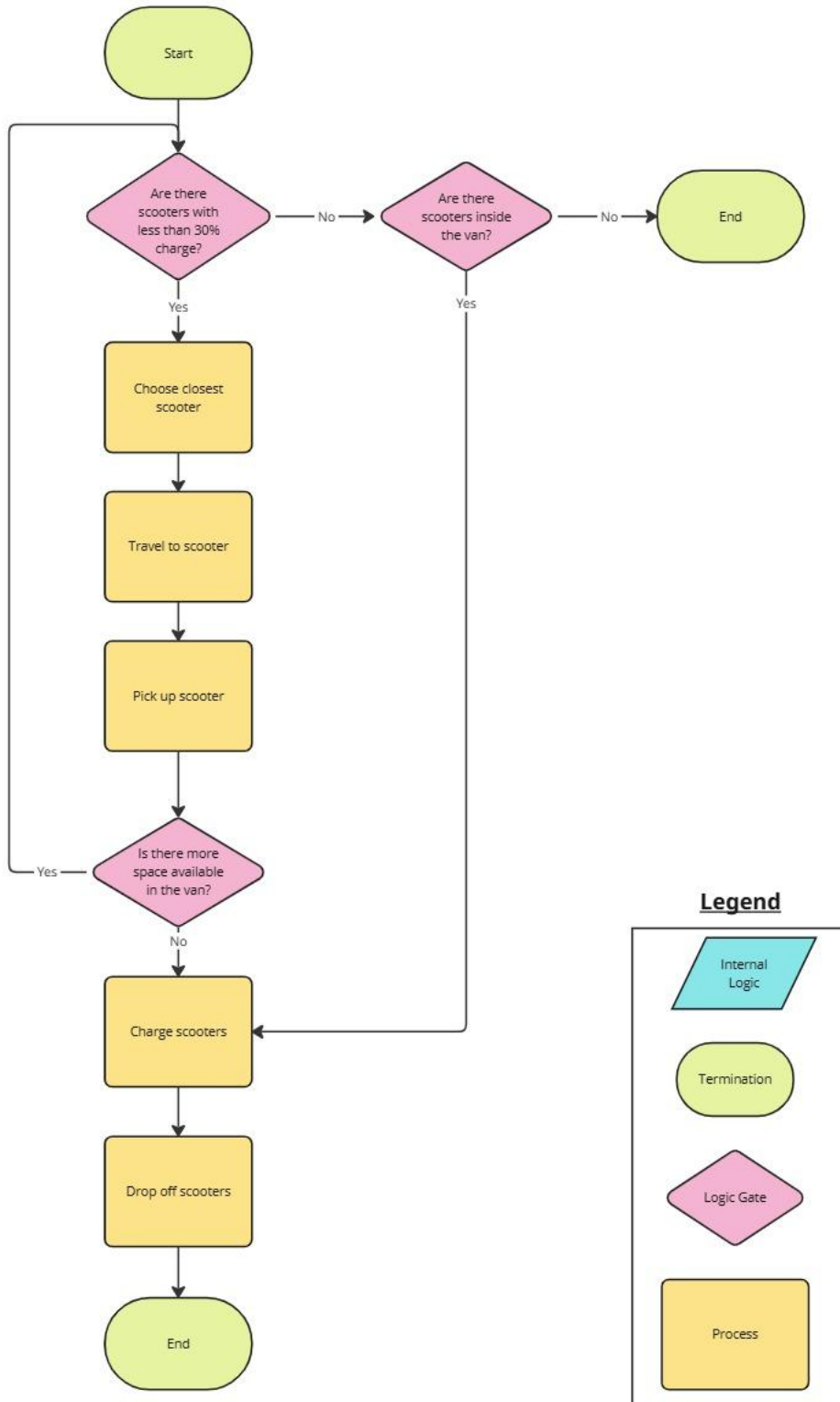


Figure 7: Flow chart of charger activity

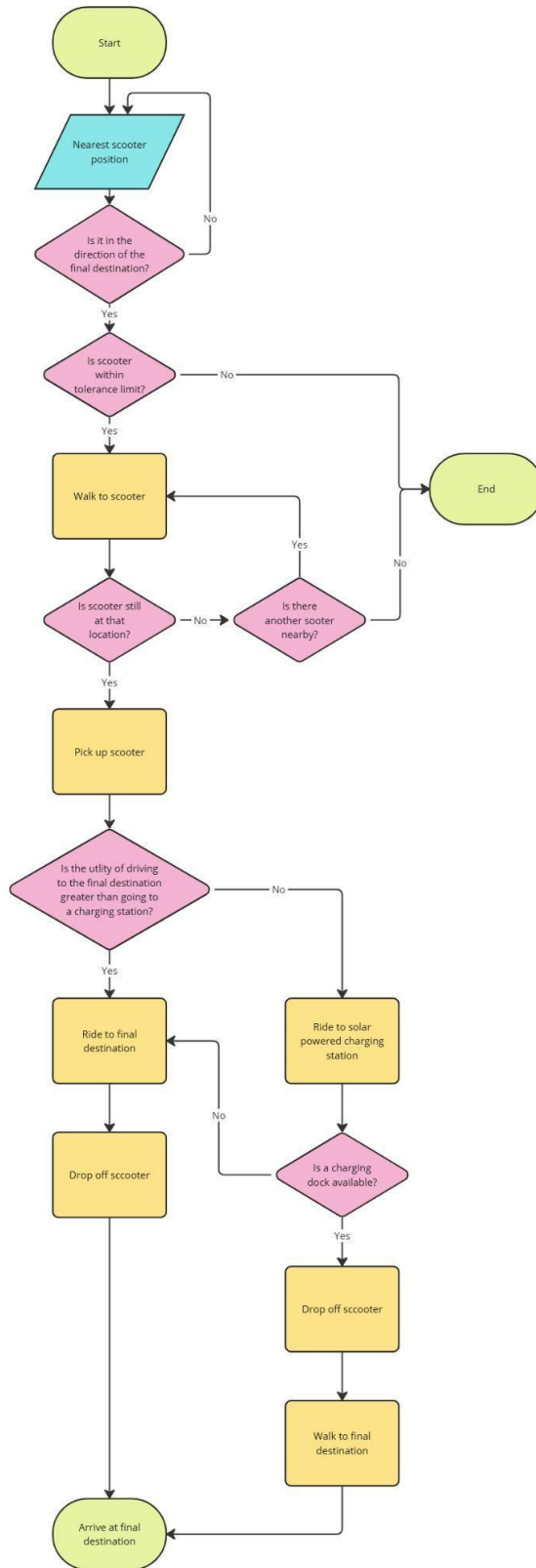


Diagram 8: Flow chart of riding activity

## 4.7 Activities

Activities are defined as actions that agents within the model should be able to undertake. The activities defined for each agent are:

### Pedestrians

- Decide whether to take an electric scooter as a means of transportation or not.
- Choose the most convenient electric scooter on the app.
- Walk to the chosen electric scooter.
- Pick up the electric scooter.
- Evaluate whether to ride to the final destination or to a solar powered charging station and walk the rest of the way.
- Ride on the electric scooter.
- Drop-off the electric scooter.

### Chargers

- Decide whether to take an electric scooter based on the charge left and the distance to reach it.
- Travel to the electric scooter.
- Evaluates if there are more scooters to pick up nearby.
- If the van is not full and repeats the previous 2 actions.
- If the van is full or there are no more scooters, then he proceeds with the charging of the scooters.
- Drop-off electric scooters

## 4.8 Parameters

Parameters are simulation inputs that dictate the behavior of the simulation run, the parameters used for this simulation are:

- Warm-up: the number of days the model is run before the start of data collection. A 7-day warm-up period was chosen, as reference values enter a stationary regiment by that time. This was observed empirically during the construction of the model.
- Window: the time window over which a run will be conducted for data collection. A half-a-year window is chosen, as reference values are not expected to change significantly due to computational limitations and the repetition of arrival rates within this time frame.

## 4.9 Exogenous and Endogenous Events

Events are triggers within the Anylogic model, like signal sending/ receiving. The purpose of events is to allow other processes in the simulation to record data or trigger other actions.

### Exogenous Events

- End of 'Warm up' period: At the end of the warmup period the statistics of resources are reset and the collection of data for reference variable commences.
- End of 'Window' period: Determines the amount of time the simulation will be run to collect data points.
- Change of the hour of the day.

### Endogenous Events

- Arrival of a pedestrian agent.

- Arrival of a charger agent.
- Pedestrians pick up a scooter on the street or at the charging station.
- Pedestrian calculates his utility in traveling to the final destination or to a solar powered charging station and makes a decision and chooses which path to undertake.
- A pedestrian arrives at the charging station.
- Pedestrian arrives at final destination.
- Pedestrian docks scooter at solar powered charging station.
- Dispatch of charger agent.
- The charger agent picks up the scooter.
- Agents leave the system

## 4.10 Process

The process begins with individuals experiencing a need to travel from one location to another within the urban setting. For this study, these individuals (referred to as pedestrian agents) will evaluate electric scooters as a potential mode of transportation. This initial consideration involves two factors: the pedestrian agent's starting location and the proximity and direction of the closest available scooter. Pedestrian agents are assumed to have a constraint of convenience; they are unwilling to move away from their final destination to access a scooter. Therefore, only scooters situated along their intended route are considered. If a scooter meets this criterion and is within a reasonable distance, the agent initiates the process of acquiring it.

Once a scooter is selected, the pedestrian agent proceeds to the scooter's location. Upon arrival, two scenarios are possible: either the scooter is still available and can be picked up, or it has been taken by another agent in the meantime. In the latter case, the agent reassesses the situation and searches for the next nearest scooter. Depending on the distance to this next option, the agent may decide to pursue it or abandon the scooter option entirely in favor of other transportation methods. A key assumption in this model is that each pedestrian agent performs a maximum of two attempts to locate a scooter; if unsuccessful after the second attempt, the agent exits the system.

When an agent successfully acquires a scooter, they then evaluate their possible travel destinations based on the concept of utility (further elaborated in Section 6.1.2). The agent has two primary choices: proceed directly to their final destination using the scooter or detour to a nearby solar-powered charging station and continue to their destination on foot from there. This thesis will explore whether implementing an incentive, such as a discount, could motivate agents to select the charging station detour as a way to optimize the distribution of scooters across the network.

If the agent opts to ride directly to their final destination, they complete the trip and leave the scooter at this endpoint. The scooter then becomes available for the next pedestrian in need of transportation.

Alternatively, if the agent selects the charging station as an intermediary destination, they ride the scooter to that location. Upon arrival, they may either find an available charging dock or find all docks occupied. If a dock is available, the agent parks the scooter, initiating a charging session, and then proceeds on foot

to their final destination. However, if no docks are available, the agent continues directly to their destination, parking the scooter upon arrival.

When scooters are left at solar-powered charging stations, they are recharged using solar energy generated by the station. Real-world solar data is incorporated into the system, ensuring that the charging behavior of scooters at these stations mirrors realistic environmental conditions and energy availability. This approach provides a basis for analyzing the potential impact of solar-powered infrastructure on the operational viability of an electric scooter network within a city.

If scooters are dropped off in street locations rather than at a charging station, they become available for monitoring by external chargers. Should a scooter's battery fall below a 30% threshold, chargers may be deployed to retrieve and charge it using conventional energy sources.

The process for chargers mirrors that of pedestrian agents. Chargers monitor available low-battery scooters in their app and prioritize the closest scooter to their current location. Once a scooter is identified, the charger travels to the location, collects it, and places it in their van. Each van can hold up to eight scooters simultaneously. After collecting a scooter, the charger evaluates whether the van has reached capacity or if there are no additional low-battery scooters nearby. If either condition is met, the van returns to charge the collected scooters. Once all scooters have been recharged, they are dropped off at designated hot spots across the map, making them available again for use by pedestrian agents.

## 4.11 Assumptions

Multiple assumptions were made in the development of the simulation model. These are categorized into market, operational, city layout, charging and battery management, environmental, logistics and operational (chargers) assumptions as follows.

### Market Assumptions

- **No Competition:** The model assumes that the simulated city has no other scooter rental companies, representing a monopoly in scooter rental services.
- **Fixed Pricing:** Prices are assumed to be fixed and independent from demand. For simplicity, the model uses average scooter rental prices in the EMEA region.
- **Simplified Charger Motivation:** Although in reality chargers prioritize scooters based on multiple factors such as battery level, proximity, and spot prices paid by the company, the model simplifies this by excluding the monetary aspect of charging. Chargers are motivated solely by proximity and a cut-off criterion of <30% battery level, assuming a fixed charging cost, while the company incurs only electricity expenses.

### Operational Assumptions

- **Scooter-to-Population Ratio:** The city model maintains a fixed scooter-to-population ratio to ensure a specified operational level. This scooter-to-population ratio will be determined empirically through the stress test.
- **Electric Scooter Model:** The base model taken to simulate the scooters in the model will be the Lime Gen4, with its energy consumption and battery capacity (Barslund, 2024).

- Average Energy Consumption: To streamline the model, scooter energy consumption is standardized to an average rate, disregarding variations due to factors such as gradient, rider weight, and road grip.
- Constant Walking Speed: Pedestrian agents are modeled with a constant walking speed, without accounting for real-life variability.
- Agent Scooter Search Behavior: Agents are assumed to use an app to locate and select a scooter before traveling to its location. Upon arrival, there is a possibility that the scooter is no longer available. In such cases, agents will search for another scooter with a certain probability. However, for the sake of simplicity, agents are limited to a maximum of two search attempts and will not search for a third time. This assumption streamlines the modeling of agent decision-making and reflects a balance between realism and computational efficiency.
- Infrastructure: Scooters are believed to be already present in the city in which the evaluation of the implementation of charging stations is taking place. Therefore the cost of purchasing e-scooters is not considered.

#### City Layout Assumptions

- City Structure: The simulated city is represented as a square and rectangular grid bounded by maximum X and Y coordinates. Each block within this grid is a regular square with 100-meter-long sides.
- Conglomerates Distribution: The city contains three types of location conglomerates (work, school, and other activities), so when referring to work/school/activity location it refers to a conglomerate.

#### Charging and Battery Management Assumptions

- Charging Status Update: To optimize resource usage, the charging status of scooters is updated on an hourly basis in the model. If a scooter is retrieved from a charging station before the next scheduled update, the battery status updates immediately upon retrieval.
- Battery size is assumed to be the same for all scooters and the same size of currently used commercial scooters.
- Idle energy consumption will be considered zero due to computational limits in the Anylogic model.
- Chargers will continue to search for scooters until either their van is full or there are no more scooters below the 30% threshold.

#### Environmental Assumptions

- Solar Radiation Levels: Solar radiation levels across the simulated city are assumed to be equivalent to the average radiation experienced at Politecnico di Torino over a sample year. For simplification, the entire city is modeled as if it receives uniform radiation, measured at a single point. Another consideration is that no shadowing effect has been considered as it may occur in a built environment.
- Uniform Solar Panel Specifications: All solar panels in the model are assumed to be identical, based on the specifications of a commercially available solar panel.

#### Logistic and Operational Assumptions for Chargers

- Average Travel Speed of Charger Vehicles: To account for factors such as start and stop times, scooter pick-up logistics, and urban traffic, charger vehicles operate at a uniform speed ranging from 20 to 40 km/h.
- Van Capacity for Scooter Transport: Each van used in charging operations is limited to a maximum capacity of eight scooters, reflecting physical transportation constraints in urban settings.

## 5. Data Model and Quantification

The Data Model and Quantification section provides a comprehensive overview of the foundational elements that define the structure and behavior of the AnyLogic simulation. It delves into how raw data is transformed into actionable inputs, ensuring that the model accurately represents the complexity of the real-world system being analyzed. A particular focus is placed on the use of stochastic variables, capturing the inherent uncertainties and randomness in agent behavior and environmental conditions. By leveraging both survey data and probabilistic modeling techniques, this section outlines the methods used to quantify variables and establish the relationships between them, laying the groundwork for robust simulation outcomes.

### 5.1 Survey Development

A survey was chosen as the primary data collection method due to its ability to capture diverse individual preferences, behaviors, and decision-making patterns in a systematic manner. Surveys offer a direct and efficient way to gather large volumes of data from a representative population, making them ideal for modeling agent-based behaviors (Bredert et al., 2006). By incorporating real-world insights into the simulation, the survey provides a robust foundation for validating the model's assumptions and outputs. This ensures that the simulation not only reflects theoretical constructs but is also grounded in actual user preferences and urban mobility trends, enhancing its credibility and applicability.

The survey (Appendix A.1) was designed to gather accurate data to model agent behavior and preferences in the simulation. Careful consideration was given to both the phrasing and sequence of questions to minimize bias and induce thoughtful, representative responses. This framing helped set the context without leading respondents toward specific answers. Participants were assured that their responses would be anonymized, to avoid biases.

The questions were constructed to extract measurable and actionable data while maintaining clarity and accessibility for respondents. Multiple-choice formats, Likert scales, and open-ended options were used to provide both structured and qualitative insights.

By aligning the survey with the key variables and hypotheses in the model, the responses obtained enabled accurate quantification of pedestrian agents' behavior, preferences for scooter use, and reactions to potential incentives. This structured approach ensured that the data collected could be seamlessly integrated into the model, providing a reliable basis for stochastic variables and agent decision-making logic.

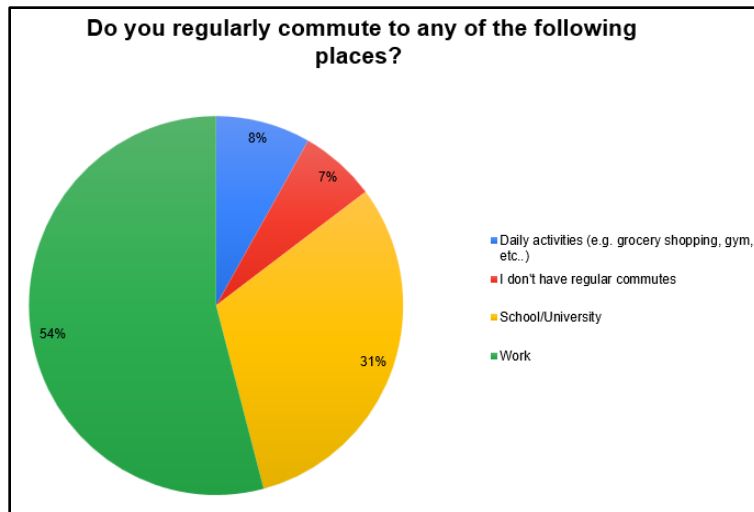
To ensure a broad and representative dataset, the survey was distributed to a diverse group of individuals spanning various age groups and geographic locations. The survey was posted on LinkedIn, WhatsApp Groups and Instagram. Nevertheless, the distribution followed a non-probabilistic, convenience sampling approach, meaning participants were selected based on accessibility and willingness to respond rather than random selection. This allows for quick data collection but may introduce biases due to the self-selection of respondents.

## 5.2 Survey results

The survey results section presents the findings from the survey conducted to gather data on urban mobility patterns and preferences, with a focus on electric scooter usage. The survey was active for three weeks from October 29, 2024, to November 19, 2024, during which 61 responses were collected. The following section will go into detail on all the data collected and their main implications.

### Commuting behavior and frequency

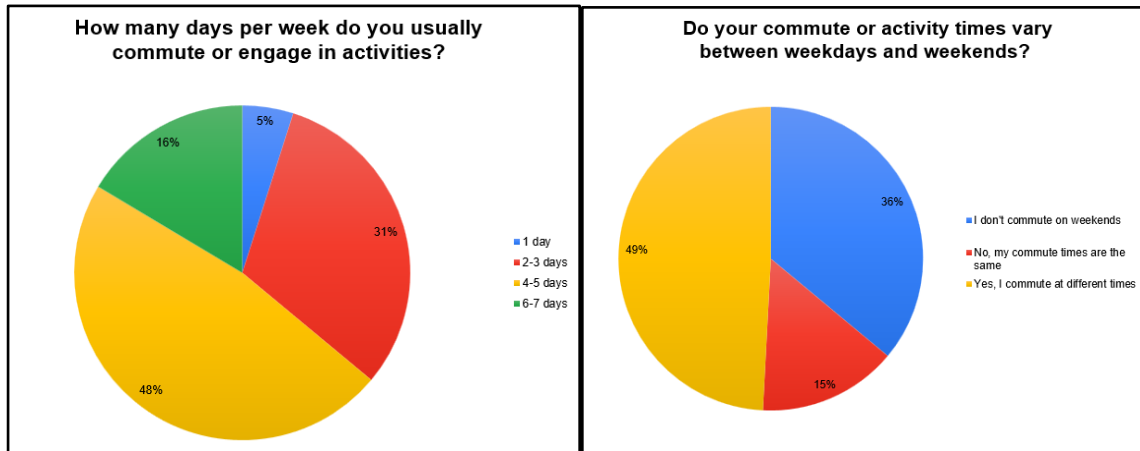
In the first series of questions, participants were asked about their regular primary commuting patterns to gain an understanding of their daily travel behaviors. The survey gathered information on where individuals commute regularly, the frequency of their commutes, and the mode of transportation they typically rely on. These questions were designed to provide a baseline understanding of urban mobility habits.



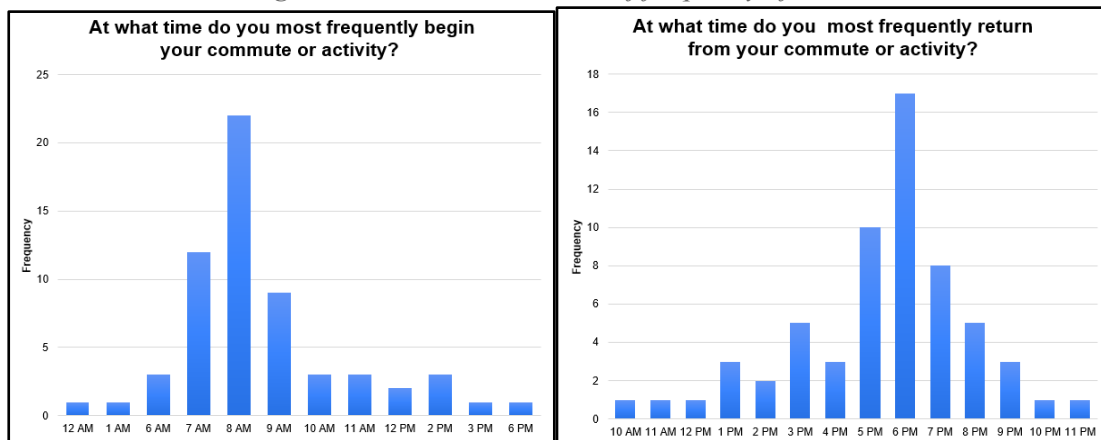
Figures 9: Pie Chart of regular commuting destinations

From the data collected it can be observed that commuting target preferred locations and the majority of commuters are not randomly choosing their final destination. We can observe the main destination frequented is work, followed by school and then other activities and no regular commutes. By looking at the histogram it would be fair to assume that the data follows a triangular distribution. Destination of agents will therefore be modeled as a triangular (1,2,4). Where in the case that the agent has no regular commute, they will be generated a random location on the map as a final destination.

Following this analysis the next step is to extract the frequency with which agents commute to their destination. In the following exhibits we can observe the results obtained.



Figures 10 and 11: Pie Charts of frequency of travel



Figures 12 and 13: Histograms of daily demand for transportation

Using the data collected a couple of conclusions may be drawn. The first is that around half of the participants travel regularly only 4 - 5 days a week, then the other half is distributed among 36% of less frequent commuters and 16% of very regular commuters. Since the percentage of users that do not hold a regular commute on weekends is the same we can assume that the users traveling 4 - 5 and 6 - 7 times a week are all commuting to work, as participants that do not travel as regularly travel have a higher probability of doing other activities.

The second is that the need for transportation may follow two gamma distributions, this is because both demands have very distinct peaks at 8 am and 6 pm respectively. This would coincide with the results obtained from the first question as these are the most common hours to commute to work.

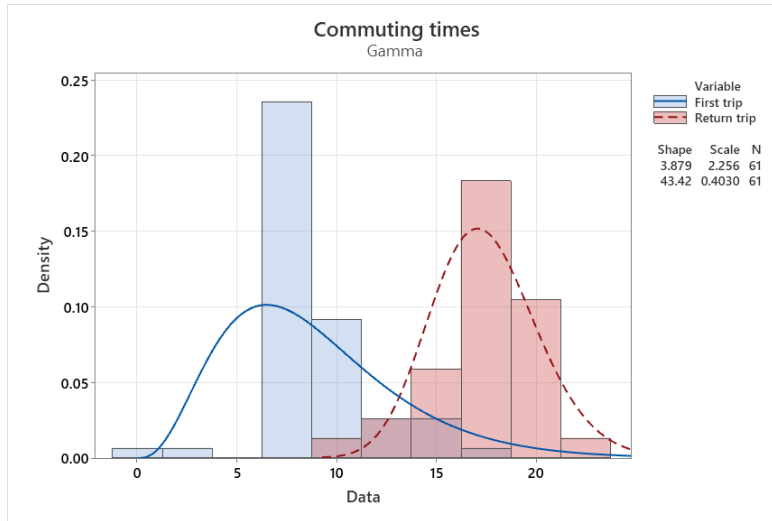
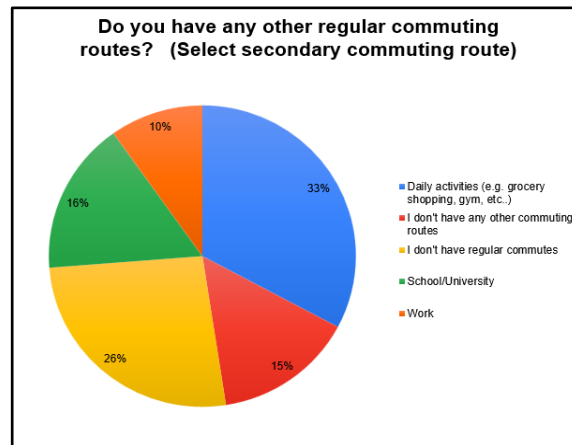


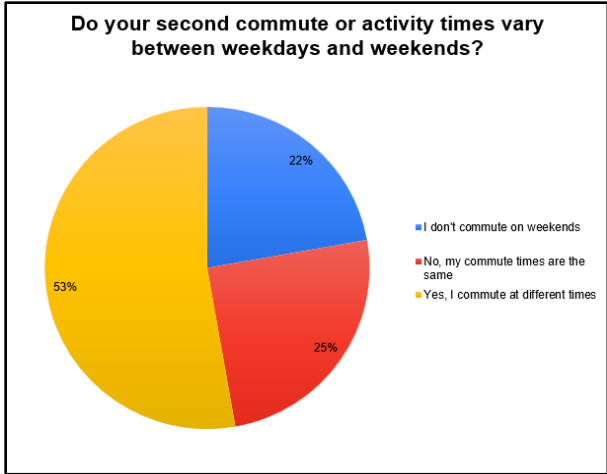
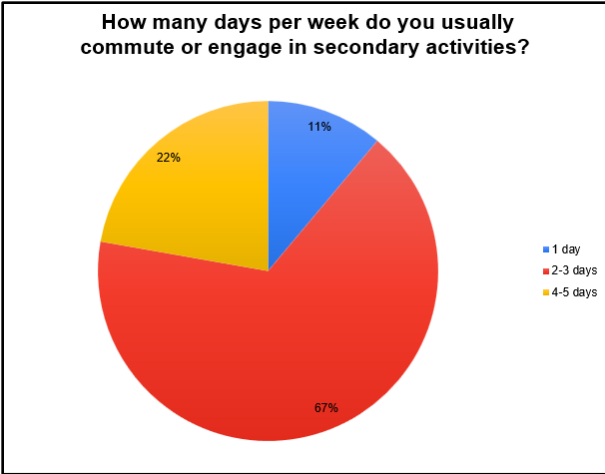
Figure 14: Histogram of frequency of travel and fit distribution

However, there is an inherent bias in this question, most people whose primary commuting activity is work might have other commuting activities they realize during the day and on weekends. It was therefore decided to re-evaluate this set of questions inquiring about secondary commuting activities. In the following diagrams secondary commuting habits may be observed.

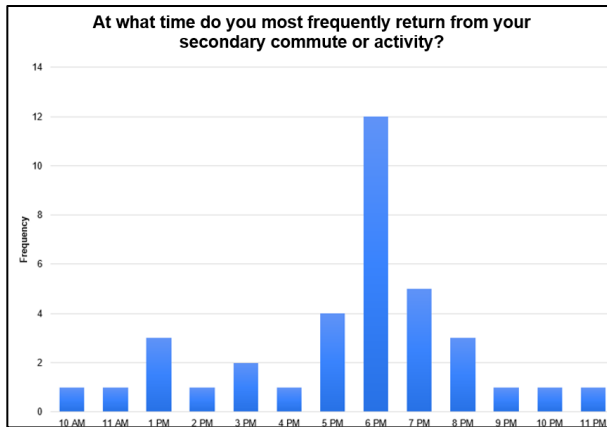
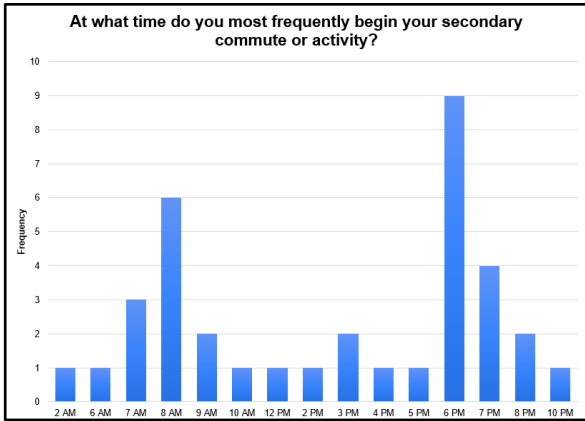


Figures 15: Pie Chart of secondary commuting destinations

The data collected reveals distinct preferences for certain locations, particularly along primary commuting routes. However, secondary routes are often less predictable, with random locations playing a more significant role. To validate the initial assumption that these locations can be modeled using a triangular distribution, further analysis is necessary. This evaluation will determine whether the observed patterns align with the assumed distribution model.

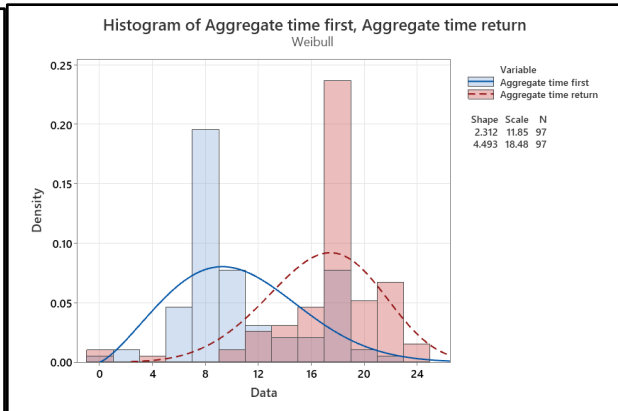
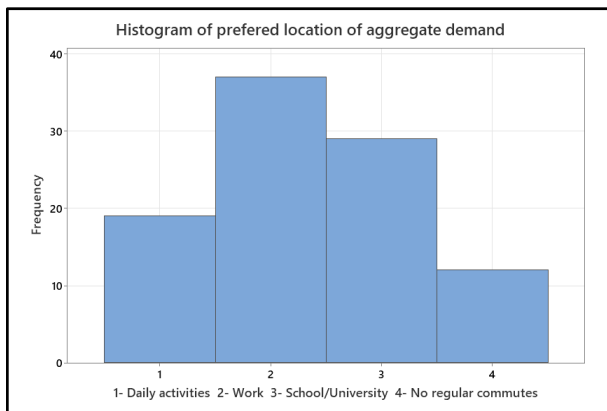


Figures 16 and 17: Pie Charts of frequency of travel to secondary locations



Figures 18 and 19: Histograms of daily demand for transportation

Building on the previous analysis, secondary commuting routes demonstrate varying frequencies across different days of the week and times of the day. To address this variability, the decision was made to aggregate the demand (primary plus secondary commuting) and analyze the results collectively.



Figures 20 and 21: Analysis of aggregated demand

As shown in Figure 20, the preferred destination for the aggregate demand can still be effectively modeled using a triangular distribution with the form  $X \sim \text{Triangular}(1, 2, 4)$ . However, upon closer observation, the hourly demand for scooters has shifted, exhibiting multiple peaks throughout the day. Consequently, the gamma distribution is no longer suitable for modeling this secondary demand. Instead, after considering various distributions it is hypothesized that the aggregate demand could be represented by a Weibull distribution, as illustrated in Figure 21. To validate this hypothesis, a goodness-of-fit test was conducted.

Goodness-of-fit tests are used to globally analyze how accurately the proposed distribution models describe the variable under study. These tests are classified as "non-parametric tests" because they do not estimate any parameters but rather assess the overall distribution. (Addelman et al., 1979)

There are various methods to analyze goodness-of-fit; in this work, the Chi-Square test will be developed. This test will allow us to determine if there is statistical evidence that the distribution does not correspond to the variable under study. It is important to note that this test only serves to find statistical evidence to reject a distribution; failure to reject the test does not prove that the chosen distribution is correct.

In the first place, the goodness-of-fit test will be conducted under the null hypothesis that the demand for transportation follows a Weibull distribution.

$$H_0 = \text{The demand for transportation follows a Weibull distribution}$$

As an initial step, it is necessary to calculate statistics for this test. First, a table is created to record the absolute sample frequencies ( $f_a$ ) for each class ( $C$ ), ensuring that classes with an absolute frequency. Next, two additional columns are added to the same table under the assumption that the null hypothesis ( $H_0$ ) is true, meaning that the variable follows a Weibull distribution. The parameters of the Weibull distribution are estimated with the Minitab Software, with their values summarized below. It is referred to as test 1 - beginning trip and 2 - return trip.

$$\begin{aligned} \widehat{k}_1 &= 2.312, \widehat{k}_2 = 4.493 \\ \widehat{\lambda}_1 &= 11.85, \widehat{\lambda}_2 = 18.48 \end{aligned}$$

Now we calculate the probabilities ( $p_i$ ) that a variable  $x$  with this Weibull distribution falls between the values of each class, i.e., the probability of each interval according to the distribution. The other column we add represents the expected frequencies of observations if the distribution were normal ( $f_e$ ), calculated as:

$$E(f_{e_i}) = N * p_i$$

where  $N$  is the number of observations, which in our case is  $N=97$ .

Similarly, the following Chi-Square statistics are used to compare the expected frequencies with the observed absolute frequencies:

$$\sum_{i=1}^{nk} \frac{(f_{a_i} - f_{e_i})^2}{f_{e_i}} = W \sim X_{nk-p}^2$$

Where  $n_k$  is the number of classes and  $p$  is the number of estimated parameters, in this case  $p = 2$ . When performing the test, we will consider a significance level of  $\alpha = 0.05$ .

The critical value ( $W_{critical}$ ) is then defined as:

$$\alpha = P(W \geq W_{critical})$$

After computing all calculations (Appendix section 4.2) ;

$$W_{obs_1} = \frac{(fa_i - fe_i)^2}{fe_i} = 22.622$$

$$W_{obs_2} = \frac{(fa_i - fe_i)^2}{fe_i} = 30.038$$

Calculating the p-value;

$$\alpha^* = P(W \geq W_{obs})$$

$$\alpha^* = P(W \geq 22.62) = 0.00015$$

$$\alpha^* = P(W \geq 30.038) \approx 0$$

Given that the p-value (0.00015) is smaller than the 5% significance level, we can conclude that there is statistical evidence to reject the null hypothesis, meaning that the variable in question does not follow a Weibull distribution.

In conclusion, the goodness-of-fit test using the Chi-Square distribution statistic indicates that the distribution should be rejected, meaning that neither the Weibull nor the Gamma distribution are suitable models for this variable.

Nevertheless, having found that neither distribution can perfectly model the empirical distribution a custom distribution will be modeled using the Weibull distribution but modifying the probability densities to accommodate for unusual peaks. This will be further developed in the operational model section 5.1.1.

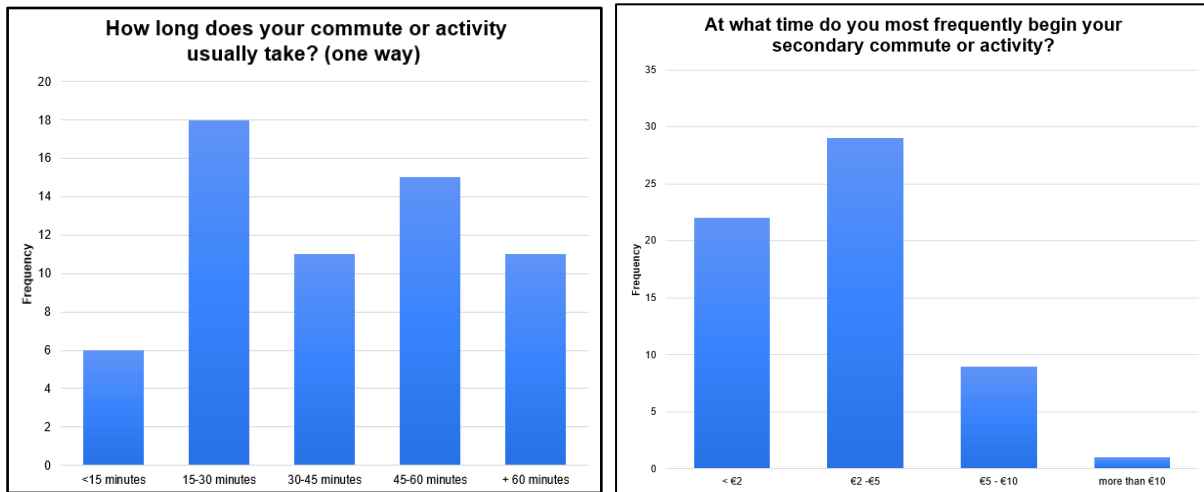
## Customer's willingness to pay

After analyzing the agents' travel behavior, the next critical piece of information to extract was participants' willingness-to-pay (WTP) for transportation. However, WTP is not a straightforward metric that can simply be asked in a survey, as it is deeply influenced by each individual's unique circumstances. Understanding this metric requires nuanced analysis, as it represents a fundamental aspect of consumer decision-making. In fact, entire industries dedicate significant resources to understanding customer WTP, recognizing it as a key factor in maximizing value from economic transactions.

Breidert et al. (2006) highlights the importance of accurately understanding customer WTP as a cornerstone for effective pricing strategies, product development, and market forecasting. It emphasizes that WTP is not a static metric but a nuanced reflection of customer preferences, influenced by factors such as product features, pricing, and market conditions. Various methods are discussed for estimating WTP, including the analysis of market data, experimental approaches, and survey-based techniques.

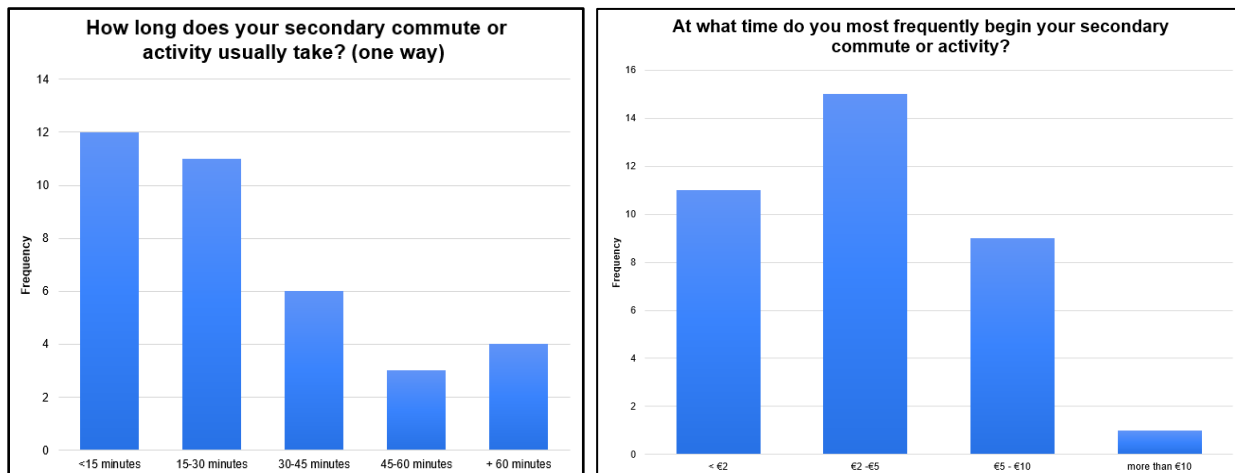
Surveys are highlighted as a widely used and cost-effective method, especially in cases where actual market data is unavailable. However, the authors caution that surveys must be carefully designed to avoid common pitfalls such as bias or inaccuracies stemming from hypothetical responses.

To address potential biases, the survey in this thesis was designed to estimate participants' current WTP by focusing on their existing transportation choices. This was achieved through two key questions: the duration of their current journey and the associated cost. Using these two data points we get the participants' willingness to pay per minute of commuting transportation. While it is acknowledged that participants may not always spend their maximum WTP, this approach provides a practical and reliable approximation. To closely simulate real-world decision-making scenarios, this level of accuracy is considered sufficient and enables meaningful insights into commuter behavior.



Figures 22 and 23: Bar charts of commuting duration and cost for primary travel

Since participants were also asked about their secondary commuting routes, the decision was made to capture their WTP in this context as well. This approach allows for an analysis of how participants' values differ between primary and secondary commuting scenarios, providing a more comprehensive understanding of their decision-making processes.



Figures 24 and 25: Bar charts of commuting duration and cost for secondary travel

As previously explained, aggregating these results allows for the calculation of participants' willingness-to-pay by dividing the amount they spend on their commute by the duration of their trip. The results are

presented in Figure 26. Based on these findings, it was hypothesized that two probabilistic distributions might fit the dataset: a lognormal distribution and a gamma distribution. After conducting the goodness-of-fit test for both, the Gamma distribution yielded a p-value of 0.13039, indicating insufficient evidence to reject the null hypothesis that WTP follows this distribution. In contrast, the lognormal distribution produced a p-value of 0.00234, leading to the rejection of the null hypothesis due to the sharpness of the lognormal curve.

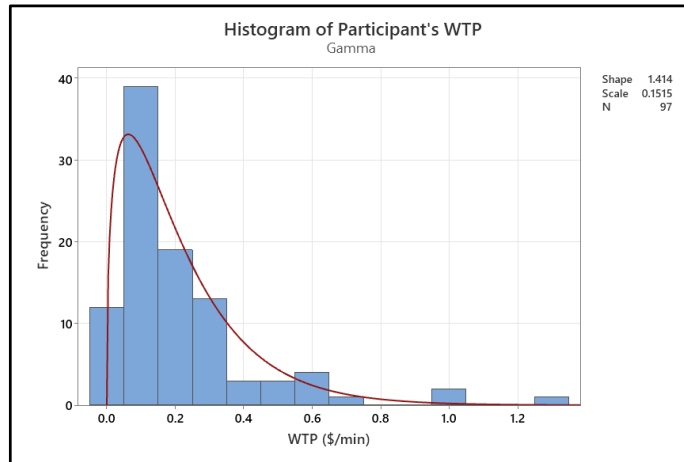
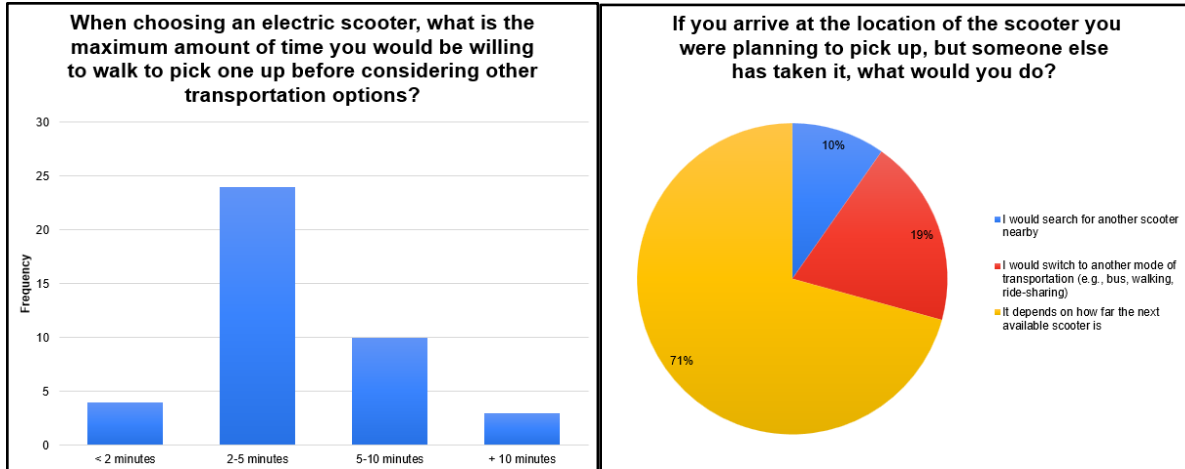


Figure 26: Histogram of participant's WTP and Gamma fit distribution

## Finding a scooter

In a subsequent series of questions, participants were asked about their behavior and decision-making when using electric scooters as a mode of transportation. Specifically, the survey explored how long individuals would be willing to search for a scooter, what actions they would take if a scooter was unavailable at their declared location, and the maximum distance they would be willing to travel to find an alternative scooter. These questions were designed to provide insights into user tolerance for inconvenience, adaptability in the face of unavailability, and the spatial limits of scooter accessibility. This information serves as a foundation for modeling agent behavior in scenarios involving scooter availability. The results can be seen in figures 27, 28 and 29.



Figures 27 and 28: Bar chart of maximum walking time and pie chart of scooter unavailability



Figures 29: Bar chart of maximum walking time to find a second scooter

The parameters will therefore be established as:

- Maximum amount of time willing to walk to pick up a scooter ~ triangular (1.5, 3.5, 10)
- Percentage of users that will abandon the system upon not finding the first scooter: 19%
- Maximum amount of time willing to walk to pick up a second scooter ~triangular (1.5, 3.5, 7.5)

### 5.3 Random Variables

1. Pedestrian Random Location Selection: When pedestrians are not traveling to a frequently visited location, such as work or school, their destination is determined randomly using a uniform distribution. This means that their destination coordinates are generated independently along the X and Y axes, with each axis having values uniformly distributed between 0 and the maximum allowed coordinate (X and Y).
2. Scooter Dispersion Before Warm-Up: Before the simulation begins, scooters are distributed across the map to ensure maximum dispersion and even availability. The code will divide the map into a grid, with each cell representing a potential placement slot for a scooter. The grid size is determined based on the map's dimensions (X and Y) and a fixed block size. Scooters are then assigned to grid positions at regular intervals, calculated to evenly spread them across the available slots. Each

scooter's specific position within a cell is determined by its row and column in the grid, ensuring a structured and uniform initial layout.

3. Charging Station Placement in Hot Zones: Charging stations are strategically placed in "hot zones" identified during the simulation's warm-up phase. The warm-up phase collects data on the most frequented travel locations. Using this data, charging stations are placed within these zones based on a uniform distribution.

## 6. Operational Model

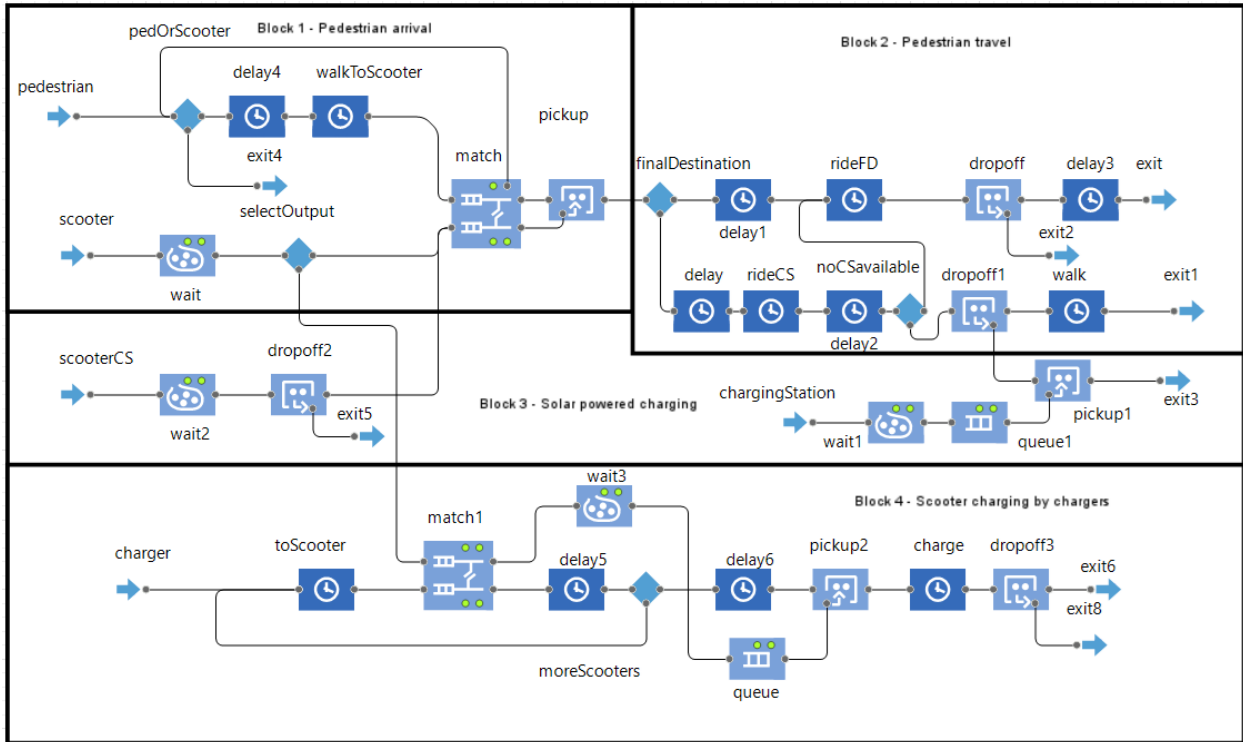
The AnyLogic model is designed to simulate a dynamic "virtual city" environment where various agents interact, representing a simplified yet realistic urban ecosystem. The Main agent serves as the core framework, encompassing the spatial and logical infrastructure required for the interactions among the primary agents: Pedestrian, Scooter, ChargingStation, Charger and supporting processes. This agent acts as the foundation for establishing the simulation's physical boundaries, agent behaviors, and the rules governing their interactions.

To define the city's structure, two parameters, maxX and maxY, are introduced, representing the maximum horizontal and vertical extents of the urban area. These parameters establish the perimeters of the city, ensuring a controlled and measurable simulation space. Within this perimeter, the city is divided into a grid of equally sized 100m x 100m square blocks, aligning with the hypotheses and assumptions defined in the conceptual model. This grid-based approach provides a logical and manageable representation of streets and blocks, facilitating agent movement and interaction while maintaining computational efficiency.

Once the city's spatial boundaries and street layout are established, the focus shifts to implementing the interaction logic within the Main agent. The Discrete Event Simulation (DES) library in AnyLogic is utilized to model the sequential and event-driven processes that drive the agents' behaviors. These include the pedestrian agents' movement patterns, the scooters' availability and utilization dynamics, and the operation of charging stations.

### 6.1 Development of Different Blocks

To enhance the clarity of the AnyLogic model's development, the process was divided into several distinct blocks, each of which will be explored independently. The following sections will delve into each block in detail.



Figures 30: Complete main agent logic flows

## 6.1.1 Block 1: Pedestrian arrival and scooter matching

### 6.1.1.1 Pedestrian Agent

First, the process of pedestrian arrivals was modeled. During the model's startup, the pedestrian population is generated based on a parameter called `nrPedestrians`, which defines the size of the population. This parameter allows for flexibility in setting the number of pedestrian agents at the beginning of the simulation, enabling the model to scale based on varying urban scenarios. At time = 0, all non-operational parameters of the pedestrian agents are initialized to zero, ensuring that the agents are in a neutral state at the start of the simulation. In this initial state, the agents are placed in their “base” state within the statechart, which governs their behavior and transitions throughout the simulation.

In the context of agent-based modeling (ABM), statecharts play a crucial role in defining the decision-making process and behavioral transitions of agents. ABM simulates the actions and interactions of autonomous agents within a defined environment, with each agent responding to both internal states and external conditions. The statechart functions as the “brain” of the pedestrian agents, determining how they react to various events and changes in their environment. It consists of different states and the transitions between them, which are triggered by specific conditions. These state transitions allow pedestrian agents to adapt their behavior dynamically, such as transitioning from a base state to a searching state upon deciding to acquire a scooter. The statechart function is utilized by all agents to different extents depending on the requirements.

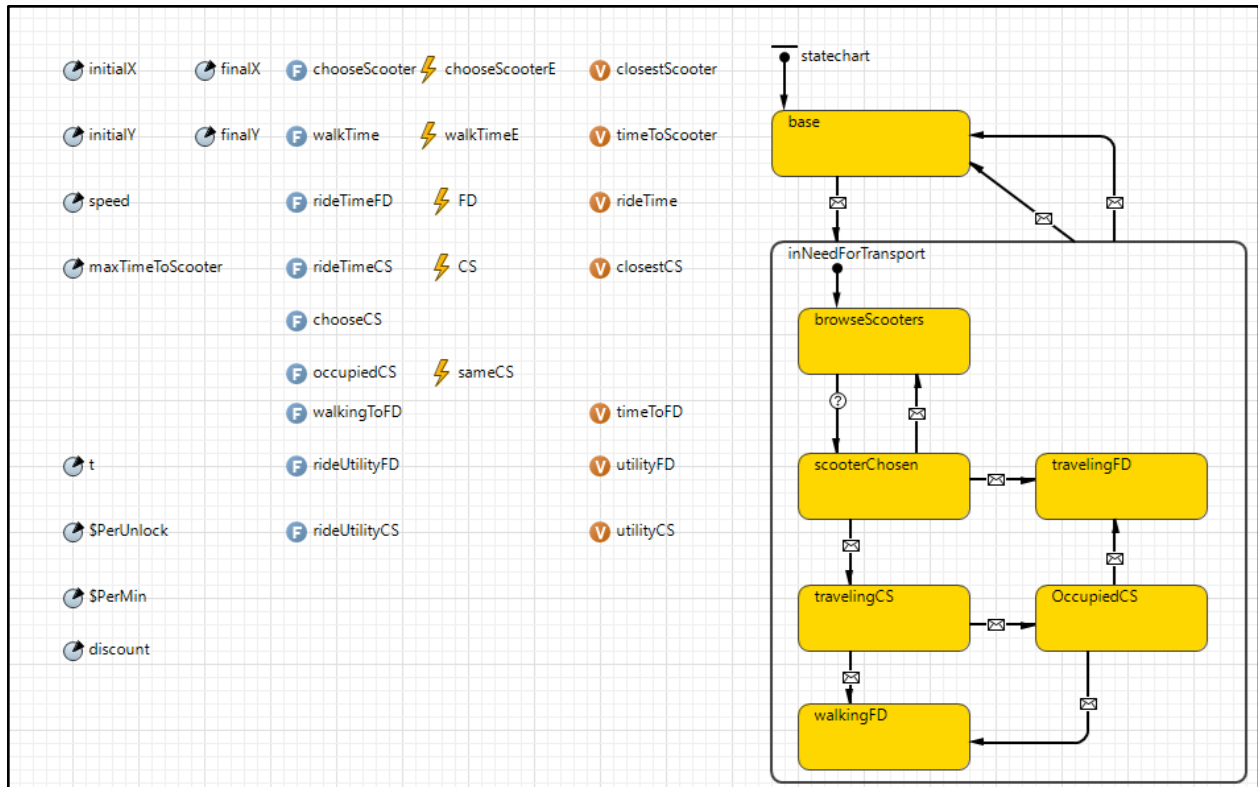


Figure 31: Complete pedestrian agent parameters, functions, events and statechart

Once the model has created the virtual city and generated the pedestrian agents, the agents begin entering the system throughout the day, following a custom distribution developed specifically for this study. As detailed in the *Data and Quantification* section of this thesis, the custom distribution was constructed after determining that distributions, such as the Weibull and Gamma, were unsuitable for modeling the empiric results obtained in the survey. This conclusion was reached based on the results of the Chi-Square goodness-of-fit test, where a p-value of 0.00015 provided statistical evidence to reject the null hypothesis, indicating that these distributions could not adequately represent the observed data.

To address this limitation, a custom distribution was created using the tools provided by AnyLogic. This approach leverages the Weibull distribution as a base but adjusts its probability densities to account for observed irregular peaks in the data. By incorporating these modifications, the custom distribution better reflects the behavior observed in the survey data. This methodology ensures the arrival patterns of pedestrian agents into the system, with separate distributions tailored for the outward and return trips.



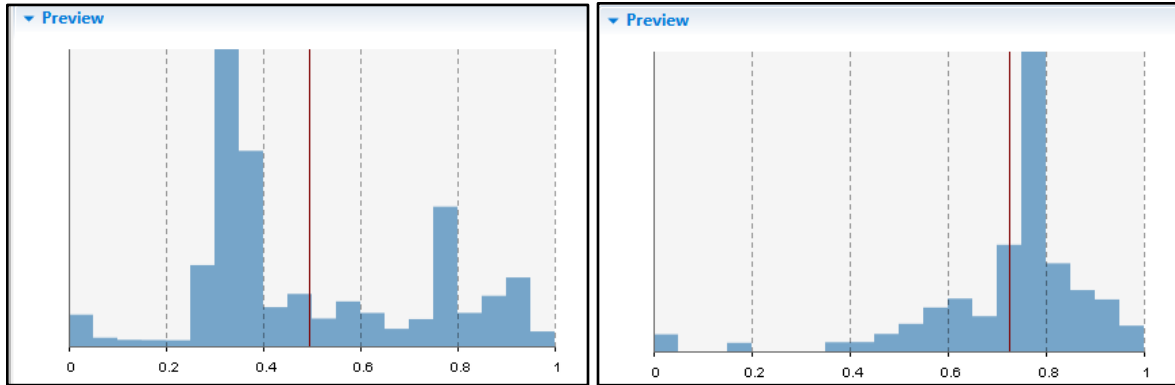


Figure 32: Preview of custom distribution to model agent's arrival outward and return respectively

Furthermore, the schedule tool in AnyLogic is utilized to proportionally adjust the total number of arrivals based on the day of the week. This adjustment accounts for variations in travel behavior observed in the survey results, where differences were noted in the proportion of individuals traveling on weekdays versus weekends. The schedule tool enables the integration of these proportions into the model, ensuring that the distribution of pedestrian arrivals aligns with the survey information.

Once the schedule triggers the arrival of an agent, an event is executed that iterates through all the pedestrians in the population. From this population, a random pedestrian currently in the “base” state is selected, indicating they are not yet active within the system. This pedestrian is sent a message labeled "Inject", which transitions them out of the base state and into the macro state *inNeedsForTransport*.

This transition initiates a series of subsequent activities. Upon leaving the base state, the pedestrian agent is assigned both an initial location and a final destination, defining their specific journey within the virtual city. As discussed in Section 5.2, the initial and final locations for pedestrian agents are determined using a triangular function with the shape triangular (1,2,4). This function generates four distinct cases for assigning locations: 1) other activity, 2) work, 3) school/university, and 4) random location. To implement this, during the startup of the model within the Main agent, a certain number of conglomerates, representing frequently traveled locations, are generated at specific coordinates. These locations are stored in vectors (or collections, as referred to in AnyLogic). The generation of these locations is random, ensuring that each simulation run has a unique configuration of coordinates, which are preserved throughout the run. For example, if a pedestrian's case falls under the "work" category, they will be randomly assigned to one of the work locations created during the simulation startup. This process ensures that each pedestrian has a starting point and a destination that aligns with realistic urban patterns. Refer to appendix A.4.2 to view how these locations are generated.

After exiting the base state, the Main agent takes over, inserting the pedestrian into the “pedestrian” enter block, which serves as the entry point for the agent’s journey within the system. At this time, it’s important to highlight that the explanation of the model will occur in parallel, what happens within the DES in the main agent and what happens within the pedestrian agent in the statechart, please refer to figures 30 and 31 respectively.

Once the pedestrian agent enters the “*inNeedsForTransport*” macrostate, it transitions into the *browseScooter* state. Upon entering this state, the *walkTime* function is executed, and its result is stored in

the variable *timeToScooter*. This function models the process of an agent, in real life, opening their mobile app and searching for the nearest available scooter on the map.

In the AnyLogic model, we replicate the decision-making process that occurs in the agent's mind. The pedestrian begins by scanning through the entire scooter population, evaluating which scooters are available. Once an available scooter is identified, the agent checks to determine whether the scooter is in the right direction. Additionally, the agent verifies whether the scooter has enough battery to reach the final destination. When all these conditions are met (availability, direction, and battery), the agent selects the scooter that is closest and meets all criteria. For the purposes of the *statechart*, the agent identifies the closest scooter and calculates the walking time required to reach it.

Each pedestrian agent is assigned a specific tolerance for walking to reach the closest scooter. This tolerance represents the maximum time a pedestrian is willing to walk and is modeled using a triangular distribution with the parameters triangular (90, 210, 600), where the values are expressed in seconds.

When an agent identifies a scooter that meets all criteria during the “*browseScooter*” state, the walking time to that scooter, stored in “*timeToScooter*”, is compared against the pedestrian’s tolerance limit. If the calculated walking time falls within the tolerance threshold, the agent transitions from the “*browseScooter*” state to the “*scooterChosen*” state. If not, the agent will exit the system.

At this stage, the pedestrian agent transitions from the “enter” block to the “decision” block labeled “pedOrScooter” within the Main agent. Here, a critical condition is evaluated to determine the agent’s next action. The condition is defined as: `agent.statechart.isStateActive(agent.scooterChosen)`. This condition checks whether the pedestrian has successfully transitioned from the “*browseScooter*” state to the “*scooterChosen*” state in their statechart. If the condition is true, it indicates that the pedestrian has found a scooter within their tolerance limit and is prepared to continue their journey using the selected scooter. The agent proceeds along the process flow to begin the scooter journey. However, if the condition is false, it implies that the agent either did not find a suitable scooter or chose not to pursue one due to the constraints of direction, battery sufficiency, or walking tolerance. In such cases, the pedestrian exits the system, symbolizing their decision to either walk to their final destination or opt for an alternative mode of transportation outside the scooter-sharing network. In the case the agent exits the system at this stage he will be sent a “No nearby scooter” message forcing him to exit the “*inNeedForTransport*” state and returning to the base state, this will reset the agent’s coordinates.

Once a pedestrian agent identifies a suitable scooter that meets all requirements, the agent begins walking toward the scooter, utilizing the time previously calculated and stored in the variable *timeToScooter*. This walking time reflects the pedestrian’s physical movement in the block “*walkToScooter*”. While in the “*scooterChosen*” state, the agent executes the function *chooseScooter*. This function uses the same logic as *walkTime* but with a key difference: instead of outputting the time required to reach the scooter, it outputs the object reference of the chosen scooter agent. This object reference is stored in a variable within the pedestrian agent, enabling ongoing communication and interaction between the paired pedestrian and scooter agents throughout the simulation.

When the walking phase ends, two outcomes are possible, the scooter is available upon arrival, or the scooter has been taken before arrival.

If the scooter is no longer at the expected location (e.g., taken by another pedestrian), the agent experiences a failure in pairing. This situation is managed in the Match block, where the pedestrian will not find its counterpart in the other queue and eventually time out. The pedestrian is sent a message "scooter was not there" and transitions back to the browseScooter state. When returning to "browseScooter", the pedestrian agent has a 19% chance of immediately abandoning the search. This is implemented by setting their "maxTimeToScooter" variable to zero, causing the agent to exit the system at the subsequent logic gate. If the pedestrian does not leave, their patience is reduced, modeled with a new triangular distribution~triangular (90, 210, 450), reflecting a diminished willingness to continue searching. The process of browsing and selecting a new scooter then repeats under these adjusted parameters.

However, when the pedestrian agent successfully walks to the chosen scooter when exiting the walkToScooter block, they immediately send a message "in use" to the scooter agent they have selected.

### 6.1.1.2 Scooter Agent

During the model's startup, the scooter population is generated based on a parameter called nrScooters, which defines the size of the population. This parameter allows for flexibility in setting the number of scooter agents at the beginning of the simulation, enabling the model to scale based on varying urban scenarios. At time = 0, all non-operational parameters of the scooter agents are initialized to zero, ensuring that the agents are in a neutral state at the start of the simulation. In this initial state, the agents are placed in their "available" macro state within the *statechart*. Lastly, all scooters when available are found in the wait block "wait" to facilitate the search throughout the model.

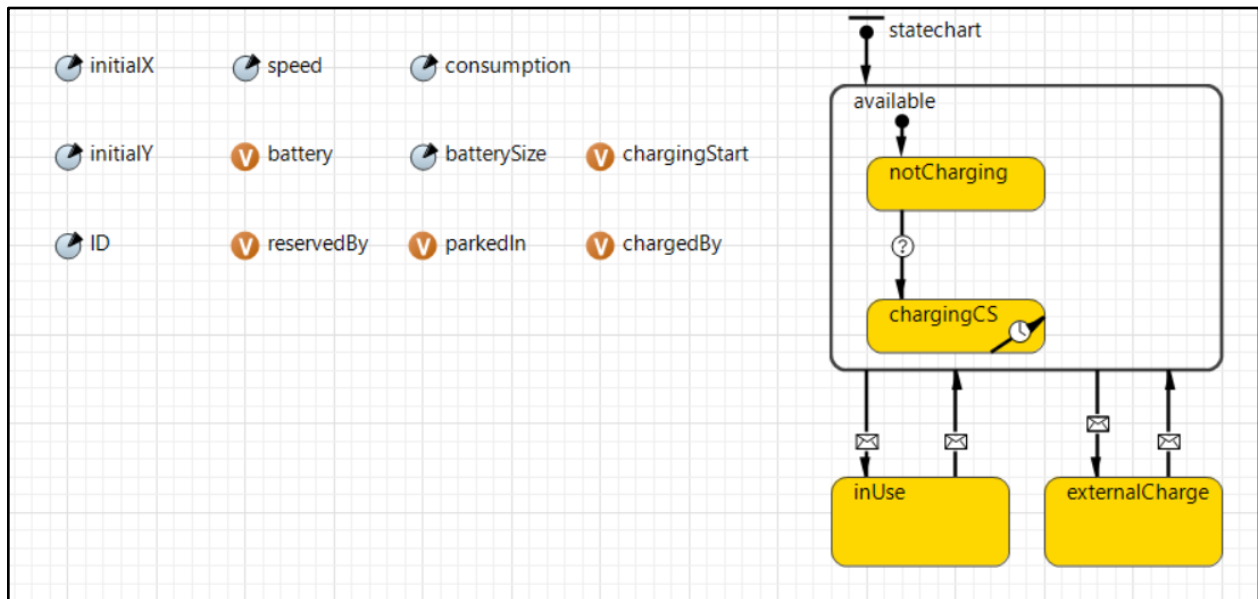


Figure 33: Complete scooter agent parameters, variables and statechart

When the scooter agent receives the message "in use", it triggers an immediate transition in its *statechart*. Regardless of the specific state the scooter is currently in, it is forced to exit the macrostate "available" and transition into the "inUse" state. This transition signifies that the scooter has been claimed by a pedestrian

and is no longer available to other agents. Upon entering the “inUse” state, the scooter agent is released from the “wait” block, where it was previously held as an available resource. Once released, the scooter is sent to the match block to await being paired with the pedestrian who has claimed it, marking the next stage in the interaction between the two agents.

The pairing process in the “Match” block is designed to match the scooter object stored in the pedestrian's variable “closestScooter” with its corresponding scooter agent. This ensures that the pedestrian is paired with the specific scooter they selected during the browseScooter state. Both agents exit the match block simultaneously and the pedestrian agent object will incorporate the scooter agent object in the pick up block. This implies that the pedestrian agent will for some time “contain” the scooter while traveling.

Lastly, a key process occurs when pedestrian agents enter the “scooterChosen” state in their statechart. At this point, they execute two utility functions: *rideUtilityFD* and *rideUtilityCS*, with their respective outputs stored in the variables “utilityFD” and “utilityCS”. These variables represent the utility that pedestrians derive from taking the scooter directly to their final destination or to a solar-powered charging station, respectively. The detailed mechanics and implications of these utility functions will be further developed and analyzed in section 5.1.2.

### 6.1.2 Utility function

The Hotelling model of spatial competition (1929) is a framework in economics that explains how businesses strategically position themselves in a market to attract consumers. In its simplest form, the model considers two firms competing along a linear market where consumers are uniformly distributed. Consumers incur transportation costs, which increases with the distance between their location and the firm's location. The framework derives a utility function  $v - P - t * (x_j - x)$ , where  $v$  is the inherent value of the product,  $P$  is the price,  $t$  is the cost of transportation and  $(x_j - x)$  is the distance from the consumer to the firm. This formulation captures the trade-off between price, product value, and accessibility, offering insights into real-world consumer choices.

Drawing inspiration from the Hotelling model, the utility function incorporates similar principles to represent the decision-making process of pedestrians in my AnyLogic model. Here, utility is framed as a trade-off between the benefits of using a scooter (value), the costs of renting ( $P$ ), and the “travel cost” associated with reaching a scooter and completing the journey. This approach simplifies the complexity of human behavior while maintaining realism, reflecting how users weigh convenience, cost, and time when making transportation choices. By adapting Hotelling's formula to this context, the model captures user decision-making in a way that is grounded in economic theory.

The utility functions implemented in the model serve as the decision-making mechanism for pedestrian agents, allowing them to evaluate and choose between two potential options:

1. Riding the scooter directly to their final destination (FD).
2. Riding the scooter to a charging station (CS) and then walking to the final destination.

The choice is based on the calculated utility for each option, with agents selecting the path that maximizes their overall utility.

## Utility of Going Directly to the Final Destination

The utility of traveling directly to the final destination is computed as:

$$Utility = Benefit\ of\ riding\ the\ scooter - Cost\ of\ renting\ the\ scooter$$

Benefit of riding the scooter is calculated as:

$$Benefit\ of\ riding\ the\ scooter = t * (time\ it\ would\ take\ to\ walk - time\ it\ would\ take\ to\ ride)$$

Here:

- $time\ it\ would\ take\ to\ walk = \frac{total\ distance\ to\ travel(origin \rightarrow FD)}{walking\ speed}$
- $time\ it\ would\ take\ to\ ride = \frac{Total\ distance\ to\ travel(scooter \rightarrow FD)}{scooter\ speed} + time\ to\ walk\ to\ scooter$

$t$ : the utility a pedestrian receives from every minute that they don't have to walk to their final destination

The cost of renting the scooter includes:

- $Cost\ of\ renting\ the\ scooter = cost\ to\ unlock + cost\ per\ minute$

The corresponding code logic in AnyLogic is expressed as:

---

```
double utility = 0;
double distanceFD = Math.abs(initialX - finalX) + Math.abs(initialY -
finalY);
double distanceSFD = Math.abs(closestScooter.initialX - finalX) +
Math.abs(closestScooter.initialY - finalY);
utility = t * ((distanceFD / speed) - ((distanceSFD / closestScooter.speed
)+ timeToScooter))
    - $PerUnlock
    - $PerMin * (distanceSFD / closestScooter.speed);
return utility;
```

---

## Utility of Going to a Charging Station and Walking

For this option, the utility considers the additional discount offered for returning the scooter to a solar-powered charging station. The calculation is:

$$Utility = Benefit\ of\ riding\ the\ scooter - Cost\ of\ renting\ the\ scooter$$

Benefit of riding the scooter is modified as:

$$Benefit = t * (time\ it\ would\ take\ to\ walk - time\ it\ would\ take\ to\ ride + discount)$$

- $time\ it\ would\ take\ to\ walk = \frac{total\ distance\ to\ travel(origin \rightarrow FD)}{walking\ speed}$
- $time\ it\ would\ take\ to\ ride = \frac{Total\ distance\ to\ travel(s \rightarrow FD)}{scooter\ speed} + time\ to\ walk\ to\ scooter$

+time to walk to final destination

The cost of renting the scooter includes:

- $Cost\ of\ renting\ the\ scooter = cost\ to\ unlock + cost\ per\ minute$

The "time to walk to a scooter/ final destination" is determined by the function *walkTime* which takes the distance to the closest scooter and divides it by the pedestrian speed.

The corresponding code logic in AnyLogic is expressed as:

---

```
double utility = 0;
chargingStation cs = null;
cs = chooseCS();

double distanceFD = Math.abs(initialX - finalX) + Math.abs(initialY -
finalY);
double distanceSCS = Math.abs(closestScooter.initialX - cs.X) +
Math.abs(closestScooter.initialY - cs.Y);
utility = t * ((distanceFD / speed) - (timeToScooter +
(distanceSCS/closestScooter.speed)+ timeToFD))
- $PerUnlock
- $PerMin * (distanceSCS / closestScooter.speed)
+ discount;
return utility;
```

---

### 6.1.3 Block 2: Pedestrian's travel

Moving on from block 1, the simulation of agents' travel begins at the point where pedestrians make a decision regarding their route based on calculated utilities. As depicted in Figure 31, the *statechart* splits into two primary branches, governed by a logic gate. This gate evaluates the utility functions discussed in Section 5.1.2, acting as the condition for the agents' trajectory.

If the utility of traveling directly to the final destination surpasses the utility of traveling to a charging station followed by walking the remaining distance, the agent will proceed along the upper branch. Otherwise, if the utility of heading to the charging station is greater, the agent will exit downward to follow the corresponding path.

#### 6.1.3.1 Traveling to final destination

When the utility for traveling directly to the final destination is greater than the alternative, the pedestrian agent proceeds through the logic gate and receives a message labeled "FD". This message signifies the decision to travel directly to the final destination and triggers a transition in the pedestrian's *statechart* from

the *scooterChosen* state to the *travelingFD* state. Upon entering this state, the *rideTimeFD* function is executed. This function calculates the time required for the pedestrian to reach their final destination using the scooter by dividing the distance between the scooter's initial location and the final destination by the scooter's average speed. The resulting value is stored in the *rideTime* variable.

---

```
// Riding function in the FD case
double rideTime = Double.MAX_VALUE;
    rideTime = (Math.abs(closestScooter.initialX - finalX) +
Math.abs(closestScooter.initialY - finalY))/closestScooter.speed;
return rideTime;
```

---

The pedestrian agent then enters the “*rideFD*” delay block, which utilizes the calculated “*rideTime*” as a dynamic delay, ensuring that travel times differ across agents based on their specific journey parameters. Upon exiting the *rideFD* block, symbolizing the completion of the journey, two simultaneous events occur, first the scooter agent is dropped off by entering the “drop-off” block, after which it is looped back to the “enter” block for scooters. In this operation the scooter is sent an “available” message which triggers a change in its statechart from the “inUse” state back to the “available” macrostate. Here, it is stored once again in the “wait” block, making it available for future users.

Then pedestrian agents exit the system, receive an "end" message, and transition out of the “inNeedForTransport” macro state back to their “base” state. In this state, the pedestrian agent's initial and final coordinates are reset to prepare for a potential subsequent simulation run or behavior.

To calculate the amount of energy consumed by the scooters, the simulation takes the distance traveled by each scooter and multiplies it by the standard energy consumption rate. This straightforward calculation provides an accurate estimate of energy usage based on the individual travel patterns of each scooter.

### 6.1.3.2 Traveling to solar powered charging station

When the utility of traveling to a charging station (CS) and subsequently walking to the final destination is higher, the pedestrian agent exits the logic gate and receives a "CS" message. This message triggers a transition in the pedestrian's statechart from the *scooterChosen* state to the *travelingCS* state. Upon entering this state, several events are initiated.

First, since the pedestrian does not initially know which charging station is closest to their final destination, the function *chooseCS* is executed. This function iterates through the entire charging station population, calculating the Euclidean distance between each station and the pedestrian's final destination. After evaluating all possible charging stations, the function identifies the closest station, saves it as an object in the variable “closestCS”, and returns it for subsequent use.

---

```
chargingStation closestCS = null;
double minDistance = Double.MAX_VALUE;
double closestCSID = 0;
// Loop through the entire population of charging stations
for (chargingStation cs : main.chargingStations) {
```

---

```

    // Calculate Euclidean distance between the person's final destination and
    the CS
    double distance = Math.sqrt(Math.pow(cs.X - finalX, 2) + Math.pow(cs.Y -
finalY, 2));
    // Check if this is the closest CS so far
    if (distance < minDistance) {
        minDistance = distance;
        closestCS = cs;
        closestCSID = cs.chargingStationNumber;
    }
}
return closestCS;

```

Once the closest charging station is determined, the *rideTimeCS* function is executed to calculate the time required for the pedestrian to ride the scooter to the selected charging station. This function operates similarly to the *rideTimeFD*, with the calculated time stored in the “rideTime” variable. Additionally, the pedestrian agent also calculates the time it will take to walk from the charging station to their final destination. This secondary calculation is handled by the *walkingToFD* function, with the result saved in a variable called “timeToFD”.

Once all calculations are complete, the simulation progresses along the DES system. After exiting the logic gate and deciding to travel to the charging station, the pedestrian agent encounters the “rideCS” delay block. This block functions similarly to the “rideFD” block: it uses the previously calculated “rideTime” variable for each agent to create a dynamic delay. This delay represents the time taken for the pedestrian to travel on the scooter to the chosen charging station, effectively simulating the scooter ride.

When exiting the rideCS block, an “on at exit” action is triggered. The Main agent verifies whether the selected charging station, stored in the pedestrian agent’s “closestCS” variable, is available for use. This verification ensures that the pedestrian can proceed with the next steps of their journey. It can be observed on the following block how the main agent calls the charging station agent through the pedestrian agent.

Before continuing with the logic for pedestrians to drop off their scooters at a charging station, it is essential to introduce the *charging station* agent. For the AnyLogic model to be accurate, the charging station is represented by individual charging docks, as each dock can accommodate only one scooter at a time. This approach ensures that the model reflects the one-to-one relationship between scooters and docks.

The creation of charging dock agents follows a structured process. In the base case scenario, the solar-powered charging stations are distributed randomly across the map, with their positions constrained to intersections of roads for simplicity. Two parameters govern the number of charging docks:

- *nrChargingStations*: Specifies the number of charging stations to be created.
- *maxNumCS*: Defines the maximum number of charging docks per station.

To generate the charging docks, a nested loop structure is employed (appendix section A.4.4):

1. Outer loop: Iterates for the number of charging stations (*nrChargingStations*). For each iteration, an X, Y coordinate is randomly generated for the charging station. To avoid duplicate locations, this coordinate is stored in a collection called “occupiedPositions”, which ensures that no two charging stations share the same coordinates.

2. Inner loop: For each charging station coordinate, the loop assigns the number of docks located at each charging station (*locationmaxNumCS*) the same X,Y coordinate , effectively creating multiple charging docks that belong to the same station but are modeled as individual agents. *locationmaxNumCS* is a parameter and will be utilized to test various scenarios.

Once created, each charging dock agent is initialized in its “available” state, meaning it is not currently holding a scooter. More detail on the creation and behavior of *chargingStation* agents in Section 6.1.4.

---

```
if (agent.closestCS.statechart.isStateActive(agent.closestCS.charging)) {
    send("CS Occupied", agent); }
else if (agent.closestCS.statechart.isStateActive(agent.closestCS.available)) {
    send("walking", agent); }
```

---

As shown in the code above, upon exiting the “rideCS” block, the Main agent verifies whether the charging dock selected by the pedestrian is in the “available” state in its statechart.

If the dock is available, the pedestrian is sent a message, "walking", which triggers a transition in the pedestrian's statechart from “travelingCS” to “walkingFD”. This transition marks the start of the pedestrian's journey on foot from the charging station to their final destination.

Upon entering the “walkingFD” state, the pedestrian sends a message, "CS taken," to the charging dock they have selected. This action triggers a transition in the charging dock’s statechart from “available” to “charging”, marking the dock as occupied and initiating the charging process for the scooter.

The pedestrian then proceeds through a logic gate that verifies they are in the “walkingFD” state and subsequently enters the “walk” delay block. Similar to previous delay blocks, this one is dynamic, using the “timeToFD” variable, which represents the time calculated for the pedestrian's walk from the charging station to their final destination.

Once the pedestrian completes this final delay, they have effectively arrived at their destination. The pedestrian exits the system, resetting their coordinates and variables, thereby preparing them for potential re-entry into the simulation at a later time.

If the initially selected charging dock is not available, the pedestrian will receive a message, "CS occupied," prompting a transition in the pedestrian's statechart from “travelingCS” to “occupiedCS”. Upon entering this state, the *occupiedCS* function is triggered. This function evaluates whether any other charging docks within the same charging station are available.

The function accomplishes this by looping through the charging dock population and checking two conditions for each dock:

1. The distance between the dock and the originally selected charging station is zero (ensuring it belongs to the same station).
2. The dock is in the available state.

If an alternative charging dock meeting these criteria is found, the pedestrian assigns this dock as their new charging dock. The pedestrian then continues the process as if the initially chosen dock had been available. They transition to the “walkingFD” state, pass through the logic gate, drop off their scooter, and proceed to their destination on foot via the “walk” delay block.

However, if the *occupiedCS* function determines that no other docks are available at the same charging station, the pedestrian receives a message, "no other CS." This prompts the pedestrian to transition to the “travelingFD” state, effectively abandoning the search for a charging station. The pedestrian proceeds

through the top branch of the logic gate and enters the “rideFD” block, where they travel directly to their final destination by scooter. The subsequent process follows the same steps as outlined earlier for pedestrians who initially chose to travel to their final destination instead of a charging station.

### 6.1.4 Block 3: Solar Powered Charging

In this section, the charging station agent is examined in greater detail, including its creation process and interactions within the model. While the agent's basic mechanics were introduced earlier, this section focuses on the placement strategies for charging stations and their charging role within the simulation.

#### 6.1.4.1 Placement of Charging Stations

There are two primary methods for distributing charging stations across the map:

1. Base Case - Random Placement:

As discussed previously, charging stations can be randomly positioned on the map, constrained to intersections of roads for simplicity. This approach ensures an even spatial distribution, making it useful for baseline scenarios or simulations where pedestrian movement patterns are unpredictable.

2. Optimized Case - Metaheuristic Placement:

The second method relies on analyzing pedestrian movement patterns during the warm-up phase of the simulation. All origins and destinations of pedestrian trips are gathered and rounded to the nearest 100 to aggregate coordinates into road crossings. The resulting data forms a vector containing all the visited crossings during the warm-up phase. The frequency of visits to each crossing is counted, and the crossings are ranked from most to least visited. The top n crossings, corresponding to the number of charging stations, are selected, and charging stations are placed at these locations. This algorithm is inspired by the ant colony metaheuristic.

This approach creates a heat map of high-traffic areas as shown in Figure 34, ensuring charging stations are strategically located where pedestrian demand is greatest.



Figures 34: Heat-map example

Similar to the scooter agent, all charging station agents are generated at the start of the simulation. These agents are initially stored in the “wait1” block, where they remain until a scooter claims the charging dock. When a pedestrian drops off a scooter at a charging station, the charging station receives a message "CS taken", prompting it to change its state from “available” to “charging” in its *statechart*. This transition reflects firstly the occupation of the charging dock, ensuring that other agents recognize the dock as unavailable for further use and secondly the release of the *chargingStation* agent from the “wait1” block to be picked up. Simultaneously, the Main agent sends a message "available" to the scooter agent, signaling it to exit the “inUse” state as seen in Figure 5.1.3.1. As discussed before, this allows the scooter to update its location to the coordinates of the charging dock and adjust its battery level.

Additionally, when a scooter is parked at a charging dock, its “parkedIn” variable is updated to reference the specific charging station it occupies. As the scooter enters the “available” macro state, it transitions from the “notCharging” state to the “chargingCS” state. This marks the beginning of the battery charging process. While all the steps described above are happening the agent has transitioned from the “pickUp1” block to the “wait2” block where it will remain for the duration of the charge.

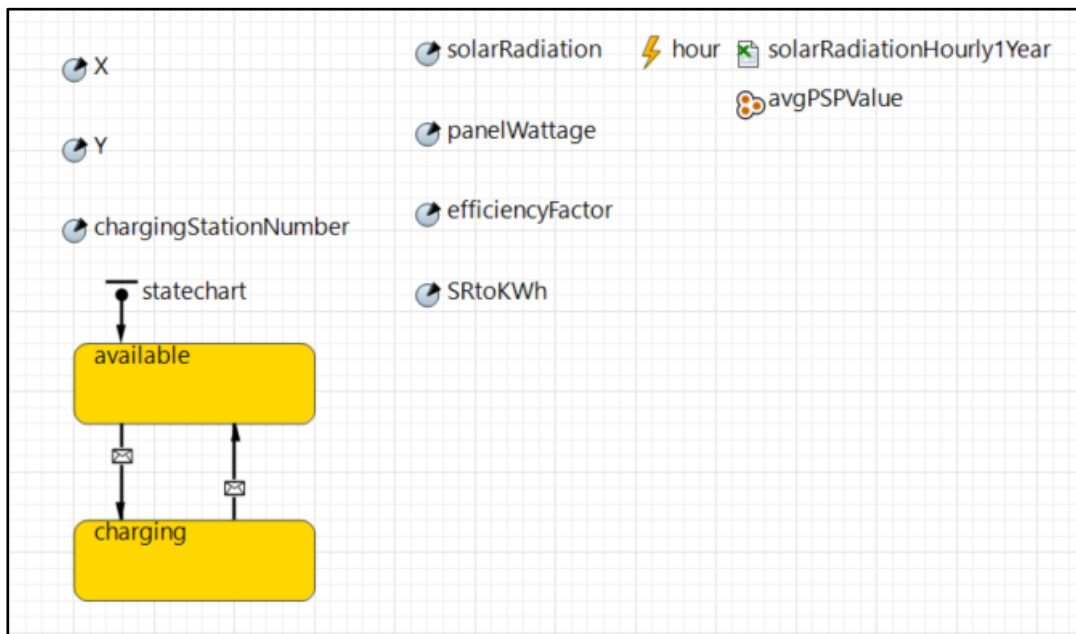


Figure 35: Complete charging Station agent with parameters, statechart and weather

The next phase of the charging process occurs within the charging station agent, where solar energy generation is calculated. As shown in Figure 5.1.4.2, the charging station agent is linked to an external database, represented by an Excel file containing hourly solar radiation data for an entire year. At the beginning of the simulation, this data is loaded into a collection named “avgPSPValue”, which stores the average solar radiation values for each hour.

An hourly event triggers a function within the charging station agent to update its parameter “solarRadiation”, with the corresponding value from the collection for the current hour bracket. This updated solar radiation value is then used to calculate the energy output of the charging station. The function multiplies the “solarRadiation” by the efficiency factor of the solar panels and by the panel’s wattage to determine the amount of energy produced, expressed in kilowatt-hours (kWh). This output is stored in the

parameter SRtoKWh (Solar radiation to KWh), which reflects the charging station's energy production for that hour.

As mentioned, when a scooter is being charged, it enters the “*chargingCS*” state within its *statechart*. This state includes a looped timeout mechanism, which triggers every hour. At each timeout, the scooter temporarily exits the chargingCS state and re-enters it. This looping behavior enables periodic updates to the scooter’s battery charge. On the exit action of the “chargingCS” state, the scooter’s battery is updated using the energy generated by the charging station, stored in the parameter SRtoKWh (expressed in kWh). Given the hourly update this value is directly added to the scooter’s current battery level.

The logic becomes more complex when accounting for scenarios where scooters are removed from the charging station before completing a full hour of charging. To handle this, two additional variables are introduced: “chargingStart” records the time when the scooter enters the charging station, and “chargingDuration” calculates the total time the scooter remains in the station upon exit. If the difference between these two variables indicates that the scooter was charged for less than a full hour, a fractional energy calculation is performed. The fraction of time spent charging (relative to an hour) is multiplied by SRtoKWh to estimate the additional battery charge for the incomplete hour. Finally, it is ensured that the scooter’s battery level does not exceed its maximum capacity.

---

```
chargingStart = time();
double chargingDuration = time()-chargingStart;
double chargingTimeFactor = chargingDuration / 60;
    if(battery < batterySize){
        battery += parkedIn.SRtoKWh * chargingTimeFactor;
        if(battery > batterySize){
            battery = batterySize;
        }
    }
    else battery = batterySize;
chargingStart = 0;
```

---

Scooters remain in the charging station even after their batteries have been fully charged. The only way for scooters to leave the charging station is when pedestrians pick them up. When a pedestrian chooses to pick up a charged scooter, the process follows the same logic previously described for regular scooters. Once a scooter is picked up, it is removed from the charging dock, passes through the drop-off block, and sends "CS free" message to the charging dock. This message changes its state back to "available" and returns the dock to the wait1 block, ready to accept another scooter. This concludes with the solar powered charging loop.

### 6.1.5 Block 4: Scooter Charging by Chargers

The behavior of chargers in is guided solely by the need to maintain operational efficiency, without monetary considerations. In practical terms, this means that during the simulation, an hourly event is triggered in which charger agents assess whether there are scooters with low battery levels. As outlined in the assumptions, a scooter is considered to have a low battery if its charge falls below 30%. If this condition is met, one charger agent is released to pick up the low-battery scooters. In cases where more than eight

scooters (which exceeds the van's capacity) require charging, additional charger agents will be released to handle the surplus.

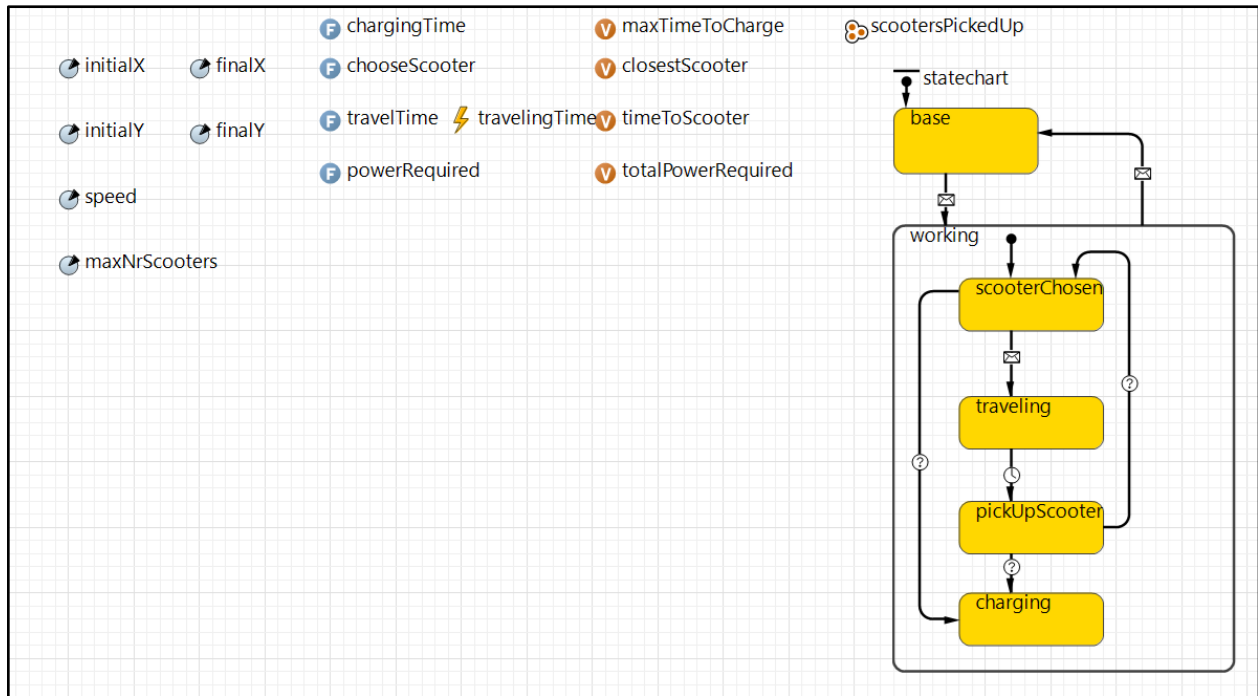


Figure 36: Complete charger agent with parameters, functions and statechart

Upon being released, charger agents will receive an "inject" message, which triggers a transition from their "base" state into the "working" macrostate, specifically entering the "scooterChosen" state. During this transition, several actions take place.

First, just like pedestrian agents, chargers are assigned a random starting location. However, their final destination is determined by the list of "occupiedPositions", which contains the coordinates of the charging station locations where charged scooters will ultimately be dropped off. It has been decided to drop off the scooters near the charging stations as it is believed that these are high traffic areas and have the highest probability of being picked up again.

Once their destinations are determined, the charger agents are injected into the main agent through the "charger" enter block, which integrates them into the broader simulation environment.

When the charger agent enters the "scooterChosen" state, the *chooseScooter* function is triggered. This process closely mirrors how pedestrian agents select a scooter. The charger loops through the entire scooter population, evaluating each one to determine if it meets two key criteria: the scooter must be in the notCharging state, and its battery level must be below the defined threshold. Among the scooters that satisfy these conditions, the charger selects the one closest to its current location.

Once a scooter is chosen, the charger proceeds to travel to its location. To accomplish this, the *travelTime* function is executed, calculating the time required for the charger to reach the scooter. The "timeToScooter" variable is updated with this value, and the "toScooter" delay block uses it to dynamically adjust the travel time for each charger. Entering this delay block triggers a state transition in the charger from "scooterChosen" to "traveling".

Since the chargers' interactions with scooters are simplified in this simulation, a precautionary measure ensures that the scooter selected by a charger becomes unavailable to other chargers and pedestrians. Upon selection, the charger sends a message, "external Charge", to the chosen scooter, prompting a state change from "available" to "external Charge".

When the scooter transitions to the "external Charge" state, it is released from the wait block. This happens because chargers can only collect scooters that are not currently at charging stations (wait 2). As the scooter exits the wait block, it encounters a logic gate that checks whether it is in the "inUse" state. However, since the scooter is in the "external Charge" state, it takes the alternate path defined for this condition and heads towards the "Match1" block.

Finally, the "external Charge" state updates the scooter's location to match the charger's final destination. This ensures that when charging is completed all parameters are updated.

The next step in the charger's journey involves picking up scooters in the "Match" block. This happens through two parallel processes. First, in the main agent, the charger agent matches with the scooter it has chosen, which is stored in the "chargedBy" variable. Second, the "traveling" state is a timed state, meaning that when the charger arrives at the scooter, the state automatically transitions to "pickUpScooter," where the scooter is added to the "scootersPickedUp" collection. Since chargers can pick up to 8 scooters, this collection keeps track of which charger has picked up which scooters.

At this point, the statechart may follow one of two paths. If the number of scooters collected is less than the maximum capacity of the charger, the charger loops back to the "chooseScooter" state to select another scooter. If there are no additional scooters meeting the criteria, the charger is forced into the "charging" state. However, if eligible scooters remain, the loop repeats until the van is full, at which point the charger transitions to the "charging" state. Once in the "charging" state, the charger proceeds through the logic gate and begins the process of charging the collected scooters.

Once the charger proceeds to the "charge" delay block, the time spent charging the scooters is determined by the scooter with the lowest battery level and the time it takes to charge. This is accomplished using an iterative loop that evaluates the battery levels of all scooters in the charger's "scootersPickedUp" collection. The result of this calculation is stored in a variable, which is then used to dynamically adjust the delay duration for the charger.

---

Code for calculating charging time for chargers

```
double maxTimeToCharge = 0.0;
// Constants for the charger
double chargerOutputVoltage = 42.0; // Volts
double chargerOutputCurrent = 2.0; // Amps
double chargerPower = chargerOutputVoltage * chargerOutputCurrent;
// Iterate through the scooters in the scootersPickedUp collection
for (scooter s : scootersPickedUp) {

    double batteryDifference = s.batterySize - s.battery;

    // To convert the battery difference to watt-hours
    double batteryDifferenceWh = batteryDifference * 1000.0;
```

```

double timeToCharge = batteryDifferenceWh / chargerPower;

    if (timeToCharge > maxTimeToCharge) {
        maxTimeToCharge = timeToCharge;
    }
}
return maxTimeToCharge;

```

---

Once the charger finishes charging the scooters, he proceeds to the “drop off” block, where he unloads all the scooters he had picked up during his route. After completing this task, the charger exits the system and transitions back to his “base” state. Upon re-entering this state, the charger’s coordinates are reset, and the stored scooters collection is cleared to prepare for the next cycle of operation.

For the scooters that are dropped off, they are sent an “available” message, which triggers a transition in their statechart from the “external Charge” state back to the “available” macro state. During this transition, the scooter’s “chargedBy” variable is reset, ensuring no residual assignments remain, and the battery level is updated to its maximum capacity, marking the completion of the process.

The final operational logic to be addressed is the looping and sequential picking up of multiple scooters by the charger agents. While this was briefly mentioned earlier to provide an overview of the model's macro functioning, it warrants a more detailed explanation due to its complexity. AnyLogic operates as a sequential simulation system, which introduces challenges in modeling parallel processes.

To revisit the earlier discussion in Section 6.1.3, scooter agents are released from the “wait” block by chargers through the sending of a message. This process occurs sequentially, as only one charger can exit the model at a time. Consequently, the order in which chargers leave the enter block dictates the sequence in which scooters arrive at the “match1” block. However, the “toScooter” delay block is a dynamic block where the travel time of each charger varies depending on the distance to their assigned scooter. This variability can result in a situation where the charger arriving at the match block does not align with the scooter waiting for them.

To address this, the queue for scooters in the match block (Queue 1) is configured with a priority-based system. This means that scooters that satisfy specific conditions are prioritized, allowing them to move forward in the queue and ensuring that the intended charger matches with the correct scooter.

---

```
(match1.queue1.size() > 0 && match1.queue1.get(0).chargedBy == agent) ? 1 : 0
```

---

As illustrated by the priority equation, when the scooter queue (Queue 1) has a size greater than zero, and the chargedBy variable of the scooter matches the charger currently waiting in the corresponding charger queue, the scooter is assigned priority.

Differently than what we saw in the pedestrian logic, the pickup block is not immediately after the match block, since the charger evaluates if there are other scooters he may pick up. Because of this the scooters that were released from the match block will proceed to the “wait3” block and only once the charger is in the “charging” state will the scooters be allowed to pass the logic gate and proceed to pick up block all at once. This is done with the following function:

---

```
for (int i = 0; i < agent.scootersPickedUp.size(); i++) {
```

```
    // Access each scooter in the scootersPickedUp collection
    scooter pickedUpScooter = agent.scootersPickedUp.get(i);
    // Free the scooter from wait3
    wait3.free(pickedUpScooter);
}
```

---

As observed, the process involves a “for” loop function within the charger agent that iterates through the entire collection of scooters associated with that charger. This loop ensures that all scooters corresponding to the charger agent passing through the logic gate are freed and subsequently picked up.

A formula was implemented within the quantity field of the pick-up block. This formula dynamically determines the number of scooters in the collection for the specific charger agent, allowing the pick-up block to adapt its operation based on the actual count. By doing so, the system ensures that all scooters associated with the charger agent are picked up effectively, regardless of their number. This was created since the pick-up block in AnyLogic imposes a constraint: it requires a predefined quantity of agents to pick up.

Once this process is completed, the charger agent transitions to the drop-off logic, as previously described, completing its operational cycle.

## 6.2 Reference Variables Definition

As outlined in section 4.2.2, ten reference variables were identified for analysis to obtain tangible outcomes from the simulation runs.

### 6.2.1 Energy Consumption (Conventional and Solar) and Solar Power Production (KWh)

The process of calculating energy consumption follows a similar approach for both conventional energy and renewable solar energy sources. When a scooter completes its charging cycle, it exits the respective charging state: “chargingCS” for solar-powered stations and “externalCharge” for conventional charging. At this point, the amount of energy transferred to the scooter is recorded in a respective cumulative variable within the main agent and subsequently stored in a connected database to calculate the amount of energy consumption.

A parallel mechanism is implemented for the charging station agent. At the start of each hour, the current value of the SRtoKWh variable, as previously discussed, is saved into a cumulative variable that tracks the total solar energy generated. To provide a real-time visualization of these dynamics, two cumulative line graphs are employed. These graphs display the aggregated energy consumption by scooters and the total solar energy produced. This visualization is essential for the next stage of the study, which focuses on validating the model and conducting stress tests to evaluate system performance under varying conditions.

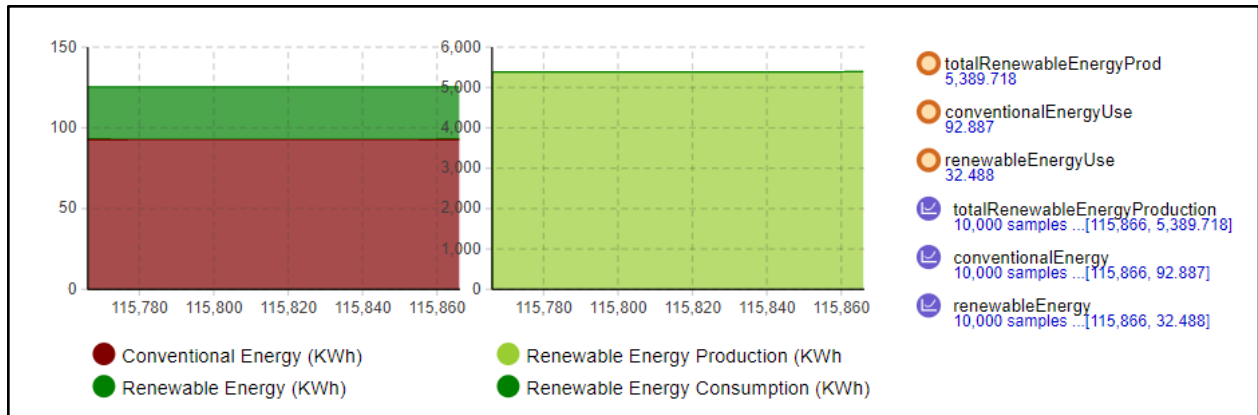


Figure 37: Energy Usage and Energy Production

Figure 37 displays two stacked line charts. The first chart compares conventional energy consumption to renewable energy consumption, while the second chart illustrates renewable energy production and consumption over the simulation time (X-axis).

The energy consumption values in KWh enable the calculation of the renewable-to-conventional energy consumption ratio. This metric provides insight into the effectiveness of solar-powered charging stations in attracting users and reducing reliance on conventional energy sources within a given simulation run.

Additionally, by aggregating the total energy consumption data, it is possible to calculate the overall energy usage by scooters (in KWh) during the simulation.

To summarize the reference variables to be analyzed in this section are:

- Conventional energy consumption
- Solar energy consumption
- Total energy consumption
- % of renewable energy consumed
- Scope 2 GHG emissions

### 6.2.2 Final destination chosen

To determine the number of agents selecting each destination, a counter variable was placed at the exit of the logic gate labeled “finalDestination.” If agents proceed to the right of the logic gate, they are counted as those traveling directly to their final destination. Conversely, if agents exit through the bottom of the logic gate, they are recorded as choosing to travel to a nearby solar-powered charging station. To visually represent this distribution within the simulation, a dynamic pie chart was implemented, as shown in Figure 38.

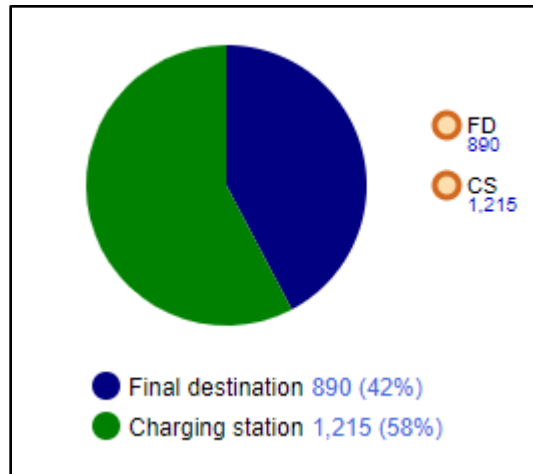


Figure 38: Destination chosen by pedestrian agents

### 6.2.3 Economic indicators

Evaluating the economic feasibility of implementing solar-powered charging stations requires a detailed analysis of both revenues and costs, these are the reference variables. The initial investment for this project comprises three primary components: the solar panel, the scooter charger, and the electrical inverter. After researching commercially available options, the costs were determined as follows: solar panels are priced at €120 per square meter, scooter chargers at €40 each, and electrical inverters at €350 per unit. (Amazon.com: Patio, Lawn & Garden, n.d.), (Amazon.com: 42V 2A Scooter Charger With 6 in 1 Plugs for 36V Pocket Mod, Sports Mod, Razor, Gotrax, Jetson, Voyage, Ninebot, Lithium Battery Device, Electric Scooter Charger : Sports & Outdoors, n.d.) (Amazon.com : SOLPERK Solar Panel 2PCS Solar Panels 100 Watt 12 Volt, 200W SOAIR Panel High Efficiency Monocrystalline PV Module Power Charger Solar Panel for Boat Car RV Motorcycle Marine : Patio, Lawn & Garden, n.d.). Other costs related to the infrastructure, were not considered. These cost values are incorporated into the simulation, allowing the model to dynamically adjust the initial investment based on the number of charging stations tested.

Operating costs have been simplified for this simulation. The only recurring cost included is electricity, and it is assumed that chargers will operate at the highest electricity prices in Europe to compensate for the lack of information on the profit they make, with data sourced from the QERY database.

Maintenance costs are assumed to be negligible within the model's time frame. Costs related to road occupation and fixed costs for connecting to the electric grid are not considered. Additionally, since the scooters are already present in the city where the charging stations are to be implemented, their costs are not considered.

Revenue generation is calculated based on several parameters, including the revenue obtained from unlocking scooters, the per-minute charge, the total ride time of pedestrians minus any discounts offered for charging at solar-powered stations and the revenue of injecting excess revenue into the grid. For this last component the average cost of electricity was taken in Europe to estimate the revenue that could be generated.

To provide a clear understanding of the financial performance, the model aggregates these revenue and cost variables into a dynamic line chart. This chart offers a visual representation of the breakeven point, serving as a critical tool for validating the economic viability of the project. It also facilitates stress testing under various conditions.

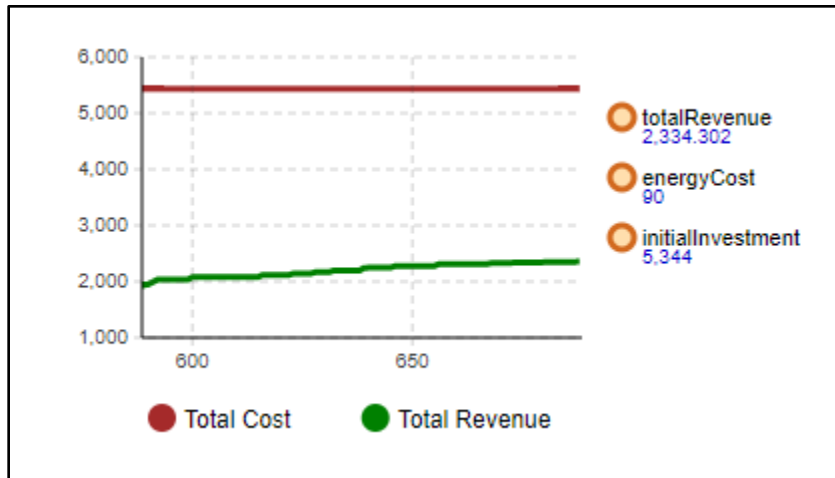


Figure 39: Total revenues and total costs in Euros

### 6.2.4 Simulation hotspots

Although not directly used to measure the effectiveness of the solar-powered charging station implementation, a 2D histogram was incorporated into the model to provide a visual representation of the underlying dynamics within the AnyLogic simulation. By plotting the X coordinates on the X-axis and the Y coordinates on the Y-axis, and mapping the locations where pedestrians originated and where they dropped off their scooters, a heatmap was generated.

As shown in Figure 5.2.3, this heat map illustrates the effectiveness of the algorithm used to place scooters within identified "hot zones." This visualization tool allows the evaluation of the effectiveness of assigning charging stations randomly or utilizing the developed algorithm. A deeper analysis of this comparison will be conducted during the experimentation phase of this thesis.

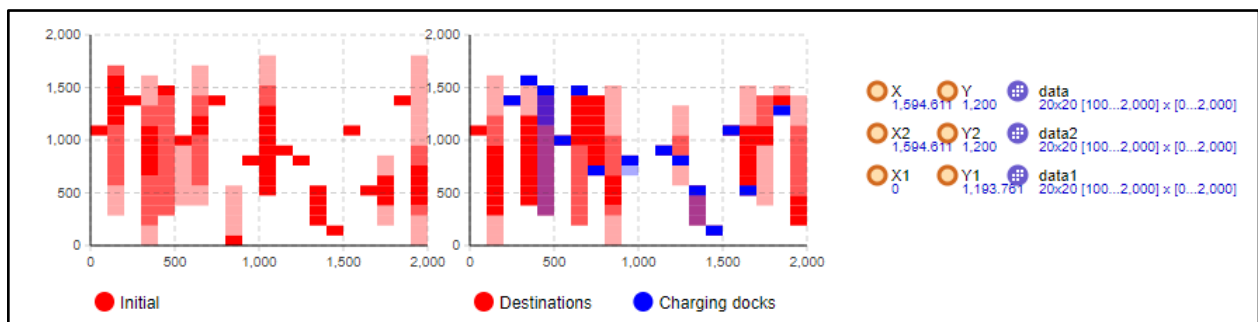


Figure 40: Heat map of location of origin, destination and charging stations

## 6.3 Stress Test

To evaluate the robustness and scalability of the simulation model, several stress tests were conducted using the key decision variables defined in the Main and Pedestrian agents. These tests aimed to assess the system's behavior under extreme conditions and to identify any potential limitations or optimization opportunities within the model.

### Zero Resources Scenario

In the first test, all solar-powered charging stations and docks were removed from the system, and no discounts were offered to pedestrians. This scenario evaluated whether the model could accurately simulate scooter usage in the absence of incentives or infrastructure for charging. The model performed as expected, with scooters operating without any charging events, and pedestrians navigating to their destinations uninterrupted.

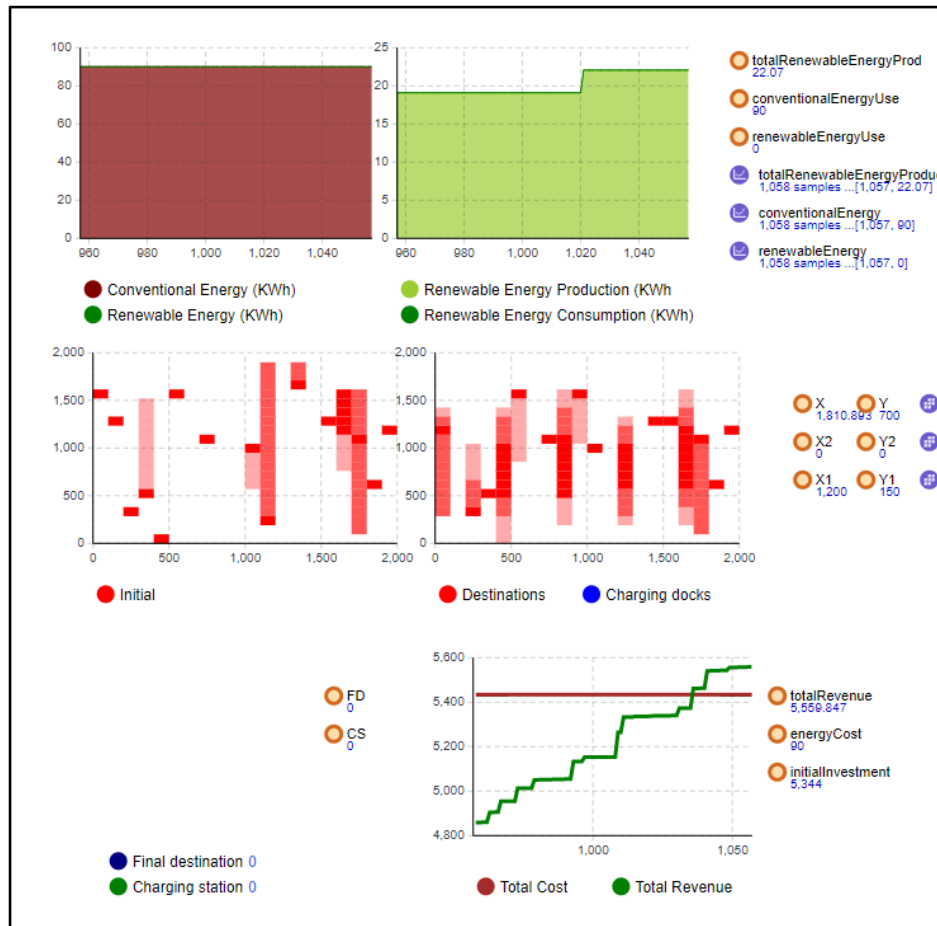


Figure 41: Reference variables under zero resources scenario

### High-Density Scenario

To test the model's capacity to handle high demand, the number of scooters increased from 200 to 500, and the maximum X and Y coordinates were extended from 2000 to 4000 meters each. Simultaneously, pedestrian entry rates were increased to simulate peak usage during the entire simulation (10 agents per second). During the simulation there was a backup of agents in different processes, particularly during matching and charging, indicating potential areas for optimization in agent interactions and resource allocation.

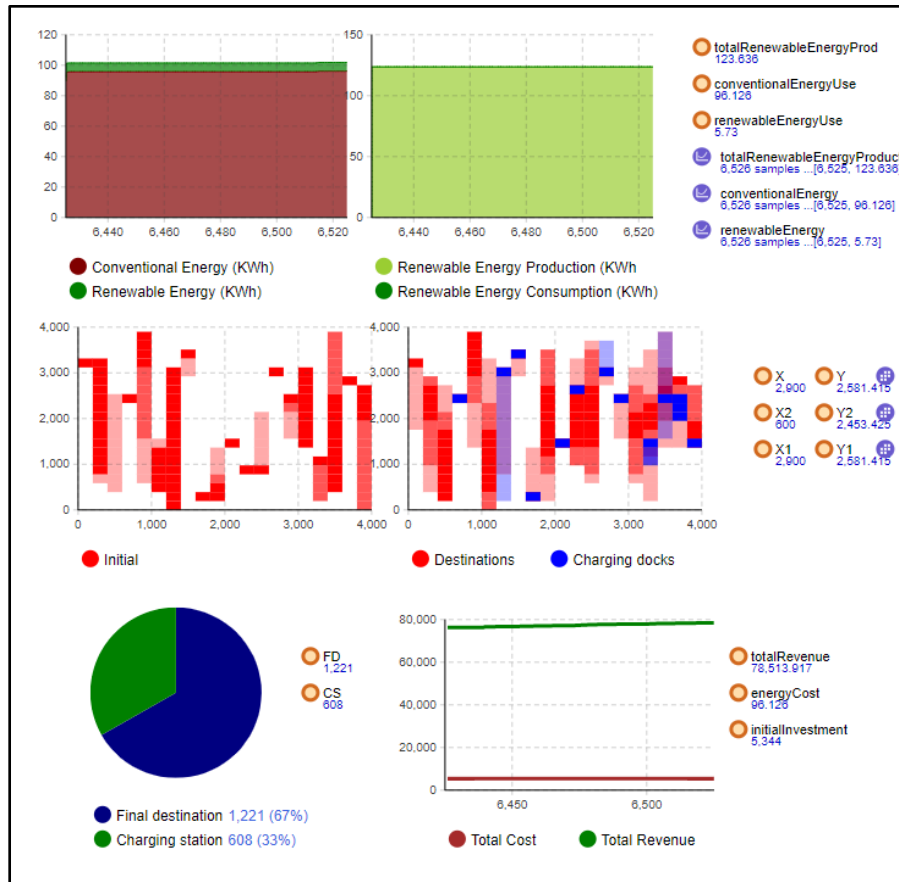


Figure 42: Reference variables under high density scenario

### Limited Resources with High Entry Rates

In this scenario, the number of scooters was reduced from 500 to 50, and only one solar-powered charging station with a single dock was introduced. Pedestrian entry rates were set to 10 agents per second, and no discounts were provided. The model experienced backups, especially in processing charging events, as the demand for the single charging dock far exceeded its capacity. This scenario highlighted the need to scale resources appropriately to maintain system efficiency.

### Balanced Scenario with Incentives

A final test involved implementing discounts for pedestrians who deviated from their route to leave scooters at solar-powered charging stations. The number of scooters was set at 200, with 10 charging stations, each equipped with 5 docks. Pedestrian entry rates were set to the custom distribution discussed earlier, and a 10% discount was introduced. The system demonstrated smooth operation with no back up of agents, with an increase in charging events and balanced utilization of charging stations. This test confirmed that strategic use of incentives can significantly enhance system performance.

Following the successful completion of the stress tests, the following key insights were obtained:

- In the stress test, the maximum entry rates were identified. By working backward using the custom distribution designed for this simulation, the population size that would generate such demand for scooters was calculated. Dividing this population by the number of scooters in the simulation, it

was found that the optimal scooter-to-pedestrian ratio ranges from 1:2 to 1:3. This balance ensures efficient resource utilization while preventing overcrowding. Nevertheless, since this thesis evaluates the economic aspect of the solution, underuse was also to be avoided, since having a surplus of scooters would incur a higher overall cost.

- Due to computational limitations, the model can support a maximum of approximately 50 solar-powered charging docks. Consequently, the simulation will be constrained to a map size of 3000 m x 3000 m to maintain performance and scalability.
- Within this defined scope, all other parameters will be systematically varied during the experimentation phase to further refine the model's performance and outcomes.

## 7. Verification & Validation: Number of Runs

In accordance with the literature (Law, 2006), to validate the simulation model and determine the appropriate number of runs ( $N$ ) required for statistical significance, a well-established iterative process was employed in this simulation. This process involves defining a baseline case and ensuring that the precision of the Half-Width (HW) of the confidence intervals for each selected variable falls below the desired threshold (HW0) at a 95% confidence level ( $\alpha = 0.05$ ). Initially, an arbitrary number of runs ( $N_0$ ) is conducted to collect reference variables and calculate sample statistics. If the resulting Half-Width (HW) exceeds the predefined HW0, indicating a greater spread in the data than is tolerable, the number of runs is increased, and the process is repeated.

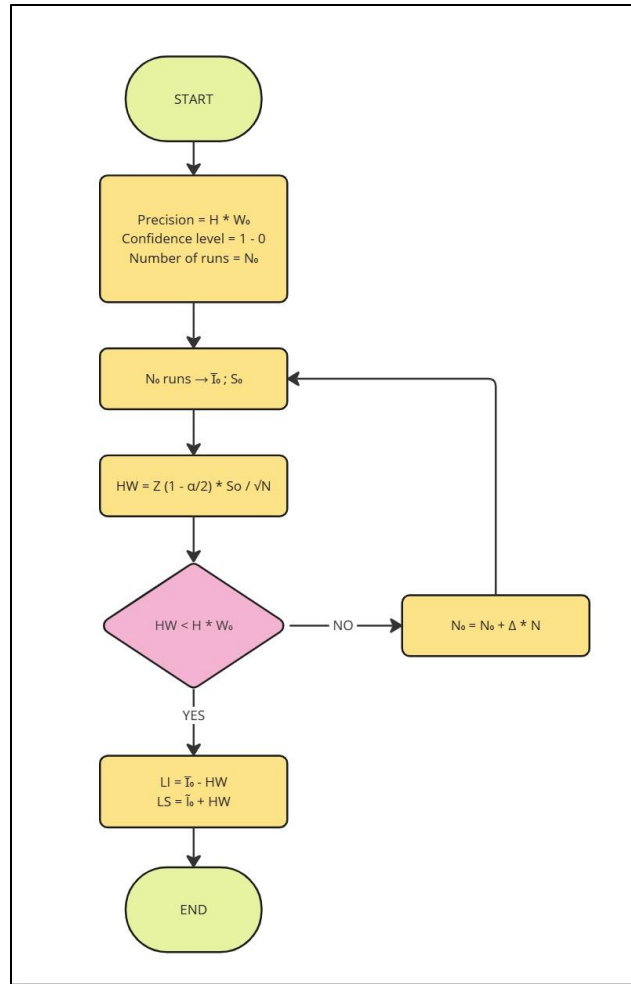


Figure 43: Methodology for validating the number of simulation runs

For this thesis, the key variables energy consumption/production (conventional and renewable), and financial performance metrics (total revenue, cost) were analyzed to validate the model. The baseline was established with 50 iterations per scenario. Using the same averages and standard deviations obtained from these runs, the Half-Widths (HW1) were calculated and compared against the predefined thresholds (HW0) to assess the precision of the results. The comparison highlights whether the variability in the simulation outputs falls within acceptable limits for statistical significance. The results of this analysis are presented in Figure 44.

Variable	Conventional Energy	Renewable Energ	FD	CS	Total Revenue	Total Cost
N	50	50	50	50	50	50
Average	108.3627958	32.21219325	54031.1	965.5	1179196.359	5452.362796
Standard deviation	20.06718804	26.13101632	3456.052883	278.3954921	182049.5247	20.06718804
HW0	10.23857019	13.33242327	1763.328274	142.0414152	92884.30615	10.23857019
Alpha	0.05	0.05	0.05	0.05	0.05	0.05
Z	1.95996	1.95996	1.95996	1.95996	1.95996	1.95996
HW1	5.562227221	7.243000366	957.9494341	77.16571855	50460.52391	5.562227221
Check	TRUE	TRUE	TRUE	TRUE	TRUE	TRUE

Figure 44: Results from the verification runs

As observed, the results confirm that 50 iterations per scenario are sufficient to achieve robust statistical results, meeting the significance level of  $\alpha = 0.05$ . This verification provides the assurance needed to proceed confidently with the experimentation process.

## 8. Experimentation Process

The following section examines the experimentation process undertaken to derive meaningful conclusions for this thesis. The discussion includes an analysis of the alternatives considered, the setup of the experimental framework, the determination of parameter ranges, the simulation duration, the warm-up period, and the methodology employed to extract results from the AnyLogic model for statistical analysis. Additionally, it is important to highlight the nomenclature utilized in this section. A single simulation run can consist of multiple iterations conducted with identical parameters. For example, running 50 iterations under the same parameter settings constitutes one simulation run.

### 8.1 Analyzed Alternatives

As discussed in the stress test and outlined in the flowchart (Figure 45), the baseline scenario for this study represents the case in which no solar-powered charging stations are utilized. This scenario reflects the current operational state of electric scooter rental services at the time of writing and serves as a critical reference point. All subsequent improvements or changes introduced in the model will be benchmarked against this baseline, enabling a clear evaluation of the impact of implementing solar-powered charging stations.

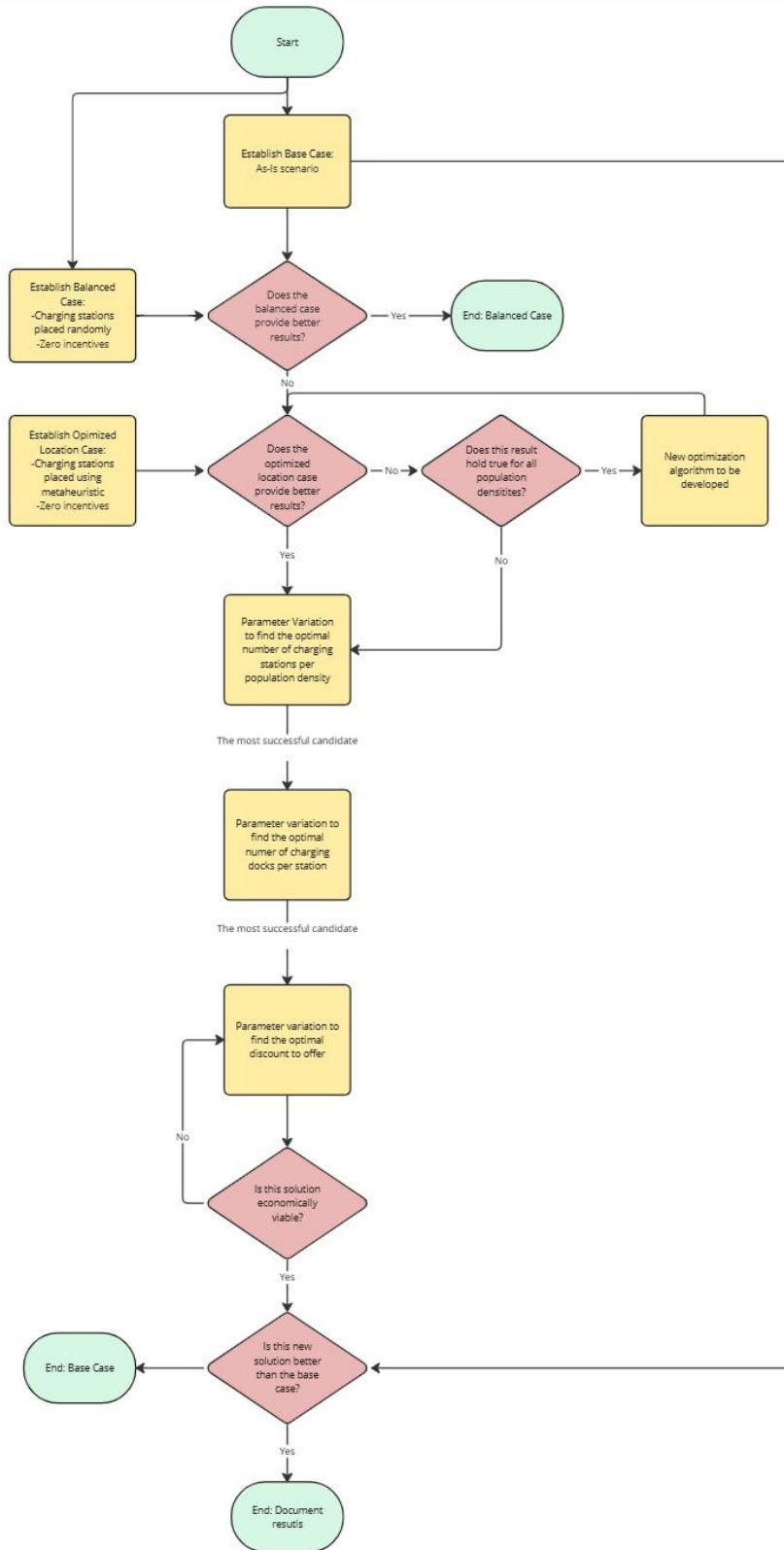


Figure 45: Flowchart of alternatives analyzed

The next step involves introducing charging stations placed randomly to assess whether users would naturally utilize these locations. If random placement proves insufficient to incentivize usage, the study will proceed with optimizing placement strategies. Once optimized, the placement method will be tested across various scenarios, including varying population densities, determining the optimal number of charging stations, and evaluating the necessity of discounts to encourage usage with the objective of optimizing the implementation strategy. To maintain the integrity of the analysis, a final comparison between the most optimized scenario and the baseline will be conducted and revisited in the results section.

In Figure 45, "better" results refer to implementing a solution whose reference variables either increase charging station utilization/ renewable energy consumption, reduce conventional energy consumption, or lowers costs. A result can only be considered "better" if at least one reference variable shows statistically significant improvement without compromising another. This ensures that one solution can be objectively classified as strictly superior to another.

### **1. Zero resource case vs. Solar-powered charging station without incentive case**

To achieve the baseline case within the AnyLogic model, a boolean variable was used to ensure that all agents select the top route in the "*finalDestination*" logic gate. This configuration forces the utility-based decision-making process, compelling all agents to travel directly to their final destination on a scooter.

This mechanism effectively recreates the base case behavior, allowing accurate reference data collection by suppressing other variables.

The baseline is then compared against a balanced scenario, where solar powered charging stations are placed randomly on the map and no incentives are provided to pedestrians for deviating from their original route to the solar powered charging stations. This comparison assesses whether the solar-powered charging stations would be utilized in the absence of incentives, or if they would be redundant. It is hypothesized that the two models should behave similarly given the structure of the utility function. If agents incur a "cost" for getting off the scooter before arriving at their final destination and having to walk, then their behaviour should be in favor of traveling to the final destination rendering both results statistically indifferentiable.

### **2. Solar-powered charging station allocation: Random vs Metaheuristic**

A very important aspect of the model is to evaluate where to place the solar powered charging stations. Two placing methods have been developed, the control case will be to randomly assign the charging stations across the map. The second will use a custom metaheuristic based on the Ant Colony Metaheuristic

The hypothesis is that optimally placed charging stations will encourage increased utilization, thereby amplifying all metrics associated with higher charging station usage.

### **3. Number of solar-powered charging stations versus population density**

Once the allocation of the charging stations is defined, the objective is to identify the optimal number of solar-powered charging stations required for specific population densities. The process will include testing various ranges of population densities versus varying numbers of charging stations simultaneously in what is called a parameter variation. This process allowed for insights into their trends and correlation. It is hypothesized that the required number of charging stations will increase as population density decreases.

In less dense populations, agents are more likely to experience big deviations on their routes, requiring a higher number of strategically placed charging stations. In this case, a one-way ANOVA test will be conducted to determine whether there are statistically significant differences among the means. Furthermore, the Tukey method will be employed to perform the comparisons and assess which specific groups differ significantly from each other.

The parameters "maxX" and "maxY" were varied to manipulate the population density within the simulation. The parameter range was set from a minimum of 1000m to a maximum of 3000m, with increments of 1000m. Given a fixed population, the different city areas gave way to the following densities being tested: 33, 50 and 100 people/ $Km^2$ . Similarly, the number of charging stations was adjusted, ranging from a minimum of 6 to a maximum of 15, with increments of 3. This setup resulted in a total of 600 iterations, enabling a comprehensive analysis of the interaction between population density and the number of charging stations.

#### **4. Optimal number of docks per solar-powered charging stations**

Following the previous comparisons, the most successful candidate from each iteration will be selected to evaluate the optimal number of charging docks required at each charging station. It is hypothesized that as the total number of charging stations decreases, the demand for charging docks at each individual station will increase. This experiment aims to provide valuable insights into the balance required between the number of charging stations and docks for a given population density. Specifically, it will help identify thresholds where the number of docks becomes insufficient or excessive, enabling the determination of an optimal configuration. As previously discussed both parameters will be varied simultaneously in a parameter variation.

#### **5. Optimal discount to offer in order to maximize the solution**

Lastly, once the configuration of the charging stations is optimized in terms of placement, number of stations, and number of docks, the next step involves determining the optimal discount to offer. This discount will aim to maximize revenue while minimizing total costs. The strategy is to set the discount at a level not exceeding the cost savings achieved from reduced conventional energy consumption. Any remaining financial surplus will contribute toward recovering the initial investment required for the project. This final analysis is critical in assessing the economic and sustainability viability of the proposed solution.

To ensure meaningful and valid comparisons between the various alternatives, several preparatory steps and assumptions must be addressed:

1. Iterative Process in Simulation Runs:

Each scenario undergoes a series of simulation runs, with each run comprising 50 iterations . Iterations introduce stochastic variability, allowing the model to account for randomness inherent in the system. A single simulation run aggregates the results of these iterations and all this data is then exported into an excel file for further analysis.

2. Graphical Analysis:

Visual tools such as boxplots or histograms are used to illustrate the distribution of results across scenarios. These plots help identify outliers, assess variance, and provide a clear visual comparison of performance metrics.

3. Since this thesis aims to compare between different scenarios to measure the effectiveness of the solutions to implement, statistical methodologies will be utilized. However, for these methodologies to be valid, it is necessary to assume the following conditions and test them:
  - a. Normal Distribution: It is necessary to verify that the data for each scenario follows a normal distribution using graphical methods (e.g., histograms or Q-Q plots) or statistical tests like the Kolmogorov-Smirnov test.
  - b. Equality of Variances: Tests such as Fisher's F-test will be conducted to determine whether the variances between groups differ significantly. It is important to note that the F-test requires the data to follow a normal distribution, meaning the data must have successfully passed the normality test beforehand. If the variances are found to be unequal, alternative methods, such as Welch's t-test, will be used.
  - c. Independence of Observations: Ensure that each observation within a group is independent. This is critical to prevent biased results that could arise from dependent data points. However, given that this is a simulation, and no runs can impact one another this third assumption can be taken as valid.
4. Hypothesis Testing:

To determine whether the differences between scenarios are statistically significant, hypothesis testing is employed. The null hypothesis ( $H_0$ ) assumes no difference in means between scenarios (e.g.,  $H_0 = \mu_A - \mu_B = 0$ ). The alternative hypothesis ( $H_1$ ) states that a difference exists ( $H_1 = \mu_A - \mu_B \neq 0$ ). Depending on the data characteristics, a t-test (for two scenarios) or ANOVA (for multiple scenarios) is used.
5. Confidence Intervals:

Confidence intervals (CIs) are calculated to quantify the range within which the true difference in means is likely to lie. This provides additional insight into the magnitude and direction of observed differences. For example, if a CI does not contain zero, it indicates a statistically significant difference between groups.
6. Contextualization and Review:

The results are interpreted with respect to the research objectives, identifying which scenarios outperform others and under what conditions. The logical structure and decision-making flow for scenario comparisons are detailed in Figure 45.

## 8.2 Experimentation Procedure

To conduct the experiments using the constructed Any Logic model this thesis used the parameter variation tool provided by the software. This tool enables systematic experimentation by varying model parameters across specified ranges. It works by running multiple simulation iterations, each with a fixed and unique combination of parameter values and will begin to vary in between simulation runs based on predefined intervals or steps. For each iteration, the model records outputs and performance metrics. This tool is particularly useful for sensitivity analysis, optimization, and understanding the impact of parameter changes on the system's behavior.

The parameter variation tool is programmed as follows: a parameter variation experiment is created in which all reference variables to be measured are specified, along with corresponding collections to store the results of each iteration. During the simulation, the specified parameters systematically vary, and the same setup is applied to decision variables, ensuring they are tracked and stored in dedicated collections. Once all iterations are completed, the results stored in the collections are printed into an Excel file. In Figure 46, the interface of the parameter variation, the reference variables, the corresponding collections and the decision variables to be varied in the panel are visualized.

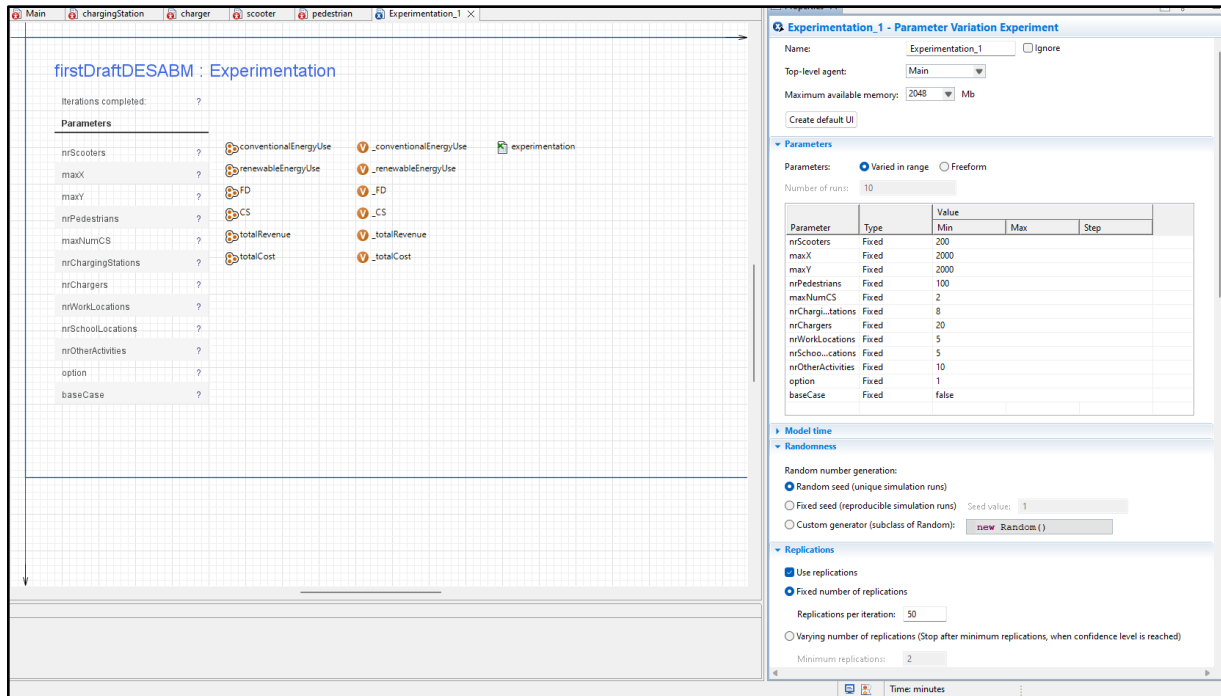


Figure 46: Parameter variation interface

Diving deeper into the implementation process, the first step is configuring the decision parameters to be varied in the experiment, including defining their range and step size. The second step sets the model runtime, which will be discussed in the following section. The third step is executing the simulation, which involves setting the number of iterations to 50 and defining the actions to be performed after each simulation run and upon completing the experiment. Once an iteration concludes, the code extracts the main reference variables from the system and stores them in a designated collection. After the experiment, the model prints the results and exports them to an Excel file, with each alternative analyzed saved on a separate sheet. This concludes with the experimentation output, now the data is ready to be analyzed.

```

After simulation run:
//Decision Variables
_populationDensity = root.nrPedestrians/((root.maxX/1000)*(root.maxY/1000));
_maxNumCS = root.maxNumCS;
_nrChargingStations = root.nrChargingStations;
_option = root.option;
_baseCase = root.baseCase;
_discount = root.discount;
//Reference Variables
_conventionalEnergyUse = root.conventionalEnergyUse;
_renewableEnergyUse = root.renewableEnergyUse;
_FD = root.FD;
_CS = root.CS;
_totalRevenue = root.totalRevenue;
_totalCost = root.energyCost + root.initialInvestment;
//add to collections
populationDensity.add(_populationDensity);
maxNumCS.add(_maxNumCS);
nrChargingStationsc.add(_nrChargingStations);
optionc.add(_option);
baseCasec.add(_baseCase);
discountc.add(_discount);
conventionalEnergyUse.add(_conventionalEnergyUse);
renewableEnergyUse.add(_renewableEnergyUse);
FD.add(_FD);
CS.add(_CS);
totalRevenue.add(_totalRevenue);

After iteration:

After experiment:
//Print collections into "experimentation" excel file
for(int i=0; i<conventionalEnergyUse.size();i++){
    experimentation.setCellValue(populationDensity.get(i),1,i+2,1);
    experimentation.setCellValue(maxNumCS.get(i),1,i+2,2);
    experimentation.setCellValue(nrChargingStationsc.get(i),1,i+2,3);
    experimentation.setCellValue(optionc.get(i),1,i+2,4);
    experimentation.setCellValue(baseCasec.get(i),1,i+2,5);
    experimentation.setCellValue(discountc.get(i),1,i+2,6);
    experimentation.setCellValue(conventionalEnergyUse.get(i),1,i+2,8);
    experimentation.setCellValue(renewableEnergyUse.get(i),1,i+2,9);
    experimentation.setCellValue(FD.get(i),1,i+2,10);
    experimentation.setCellValue(CS.get(i),1,i+2,11);
    experimentation.setCellValue(totalRevenue.get(i),1,i+2,12);
    experimentation.setCellValue(totalCost.get(i),1,i+2,13);
}

```

Figure 47: Parameter variation java actions

### 8.3 Experiment Conditions

Most simulation projects can be divided into two distinct phases: the transition period and the stationary period (Banks, 1998). The transition period occurs at the beginning of the simulation run, characterized by the system adjusting from an initial state to a steady operational flow. In the context of this project, this phase begins with agents entering the system for the first time, and scooters being evenly distributed across the map. During this period, the system dynamics have not yet stabilized, and the data generated does not reflect the typical behavior aimed at evaluating. (Banks, 1998)

To address this issue, a warmup period is implemented at the beginning of the simulation. During this period, the model allows the agents to interact and adjust within the system without recording any data. This ensures that transitory effects, such as agents finding their initial positions and scooters dispersing naturally, do not influence the results. The system is essentially given time to settle into a stationary regime, where the behavior and metrics observed are stable and representative of normal operation.

Empirical observation revealed that the system typically enters a stationary state within 3-4 days under regular conditions. However, in scenarios with lower population densities, the transition period can extend to 6-7 days as agents require more time to interact and stabilize within the system. To account for these

variations and ensure an unbiased experiment, the warmup period was set to 7 days. This duration guarantees that all possible cases, regardless of population density, are adequately covered before data collection begins. Furthermore, the choice of a 7-day warmup period aligns with the cyclic nature of agent behavior, as the number and distribution of agents throughout the simulation is repeated on a weekly basis.

Due to computational constraints, the simulation model cannot be run for extended periods. Given the available computational capacity at the time of writing, the duration of each simulation run was limited to six months. To avoid biases on the period of the year analyzed the simulation will begin to run at a random date throughout the year. While this timeframe may not fully capture the long-term outcomes of the model (considering the projection period for solar-powered charging stations is typically several years) it is expected to provide enough insights to analyze agent behavior, as well as to estimate short-term environmental and economic benefits, potentially inferring on their long-term development. This includes insights into emission reductions and cost savings that the company might achieve. Refer to the appendix section A.0 for the information about the computer used to run the simulations in this thesis.

With the experimentation fully built, the scenarios outlined, and the AnyLogic model validated, the next step involves executing the simulations and analyzing the results.

## 9. Results

This section presents a statistical analysis of various scenarios to derive concrete insights. Not all reference variables will be analyzed in every experiment, as their relevance depends on the specific conditions being evaluated. For example, comparing renewable energy usage between a scenario with no charging stations and one with charging stations would not yield meaningful insights. Instead, reference variables will be selectively applied to ensure a focused and relevant analysis. However, each experiment consistently assesses three key macro areas: pedestrian behavior, energy usage, and economic viability.

### 9.1 Analysis of Results

#### 9.1.1 Zero resource case vs. Solar-powered charging station without incentive case

The simulation was conducted for two scenarios: the zero resource case and the scenario with solar-powered charging stations allocated randomly and without incentives. The initial step involved graphically plotting the results of both alternatives to qualitatively derive preliminary insights.

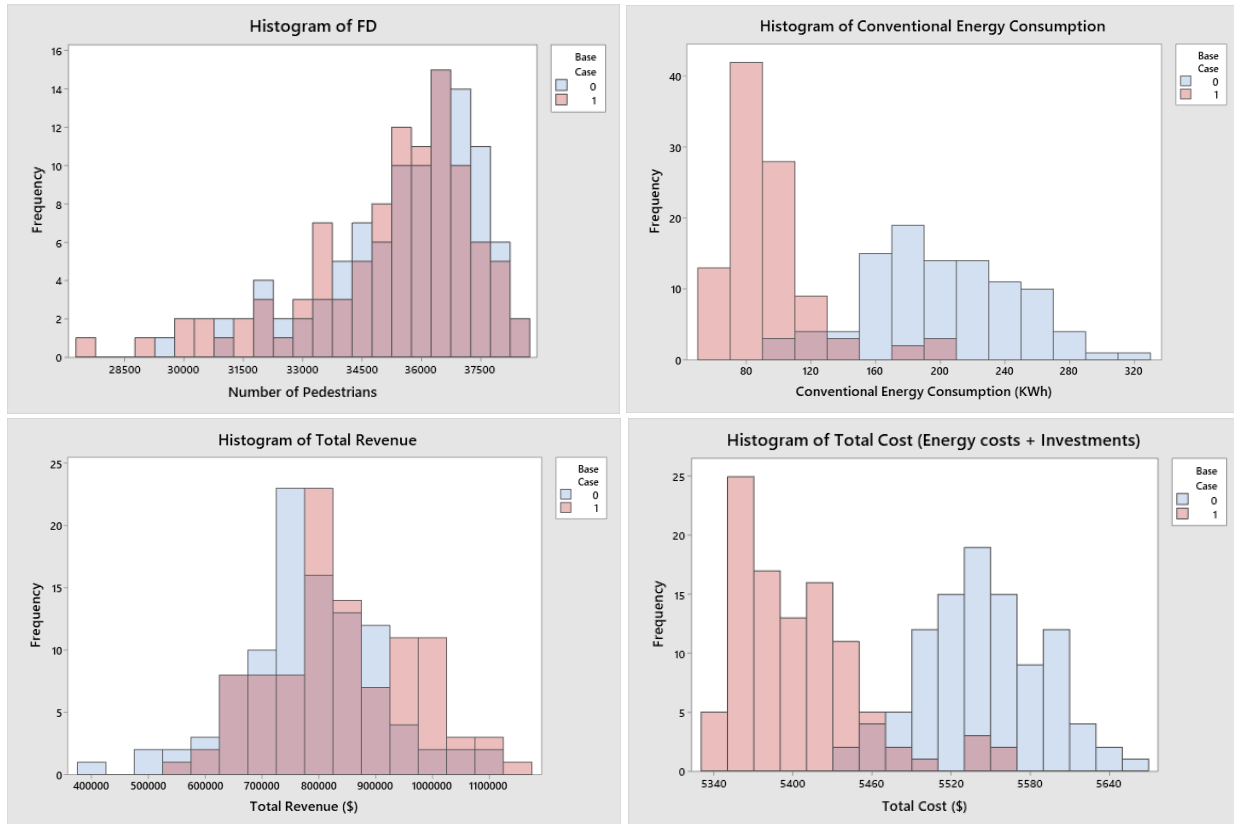


Figure 48: Histogram of reference variables in experiment - zero resource case corresponds to when the variable `baseCase` is set to 0, while the scenario with solar-powered charging stations is represented when `baseCase` is set to 1.

As in Figure 47, the insertion of solar-powered charging stations has a limited impact on the number of pedestrians who choose to deviate from their final destination to visit the charging stations. This aligns with our initial hypothesis, as the structure of the utility function imposes a cost on deviating from the intended destination. However, some pedestrians do choose to travel to the charging stations. A closer analysis of individual iterations reveals that this occurs primarily when the charging stations are conveniently located at their final destination, thereby eliminating the need for significant detours.

These pedestrians, who choose to visit the charging stations, have a notable effect on other reference variables. For instance, the total energy consumed and total cost exhibit significant reductions, shifting these metrics to the left. Additionally, a slight increase in total revenues is observed.

To analyze if the results of this test are statistically significant the following hypothesis are defined:

$H_0$  = There is no significant difference between the base case and the random solar charger case for the reference variables being tested.

$H_1$  = There is a significant difference between the two cases.

The next step involves verifying the assumptions of normality and equal variance for all reference variables analyzed. The assumption of normality was satisfied for all four variables, as confirmed by the results of the Kolmogorov-Smirnov test.

Following the normality test, the analysis proceeded to evaluate the equality of variances. This assumption held true for all variables except for conventional energy usage, which, as shown in the histogram, exhibited a smaller variance compared to the base case. In this case, Welch's t-test will be employed to account for unequal variances and to determine whether there is a statistically significant difference. For the detailed analysis refer to the appendix section 9.1.1.

Once the assumptions are validated the specific hypothesis are stated: taking the mean of the base case ( $\mu_B$ ) and the mean of the Solar charging stations case ( $\mu_S$ );

$$H_0 \Rightarrow \mu_B = \mu_S \qquad H_1 \Rightarrow \mu_B \neq \mu_S$$

The data is then entered into the Minitab software and the two sample t-tests are run.

### 9.1.1.1 Pedestrian behaviour

<p><b>Method</b></p> <p><math>\mu_1</math>: mean of FD_2 when Base Case = 0  <math>\mu_2</math>: mean of FD_2 when Base Case = 1          Difference: <math>\mu_1 - \mu_2</math></p> <p><i>Equal variances are assumed for this analysis.</i></p>	<p><b>Estimation for Difference</b></p> <p><b>Pooled 95% CI for</b></p> <table border="1"> <thead> <tr> <th>Difference</th> <th>StDev</th> <th>Difference</th> </tr> </thead> <tbody> <tr> <td>556</td> <td>2015</td> <td>(-6, 1118)</td> </tr> </tbody> </table>	Difference	StDev	Difference	556	2015	(-6, 1118)	<p><b>Test</b></p> <p>Null hypothesis <math>H_0: \mu_1 - \mu_2 = 0</math>          Alternative hypothesis <math>H_1: \mu_1 - \mu_2 \neq 0</math></p> <table border="1"> <thead> <tr> <th>T-Value</th> <th>DF</th> <th>P-Value</th> </tr> </thead> <tbody> <tr> <td>1.95</td> <td>198</td> <td>0.052</td> </tr> </tbody> </table>	T-Value	DF	P-Value	1.95	198	0.052
Difference	StDev	Difference												
556	2015	(-6, 1118)												
T-Value	DF	P-Value												
1.95	198	0.052												

Figure 49: Two sample t-test for Pedestrians traveling to final destination

For pedestrians traveling to their final destination, the two-sample t-test returned a p-value of 0.052, which is slightly above the common significance threshold of 0.05. This indicates that there is just insufficient statistical evidence to reject the null hypothesis and concludes that there is a significant difference between the mean of the two samples. Additionally, the fact that 0 is included in the 95% confidence interval for the difference suggests that the true difference in mean could be zero. This outcome implies that any observed difference may be due to the charging stations being placed exactly at their final destination and not necessarily due to higher utility.

### 9.1.1.2 Conventional and Renewable Energy Consumption

<p><b>Method</b></p> <p><math>\mu_1</math>: mean of Conventional Energy_2 when Base Case = 0  <math>\mu_2</math>: mean of Conventional Energy_2 when Base Case = 1          Difference: <math>\mu_1 - \mu_2</math></p> <p><i>Equal variances are not assumed for this analysis.</i></p>	<p><b>Estimation for Difference</b></p> <p><b>95% CI for</b></p> <table border="1"> <thead> <tr> <th>Difference</th> <th>Difference</th> </tr> </thead> <tbody> <tr> <td>106.06</td> <td>(95.33, 116.80)</td> </tr> </tbody> </table>	Difference	Difference	106.06	(95.33, 116.80)	<p><b>Test</b></p> <p>Null hypothesis <math>H_0: \mu_1 - \mu_2 = 0</math>          Alternative hypothesis <math>H_1: \mu_1 - \mu_2 \neq 0</math></p> <table border="1"> <thead> <tr> <th>T-Value</th> <th>DF</th> <th>P-Value</th> </tr> </thead> <tbody> <tr> <td>19.50</td> <td>171</td> <td>0.000</td> </tr> </tbody> </table>	T-Value	DF	P-Value	19.50	171	0.000
Difference	Difference											
106.06	(95.33, 116.80)											
T-Value	DF	P-Value										
19.50	171	0.000										

Figure 50: Welch's t-test for Conventional Energy Usage

For conventional energy use, Welch's t-test returned a p-value of 0, indicating strong statistical evidence to reject the null hypothesis. This result suggests that there is a significant difference between the means of the two samples. Furthermore, since the 95% confidence interval for the difference does not contain 0, it confirms that the observed difference is both statistically significant and meaningful. This finding implies that the introduction of solar-powered charging stations has a measurable impact on conventional energy usage, which correlates with what could be observed in the histograms, since there are some pedestrians who use the charging stations, conventional energy use logically decreases.

Renewable energy usage is not analyzed as for the case in which no solar panels are introduced the amount of renewable energy used is always zero.

### 9.1.1.3 Economic viability

#### Method

$\mu_1$ : mean of Total Cost\_2 when Base Case = 0  
 $\mu_2$ : mean of Total Cost\_2 when Base Case = 1  
 Difference:  $\mu_1 - \mu_2$

*Equal variances are assumed for this analysis.*

#### Estimation for Difference

	Pooled	95% CI for
Difference	StDev	Difference
	139.66	46.48 (126.70, 152.63)

#### Test

Null hypothesis	$H_0: \mu_1 - \mu_2 = 0$
Alternative hypothesis	$H_1: \mu_1 - \mu_2 \neq 0$
T-Value	DF P-Value
21.25	198 0.000

#### Method

$\mu_1$ : mean of Total Revenue\_2 when Base Case = 0  
 $\mu_2$ : mean of Total Revenue\_2 when Base Case = 1  
 Difference:  $\mu_1 - \mu_2$

*Equal variances are assumed for this analysis.*

#### Estimation for Difference

	Pooled	95% CI for
Difference	StDev	Difference
	-57175	126368 (-92417, -21933)

#### Test

Null hypothesis	$H_0: \mu_1 - \mu_2 = 0$
Alternative hypothesis	$H_1: \mu_1 - \mu_2 \neq 0$
T-Value	DF P-Value
-3.20	198 0.002

Figure 51: Two sample t-test for total cost and revenue

For total revenues and total costs, the two-sample t-tests returned p-values less than 0.05, providing statistical evidence to reject the null hypothesis. Additionally, the 95% confidence intervals for the differences do not include 0, confirming that the observed differences are both statistically significant and meaningful. These results are expected, as a reduction in conventional energy usage directly impacts costs, leading to changes in total revenues.

After analyzing the data obtained in this experiment, we can conclude that while the implementation of solar-powered charging stations does influence the overall behavior of the system and the financial metrics, there is no statistically significant evidence to suggest that users would consistently utilize these stations unless they are located directly at their final destination. Based on these findings, the next step is to compare the random allocation of charging stations with an optimized placement strategy using the ant colony metaheuristic discussed in Section 8.1.

## 9.1.2 Solar-powered charging station allocation: Random vs Metaheuristic

The simulation was conducted for two scenarios: one with randomly allocated solar-powered charging stations and another with charging stations allocated using the metaheuristic. The initial step involved graphically plotting the results of both alternatives to qualitatively derive preliminary insights.

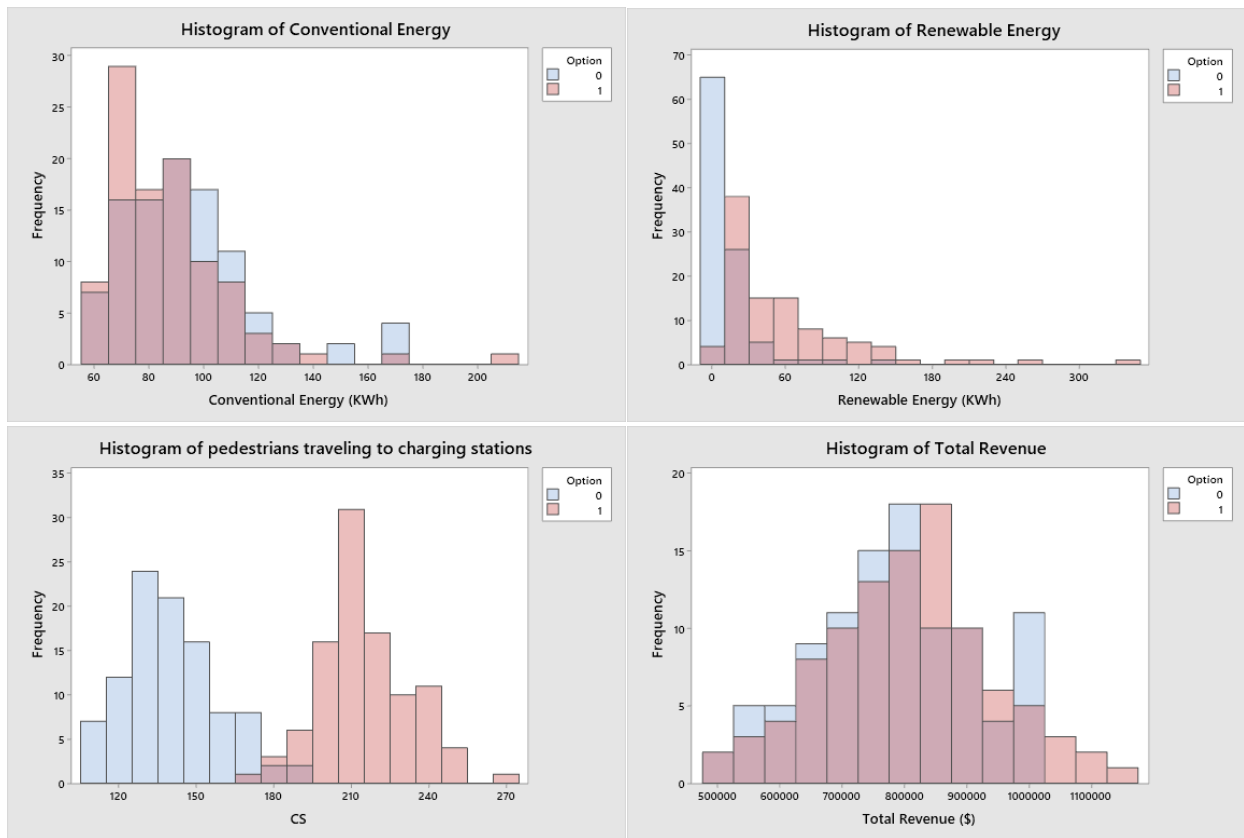


Figure 52: Histogram of reference variables in experiment 2 - the scenario with random allocation corresponds to when the variable “option” is set to 0, while the scenario with metaheuristic-based allocation is represented with a 1.

As observed in Figure 51, there is a notable improvement in the number of pedestrians traveling to their final destination under the optimized placement scenario. This suggests that strategically positioned solar-powered charging stations align better with pedestrian travel patterns, effectively incentivizing their use. The histograms reveal there is an increase in renewable energy consumption, possibly demonstrating the effectiveness of optimized charging station placement. The shift in energy usage is further reflected in the associated revenues, however it does not seem too pronounced, meaning further statistical analysis is required. With the increased reliance on solar energy, revenues display an upward trend, as evidenced by the positive shift in the revenue histogram.

With the implementation of the placement metaheuristic, the objective is to determine whether the number of pedestrians deviating from their final destination increases. Following this analysis, the goal is to evaluate whether such deviations translate into measurable economic benefits for the system.

Following the methodology already established to analyze if the results of this test are statistically significant the following hypothesis are defined:

$H_0$  = There is no significant difference between the random allocation case and the optimized allocation case for the reference variables being tested.

$H_1 =$  There is a significant difference between the two cases.

The next step involves verifying the assumptions of normality and equal variance for the reference variables analyzed. The assumption of normality was satisfied for both variables, as confirmed by the results of the Kolmogorov-Smirnov test.

Following the normality test, the analysis proceeded to evaluate the equality of variances. This assumption held true for all variables. For the detailed analysis refer to the appendix section 9.1.2.

Once the assumptions are validated the specific hypothesis are stated: taking the mean of the random allocation case ( $\mu_S$ ) and the mean of the optimized allocation case ( $\mu_{S'}$ );

$$H_0 \Rightarrow \mu_S = \mu_{S'} \quad H_1 \Rightarrow \mu_S \neq \mu_{S'}$$

The data is then entered into the Minitab software and the two sample t-tests are run.

### 9.1.2.1 Pedestrians behaviour

Method	Estimation for Difference	Test																	
$\mu_1$ : mean of CS when Option = 0 $\mu_2$ : mean of CS when Option = 1 Difference: $\mu_1 - \mu_2$ <i>Equal variances are assumed for this analysis.</i>	<table border="1"> <thead> <tr> <th></th> <th>Pooled</th> <th>95% CI for</th> </tr> <tr> <th>Difference</th> <th>StDev</th> <th>Difference</th> </tr> </thead> <tbody> <tr> <td>-74.27</td> <td>17.64</td> <td>(-79.19, -69.35)</td> </tr> </tbody> </table>		Pooled	95% CI for	Difference	StDev	Difference	-74.27	17.64	(-79.19, -69.35)	<table border="1"> <thead> <tr> <th>Null hypothesis</th> <th><math>H_0: \mu_1 - \mu_2 = 0</math></th> </tr> <tr> <th>Alternative hypothesis</th> <th><math>H_1: \mu_1 - \mu_2 \neq 0</math></th> </tr> <tr> <th>T-Value</th> <th>DF P-Value</th> </tr> </thead> <tbody> <tr> <td>-29.77</td> <td>198 0.000</td> </tr> </tbody> </table>	Null hypothesis	$H_0: \mu_1 - \mu_2 = 0$	Alternative hypothesis	$H_1: \mu_1 - \mu_2 \neq 0$	T-Value	DF P-Value	-29.77	198 0.000
	Pooled	95% CI for																	
Difference	StDev	Difference																	
-74.27	17.64	(-79.19, -69.35)																	
Null hypothesis	$H_0: \mu_1 - \mu_2 = 0$																		
Alternative hypothesis	$H_1: \mu_1 - \mu_2 \neq 0$																		
T-Value	DF P-Value																		
-29.77	198 0.000																		

Figure 53: Two sample t-test for Pedestrians traveling to charging stations

For pedestrians traveling to the charging stations, the two-sample t-test returned a p-value of 0, indicating robust statistical evidence to reject the null hypothesis and conclude that there is a significant difference between the means of the two samples. Additionally, the fact that 0 is not included in the 95% confidence interval for the difference further confirms that the observed increase is statistically significant. This outcome strongly suggests that optimizing the placement of charging stations has a measurable and positive impact on the efficiency of the solution, as it effectively incentivizes more pedestrians to utilize the charging stations.

### 9.1.2.2 Conventional and Renewable Energy Consumption

Method	Estimation for Difference	Test																	
$\mu_1$ : mean of Conventional Energy when Option = 0 $\mu_2$ : mean of Conventional Energy when Option = 1 Difference: $\mu_1 - \mu_2$ <i>Equal variances are assumed for this analysis.</i>	<table border="1"> <thead> <tr> <th></th> <th>Pooled</th> <th>95% CI for</th> </tr> <tr> <th>Difference</th> <th>StDev</th> <th>Difference</th> </tr> </thead> <tbody> <tr> <td>6.53</td> <td>23.49</td> <td>(-0.02, 13.08)</td> </tr> </tbody> </table>		Pooled	95% CI for	Difference	StDev	Difference	6.53	23.49	(-0.02, 13.08)	<table border="1"> <thead> <tr> <th>Null hypothesis</th> <th><math>H_0: \mu_1 - \mu_2 = 0</math></th> </tr> <tr> <th>Alternative hypothesis</th> <th><math>H_1: \mu_1 - \mu_2 \neq 0</math></th> </tr> <tr> <th>T-Value</th> <th>DF P-Value</th> </tr> </thead> <tbody> <tr> <td>1.96</td> <td>198 0.051</td> </tr> </tbody> </table>	Null hypothesis	$H_0: \mu_1 - \mu_2 = 0$	Alternative hypothesis	$H_1: \mu_1 - \mu_2 \neq 0$	T-Value	DF P-Value	1.96	198 0.051
	Pooled	95% CI for																	
Difference	StDev	Difference																	
6.53	23.49	(-0.02, 13.08)																	
Null hypothesis	$H_0: \mu_1 - \mu_2 = 0$																		
Alternative hypothesis	$H_1: \mu_1 - \mu_2 \neq 0$																		
T-Value	DF P-Value																		
1.96	198 0.051																		

### Method

$\mu_1$ : mean of Renewable Energy when Option = 0  
 $\mu_2$ : mean of Renewable Energy when Option = 1  
Difference:  $\mu_1 - \mu_2$

Equal variances are assumed for this analysis.

### Estimation for Difference

	Pooled	95% CI for
Difference	StDev	Difference
	-44.20	41.84 (-55.87, -32.54)

### Test

Null hypothesis	$H_0: \mu_1 - \mu_2 = 0$	
Alternative hypothesis	$H_1: \mu_1 - \mu_2 \neq 0$	
T-Value	DF	P-Value
-7.47	198	0.000

Figure 54: Two sample t-test conventional and renewable energy usage

For conventional energy use, Welch's t-test returned a p-value of 0.51, indicating there is not enough statistical evidence to reject the null hypothesis. However, when looking at renewable energy usage the test's results indicate a p-value of 0. This result suggests that there is a significant difference between the means of the two samples. Furthermore, since the 95% confidence interval for the difference does not contain 0, it confirms that the observed difference is both statistically significant and meaningful. This finding implies that the introduction of solar-powered charging stations has a measurable impact on renewable energy usage, which correlates with what could be observed in the histograms.

### 9.1.2.3 Economic viability

### Method

$\mu_1$ : mean of Total Revenue when Option = 0  
 $\mu_2$ : mean of Total Revenue when Option = 1  
Difference:  $\mu_1 - \mu_2$

Equal variances are assumed for this analysis.

### Estimation for Difference

	Pooled	95% CI for
Difference	StDev	Difference
	-23125	130914 (-59635, 13385)

### Test

Null hypothesis	$H_0: \mu_1 - \mu_2 = 0$	
Alternative hypothesis	$H_1: \mu_1 - \mu_2 \neq 0$	
T-Value	DF	P-Value
-1.25	198	0.213

Figure 55: Two sample t-test for Pedestrians traveling to charging stations

For total revenues, the two-sample t-test returned a p-value of 0.213, indicating insufficient statistical evidence to reject the null hypothesis. Additionally, the 95% confidence interval for the differences includes 0, further confirming that the observed differences are not statistically significant. This result suggests that the increase in the use of solar-powered charging stations was not sufficient to result in a meaningful impact on total revenues, highlighting that additional factors may be required to translate increased usage into significant economic benefits.

Total Costs are not explored for this alternative given that there is no added cost for allocating charging stations in optimized location as to randomly.

In conclusion, experiment 2 demonstrated that optimizing the placement of solar-powered charging stations using the metaheuristic approach significantly increases the number of pedestrians utilizing these stations. However, the increase in station usage did not translate into a statistically significant impact on total revenues, suggesting that while the optimization strategy enhances system usage, further steps are needed to monetize this increased usage and unlock its full economic potential.

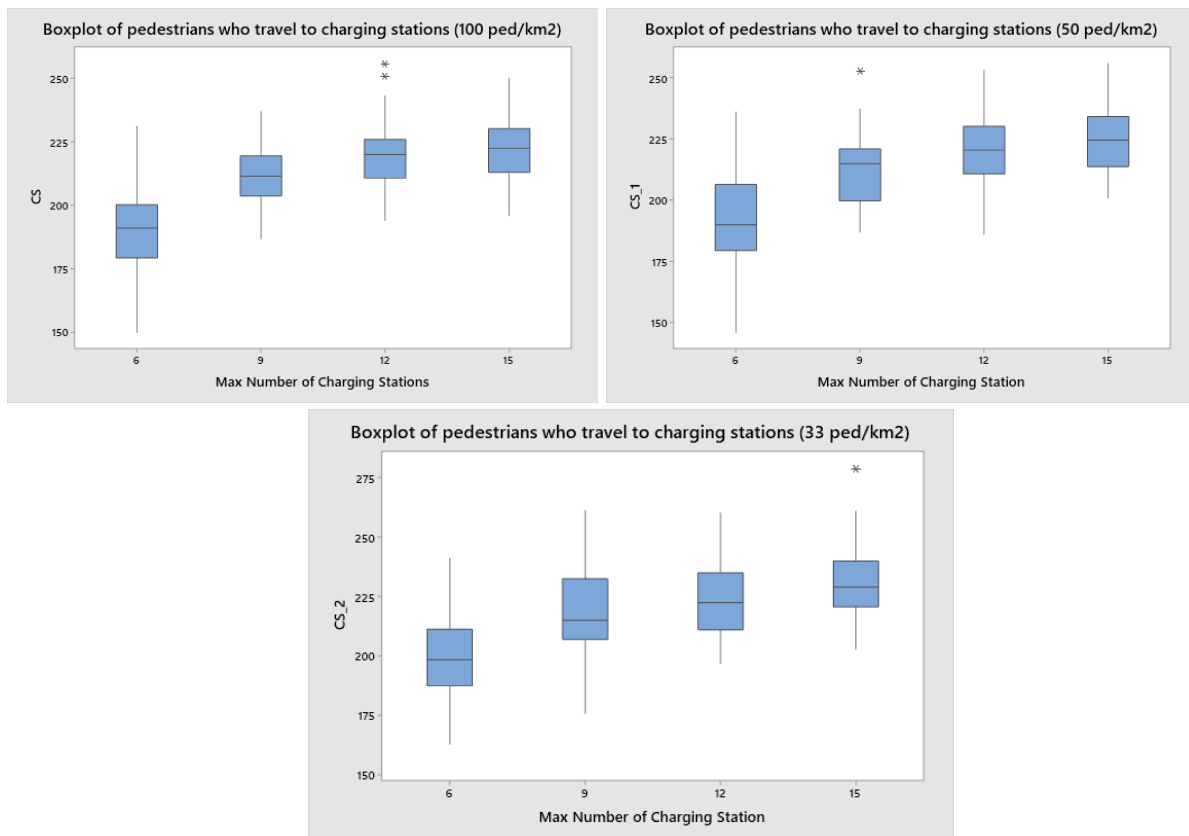
The next step is identifying the conditions required to make the optimized allocation strategy as profitable as possible. These investigations will explore factors such as varying population densities, the optimal number of charging stations, and the role of incentives like discounts to encourage usage.

### 9.1.3 Number of solar-powered charging stations versus population density

The simulation was conducted by varying two key parameters: the population density and the number of solar-powered charging stations. The number of charging docks per charging station was held constant throughout the experiment, ensuring consistency in infrastructure capacity. The initial step involved graphically plotting the results across the range of parameter values to qualitatively interpret the relationships between population density, the availability of charging stations, and the system's reference variables. The next step, unlike the previous two experiments, where a two-sample t-test was sufficient, the evaluation of the optimal number of charging stations requires analyzing multiple scenarios.

#### 9.1.3.1 Pedestrians traveling to charging stations

When the results were plotted as boxplots, it could be observed that an increase in the number of charging stations corresponds to an increase in the number of pedestrians choosing to travel to these stations across all population densities analyzed. In scenarios with lower population density, the impact of additional charging stations was more pronounced, resulting in a greater number of pedestrians selecting these stations as their destination. Conversely, in high-density scenarios, the alternatives appeared more closely grouped, indicating a diminished effect of additional charging stations on pedestrian behavior in these conditions.



Figures 56: Boxplot of pedestrians who travel to charging stations for varying number of charging stations and population densities

An ANOVA one-way test was subsequently conducted to statistically validate the patterns observed in the graphical analysis. The results of the Tukey test, providing pairwise comparisons between groups, are presented in the figures 56-58.

### Method

Null hypothesis All means are equal  
 Alternative hypothesis Not all means are equal  
 Significance level  $\alpha = 0.05$

Equal variances were assumed for the analysis.

### Analysis of Variance

Source	DF	Adj SS	Adj MS	F-Value	P-Value
Max Number of Charging Stations	3	28904	9634.7	49.93	0.000
Error	196	37824	193.0		
Total	199	66728			

### Grouping Information Using the Tukey Method and 95% Confidence

Max Number of Charging Stations	N	Mean	Grouping
15	50	222.36	A
12	50	219.78	A
9	50	212.08	B
6	50	191.72	C

Means that do not share a letter are significantly different.

Figures 57: Tukey test results for number of pedestrians traveling to charging stations for varying quantities of charging stations (Population density of 100 ped/km<sup>2</sup>)

### Method

Null hypothesis All means are equal  
 Alternative hypothesis Not all means are equal  
 Significance level  $\alpha = 0.05$

Equal variances were assumed for the analysis.

### Analysis of Variance

Source	DF	Adj SS	Adj MS	F-Value	P-Value
Max Number of Charging Statio_1	3	34498	11499.3	48.64	0.000
Error	196	46333	236.4		
Total	199	80831			

### Grouping Information Using the Tukey Method and 95% Confidence

Max Number of Charging Statio_1	N	Mean	Grouping
15	50	225.14	A
12	50	220.94	A
9	50	211.90	B
6	50	191.08	C

Means that do not share a letter are significantly different.

Figures 58: Tukey test results for number of pedestrians traveling to charging stations for varying quantities of charging stations (population density of 50 ped/km<sup>2</sup>)

## Method

Null hypothesis All means are equal  
Alternative hypothesis Not all means are equal  
Significance level  $\alpha = 0.05$

*Equal variances were assumed for the analysis.*

## Analysis of Variance

Source	DF	Adj SS	Adj MS	F-Value	P-Value
Max Number of Charging Statio_2	3	28729	9576.5	34.70	0.000
Error	196	54086	276.0		
Total	199	82816			

## Grouping Information Using the Tukey Method and 95% Confidence

Max Number of Charging Statio_2	N	Mean	Grouping
15	50	230.62	A
12	50	224.54	A B
9	50	218.26	B
6	50	198.70	C

*Means that do not share a letter are significantly different.*

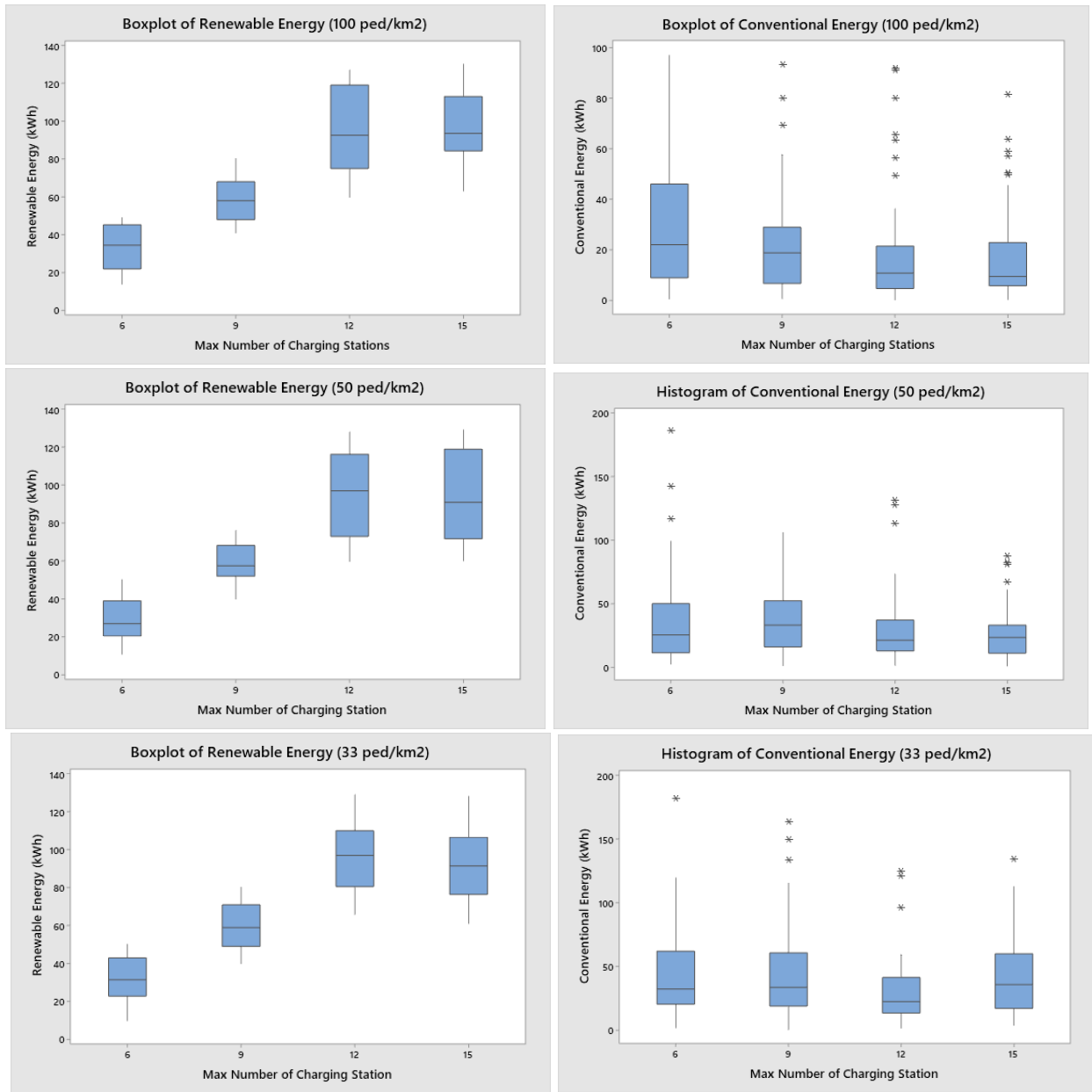
*Figures 59: Tukey test results for number of pedestrians traveling to charging stations for varying quantities of charging stations (Population density of 33 ped/km<sup>2</sup>)*

The statistical results reveal an unexpected finding: contrary to the initial hypothesis derived from the graphical analysis, the low-density scenario is the one in which the mean values between alternatives are statistically indistinguishable. As evidenced by the Tukey test results, there is no statistically significant difference between 12 and 15 charging stations or between 12 and 9 charging stations in the low-density scenario. However, apart from this specific result, the ANOVA test aligns with the patterns observed in the graphical analysis. It confirms that increasing the number of charging stations generally leads to more pedestrians traveling to these stations, a trend that holds true up to 12 charging stations. Beyond this point, the mean difference between 12 and 15 charging stations becomes statistically insignificant across all three population densities.

### 9.1.3.2 Conventional and Renewable Energy Consumption

Figure 59 reveals that the amount of conventional energy consumed does not significantly decrease with the rise in the number of charging stations. However, certain trends emerge. Notably, as the availability of solar-powered charging stations increases, the consumption of renewable energy increases consistently across all population densities, with this effect being most pronounced in lower-density scenarios.

In lower-density settings, the overall energy demand is higher, with conventional energy consumption occasionally exceeding 180 kWh. This increased demand can be attributed to pedestrians needing to travel longer distances to reach their destinations, a characteristic more typical of suburban environments compared to densely populated areas.



Figures 60: Boxplot of Energy consumption for varying number of charging stations and population densities

The following section presents the results of the Tukey test applied to renewable energy consumption.

### Method

Null hypothesis All means are equal  
 Alternative hypothesis Not all means are equal  
 Significance level  $\alpha = 0.05$

Equal variances were assumed for the analysis.

### Analysis of Variance

Source	DF	Adj SS	Adj MS	F-Value	P-Value
Max Number of Charging Stations	3	138095	46031.8	155.50	0.000
Error	196	58021	296.0		
Total	199	196116			

### Grouping Information Using the Tukey Method and 95% Confidence

Max Number of Charging			
Stations	N	Mean	Grouping
15	50	96.70	A
12	50	94.44	A
9	50	58.74	B
6	50	33.56	C

Means that do not share a letter are significantly different.

Figures 61: Tukey test results for renewable energy consumption for varying quantities of charging stations (Population density of 100 ped/km2)

#### Method

Null hypothesis All means are equal  
 Alternative hypothesis Not all means are equal  
 Significance level  $\alpha = 0.05$

Equal variances were assumed for the analysis.

#### Analysis of Variance

Source	DF	Adj SS	Adj MS	F-Value	P-Value
Max Number of Charging Statio_1	3	147753	49251.0	161.10	0.000
Error	196	59922	305.7		
Total	199	207675			

### Grouping Information Using the Tukey Method and 95% Confidence

Max Number of Charging			
Statio_1	N	Mean	Grouping
12	50	95.86	A
15	50	92.88	A
9	50	59.22	B
6	50	29.40	C

Means that do not share a letter are significantly different.

Figures 62: Tukey test results for renewable energy consumption for varying quantities of charging stations (Population density of 50 ped/km2)

#### Method

Null hypothesis All means are equal  
 Alternative hypothesis Not all means are equal  
 Significance level  $\alpha = 0.05$

Equal variances were assumed for the analysis.

#### Analysis of Variance

Source	DF	Adj SS	Adj MS	F-Value	P-Value
Max Number of Charging Statio_2	3	137924	45974.7	188.02	0.000
Error	196	47925	244.5		
Total	199	185849			

### Grouping Information Using the Tukey Method and 95% Confidence

Max Number of Charging			
Statio_2	N	Mean	Grouping
12	50	96.70	A
15	50	91.92	A
9	50	59.86	B
6	50	31.76	C

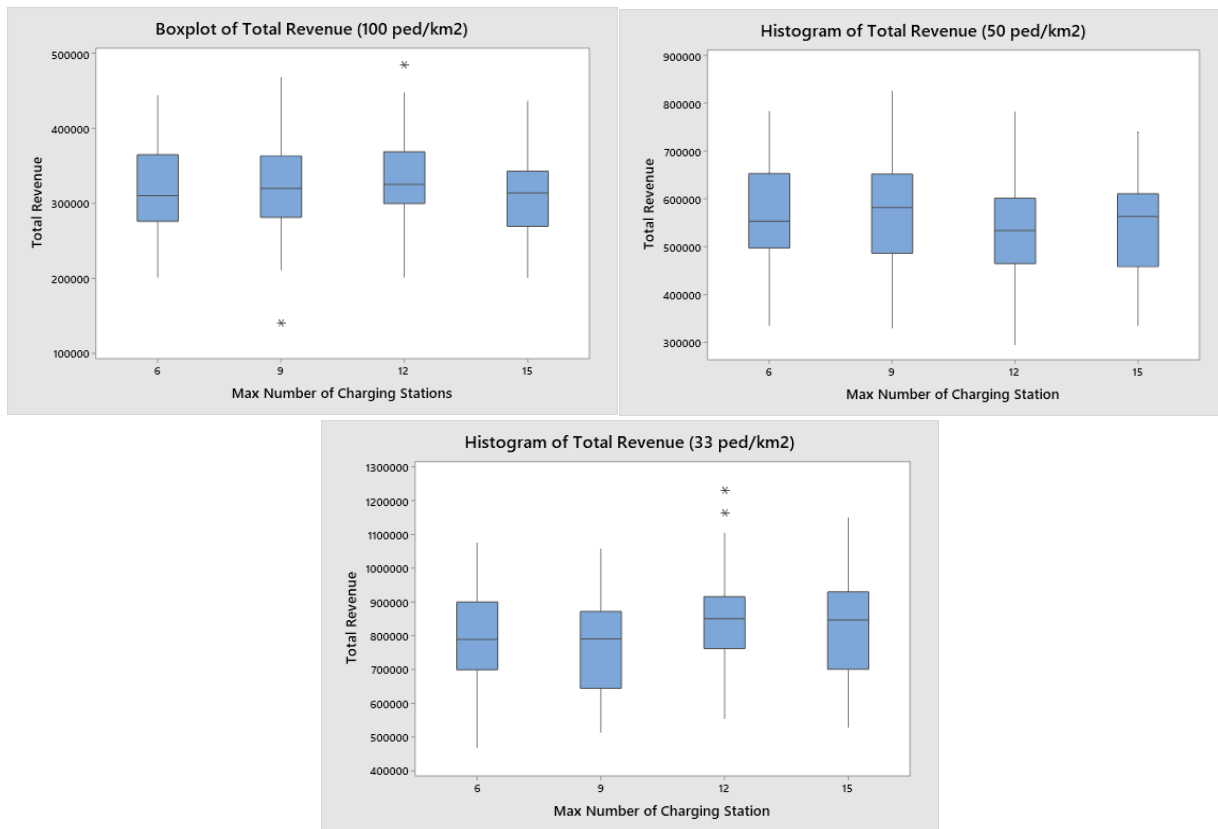
Means that do not share a letter are significantly different.

Figures 63: Tukey test results for renewable energy consumption for varying quantities of charging stations (Population density of 33 ped/km2)

As observed in the figures above, the results align with those of the ANOVA test conducted for the number of pedestrians choosing to travel to the solar-powered charging stations. Across all population densities, the mean renewable energy consumption increases with the number of charging stations, up to 12 stations. Beyond this point, there is no statistical evidence to indicate a significant difference in renewable energy consumption between 12 and 15 charging stations.

### 9.1.3.3 Economic viability

Lastly, the histograms for total revenue (Figure 63) reveal no clear differences between the varying numbers of charging stations across any of the population densities. However, it is noteworthy that revenue is consistently higher in low-density areas compared to high-density scenarios. This is likely due to the longer average trip distances in low-density areas, which increase the amount paid per trip. As a result, within the same time window of the simulation, the average revenue generated in low-density areas is nearly 300% higher, highlighting the significant impact of trip length on overall earnings.



Figures 64: Boxplot of total revenues for varying number of charging stations and population densities

Due to the relatively low impact of varying the number of charging stations on total revenue, a secondary analysis was conducted to determine the most optimal configuration of charging stations per population density. For this purpose, the average profit was calculated across all population densities and charging station quantities. The results, displayed in Table 2, indicate that the optimal number of charging stations is 12 for population densities of 33 and 100 pedestrians/km<sup>2</sup>, while for a density of 50 pedestrians/km<sup>2</sup>, the

optimal number is 9 charging stations. This result is consistent with the findings of the ANOVA test run for the number of pedestrians traveling to the charging stations in Section 9.1.3.1.

While the use of averages provides a convenient and practical approach to identify trends, it is an inherently imperfect measure and does not constitute robust statistical evidence on its own. However, for the purposes of this analysis, the average profit offers sufficient approximation to guide decision-making, particularly when coupled with the broader insights derived from the simulation. It is important to note that within columns the results are not that significant, however, the average profitability is very different between population densities.

		Population density (ped/km <sup>2</sup> )		
		33	50	100
Number of charging stations	6	802,874.67	571,248.98	317,991.07
	9	772,727.05	575,725.37	324,229.11
	12	843,394.64	529,664.28	326,708.54
	15	833,125.20	540,806.32	312,329.98

Table 2: Average profit with different population densities and number of charging stations

#### 9.1.4 Optimal number of docks per solar-powered charging stations

The simulation was conducted to determine the optimal number of docks per solar-powered charging station. This experiment utilized the previously identified optimal number of charging stations for each population density and iterated the number of charging docks per station from 2 to 6, with increments of 2. While no additional dock configurations were analyzed due to computational constraints, the chosen range is considered reasonable. Higher numbers of docks may be relevant for very busy terminals or intersections but fall outside the scope of this thesis.

Using AnyLogic’s parameter variation tool, a one-way ANOVA test was conducted, complemented by the Tukey test, to identify statistically significant differences among the means, as in the previous experiment. Graphical plotting of the results offered preliminary insights, which were then validated through statistical analysis.

##### 9.1.4.1 Pedestrians traveling to charging stations

The first clear trend observed when plotting the data onto boxplots is that the number of charging docks within a station has no effect on the number of pedestrians traveling to the solar-powered charging stations.

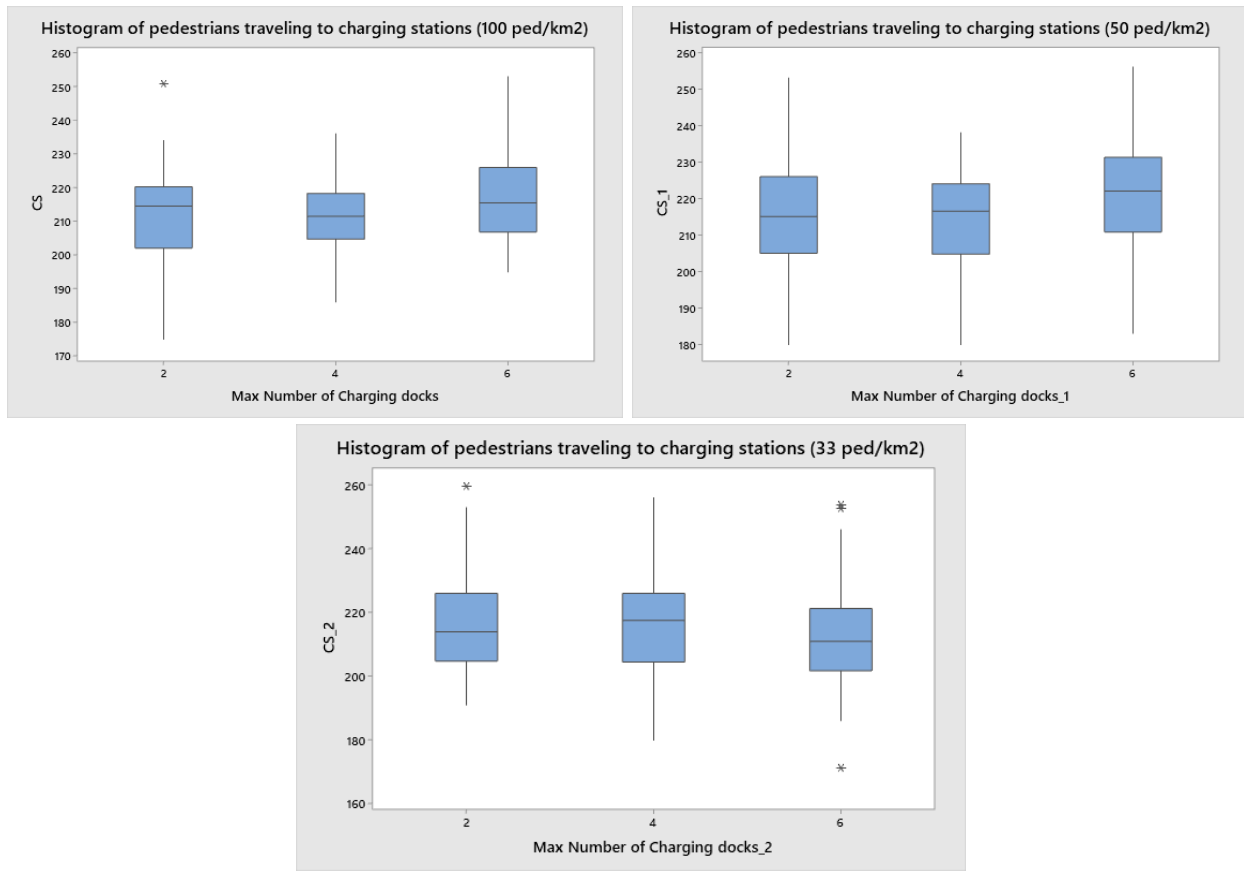


Figure 65: Boxplots of pedestrians who travel to the charging stations for varying population densities and number of charging stations

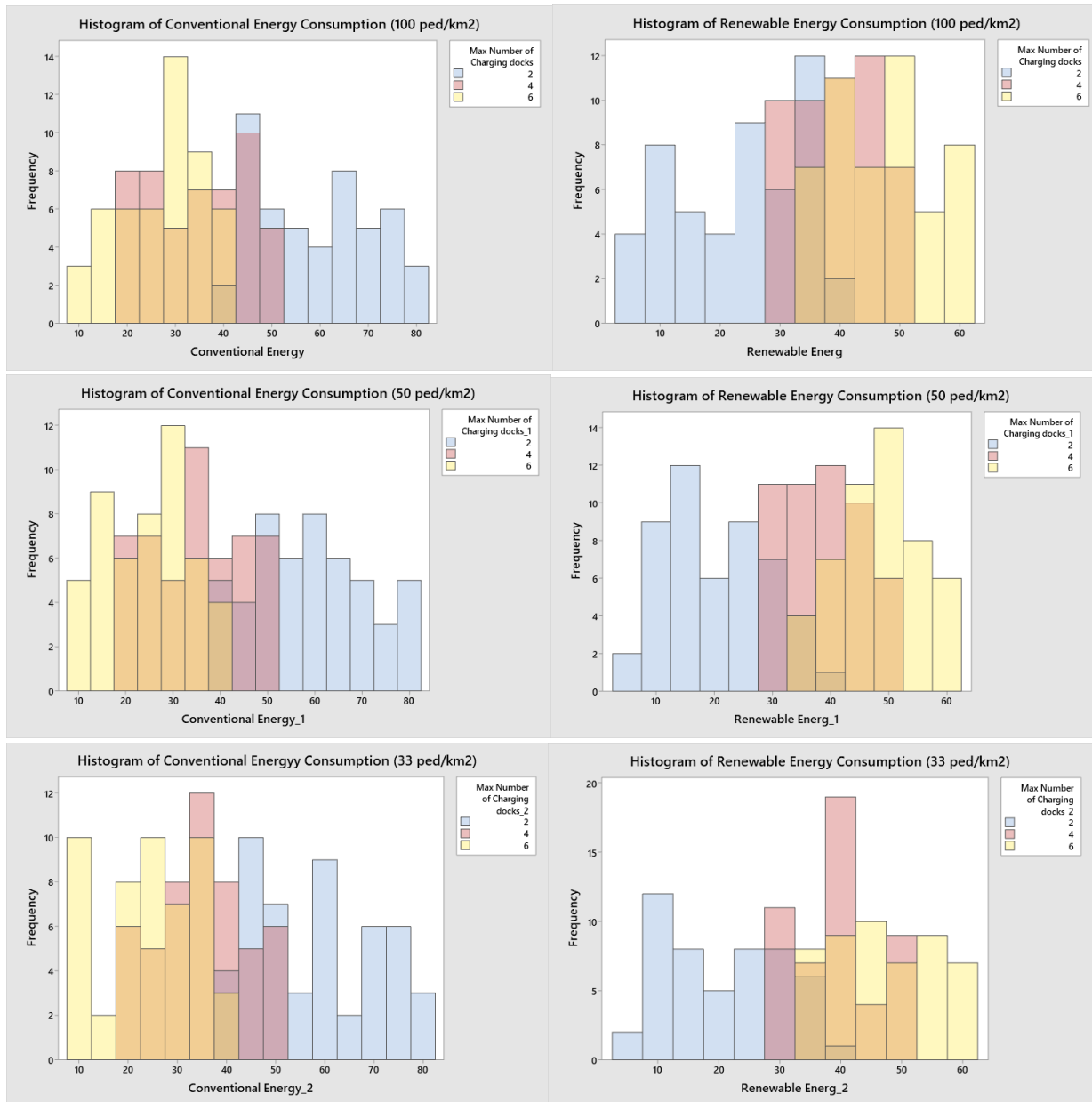
This outcome is consistent with the model's utility function as it solely considers the position of the charging station relative to the agent's final destination, assigning a cost to the deviation required. Therefore, the pedestrian's decision to travel to a charging station is unaffected by the availability of docks in the current scenario.

However, upon further reflection, in a real-world scenario, the number of charging docks within a station could influence user behavior over time. For instance, a pedestrian may initially choose to travel to a charging station based purely on utility. If, upon arrival, they find no available docks, this negative experience might affect their future decisions. Even if traveling to the charging station might provide more immediate utility, the pedestrian could opt to travel directly to their final destination to avoid a potentially frustrating experience. This behavior represents a non-ideal case that is not accounted for in the current scope of this thesis.

To address this limitation, this thesis proposes, for further researchers, the introduction of a parameter within the pedestrian agent to track the number of times they have traveled to a charging station and found no available docks. This parameter could then negatively impact the utility associated with traveling to the charging station, better reflecting real-world behavior and improving the model's accuracy.

### 9.1.4.2 Conventional and Renewable Energy Consumption

The simulation output for conventional and renewable energy consumption exhibited significant variability when the number of charging docks was altered. A clear trend emerged: as the number of charging stations increased, the consumption of conventional energy consistently decreased, while the consumption of renewable energy increased. This observation remained consistent across all population densities tested.



Figures 66: Histogram of Energy consumption for varying number of charging stations and population densities

A one-way ANOVA test was conducted for each variable analyzed in the histograms above to statistically validate the patterns observed in the graphical analysis. The results of the Tukey test are presented in Figures 66 – 71. These statistical tests confirm the initial hypotheses derived from the graphical analysis: all mean

values are statistically different across the various categories. Practically, this indicates that increasing the number of charging stations significantly improves the reference variables measured. Specifically, while adding more charging stations increases the number of pedestrians utilizing them, increasing the number of charging docks improves the overall utilization of the infrastructure, maximizing renewable energy consumption and minimizing conventional energy consumption.

### Method

Null hypothesis All means are equal  
 Alternative hypothesis Not all means are equal  
 Significance level  $\alpha = 0.05$

*Equal variances were assumed for the analysis.*

### Analysis of Variance

Source	DF	Adj SS	Adj MS	F-Value	P-Value
Max Number of Charging docks	2	15801	7900.53	107.94	0.000
Error	147	10759	73.19		
Total	149	26560			

### Grouping Information Using the Tukey Method and 95% Confidence

Max Number of Charging docks	N	Mean	Grouping
6	50	47.34	A
4	50	39.800	B
2	50	22.80	C

*Means that do not share a letter are significantly different.*

Figure 67: Tukey test results for renewable energy consumption for varying quantities of charging docks (100 Pedestrians / km<sup>2</sup>)

### Method

Null hypothesis All means are equal  
 Alternative hypothesis Not all means are equal  
 Significance level  $\alpha = 0.05$

*Equal variances were assumed for the analysis.*

### Analysis of Variance

Source	DF	Adj SS	Adj MS	F-Value	P-Value
Max Number of Charging docks	2	27090	13545.0	124.91	0.000
Error	147	15940	108.4		
Total	149	43030			

### Grouping Information Using the Tukey Method and 95% Confidence

Max Number of Charging docks	N	Mean	Grouping
2	50	58.68	A
4	50	34.70	B
6	50	27.16	C

*Means that do not share a letter are significantly different.*

Figure 68: Tukey test results for conventional energy consumption for varying quantities of charging docks (100 Pedestrians / km<sup>2</sup>)

## Method

Null hypothesis All means are equal  
 Alternative hypothesis Not all means are equal  
 Significance level  $\alpha = 0.05$

*Equal variances were assumed for the analysis.*

## Analysis of Variance

Source	DF	Adj SS	Adj MS	F-Value	P-Value
Max Number of Charging docks_1	2	20237	10118.6	189.04	0.000
Error	147	7868	53.5		
Total	149	28106			

### Grouping Information Using the Tukey Method and 95% Confidence

Max Number of Charging docks_1			
docks_1	N	Mean	Grouping
6	50	48.360	A
4	50	38.940	B
2	50	20.40	C

*Means that do not share a letter are significantly different.*

Figure 69: Tukey test results for renewable energy consumption for varying quantities of charging docks (50 Pedestrians / km<sup>2</sup>)

## Method

Null hypothesis All means are equal  
 Alternative hypothesis Not all means are equal  
 Significance level  $\alpha = 0.05$

*Equal variances were assumed for the analysis.*

## Analysis of Variance

Source	DF	Adj SS	Adj MS	F-Value	P-Value
Max Number of Charging docks_1	2	29969	14984.7	144.11	0.000
Error	147	15286	104.0		
Total	149	45255			

### Grouping Information Using the Tukey Method and 95% Confidence

Max Number of Charging docks_1			
docks_1	N	Mean	Grouping
2	50	58.74	A
4	50	35.14	B
6	50	25.00	C

*Means that do not share a letter are significantly different.*

Figure 70: Tukey test results for conventional energy consumption for varying quantities of charging docks (50 Pedestrians / km<sup>2</sup>)

## Method

Null hypothesis All means are equal  
 Alternative hypothesis Not all means are equal  
 Significance level  $\alpha = 0.05$

*Equal variances were assumed for the analysis.*

## Analysis of Variance

Source	DF	Adj SS	Adj MS	F-Value	P-Value
Max Number of Charging docks_2	2	18305	9152.51	140.34	0.000
Error	147	9587	65.22		
Total	149	27892			

### Grouping Information Using the Tukey Method and 95% Confidence

Max Number of Charging			
docks_2	N	Mean	Grouping
6	50	47.00	A
4	50	39.280	B
2	50	20.68	C

Means that do not share a letter are significantly different.

Figure 71: Tukey test results for renewable energy consumption for varying quantities of charging docks (33 Pedestrians / km<sup>2</sup>)

#### Method

Null hypothesis All means are equal  
 Alternative hypothesis Not all means are equal  
 Significance level  $\alpha = 0.05$

Equal variances were assumed for the analysis.

#### Analysis of Variance

Source	DF	Adj SS	Adj MS	F-Value	P-Value
Max Number of Charging docks_2	2	29492	14746.2	143.23	0.000
Error	147	15134	103.0		
Total	149	44627			

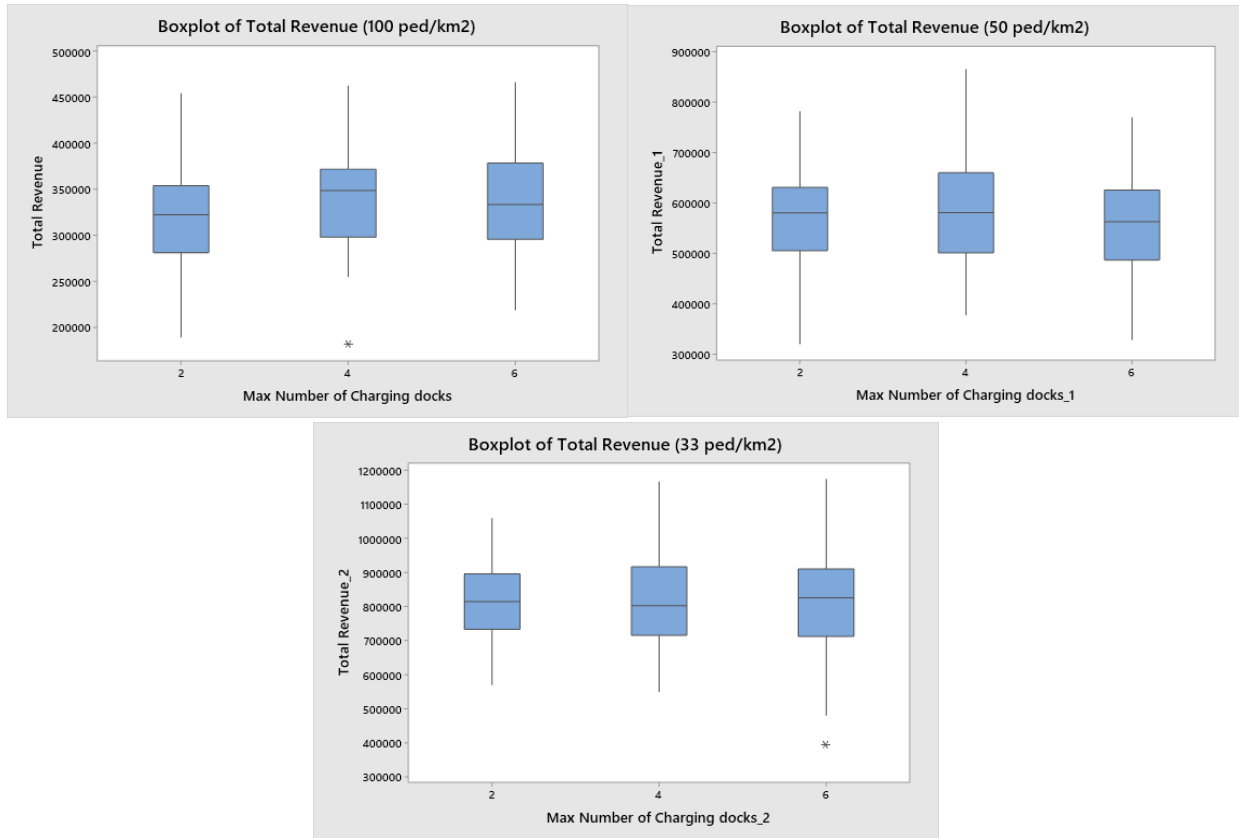
### Grouping Information Using the Tukey Method and 95% Confidence

Max Number of Charging			
docks_2	N	Mean	Grouping
2	50	58.10	A
4	50	34.72	B
6	50	24.62	C

Means that do not share a letter are significantly different.

Figure 72: Tukey test results for conventional energy consumption for varying quantities of charging docks (33 Pedestrians / km<sup>2</sup>)

### 9.1.4.3 Economic viability



Figures 73: Boxplot of total revenues for varying number of charging stations and population densities

Due to the relatively low impact of varying the number of charging docks per charging station on total revenue, a secondary analysis was conducted to determine the most optimal configuration of charging docks per population density. For this purpose, the average profit was calculated across all population densities and charging station quantities. The results, displayed in Table 3, indicate that the optimal number of charging docks is 4 for all population densities.

		Population density (ped/km <sup>2</sup> )		
		100	50	33
Max Number of Charging docks	2	314140.4	561939.8	799182.8
	4	332059.2	576051.5	805153.2
	6	324092.2	542242.2	793037.6

Table 3: Average profit with different population densities and number of charging docks

In conclusion, while to maximize renewable energy usage the optimal solution would be to install 6 charging docks, when analyzing the economic aspect, we see that this would incur higher costs and would therefore reduce the profitability of the solution.

### 9.1.5 Optimal discount to offer in order to maximize the solution

The simulation was conducted to determine the optimal discount to offer in order to maximize the performance of the solution. This experiment varied the discount rate from 0% to 100% in 10% intervals to observe how the system's behavior would change under this stimulus. The number of charging stations was held constant at 9 to 12, depending on the population density, and 4 charging docks per charging station as discussed in Section 9.1.3 and 9.1.4.

Using AnyLogic's parameter variation tool, a one-way ANOVA test was conducted, complemented by the Tukey test, to identify statistically significant differences among the means, as in the prior experiments.

#### 9.1.5.1 Pedestrian behaviour

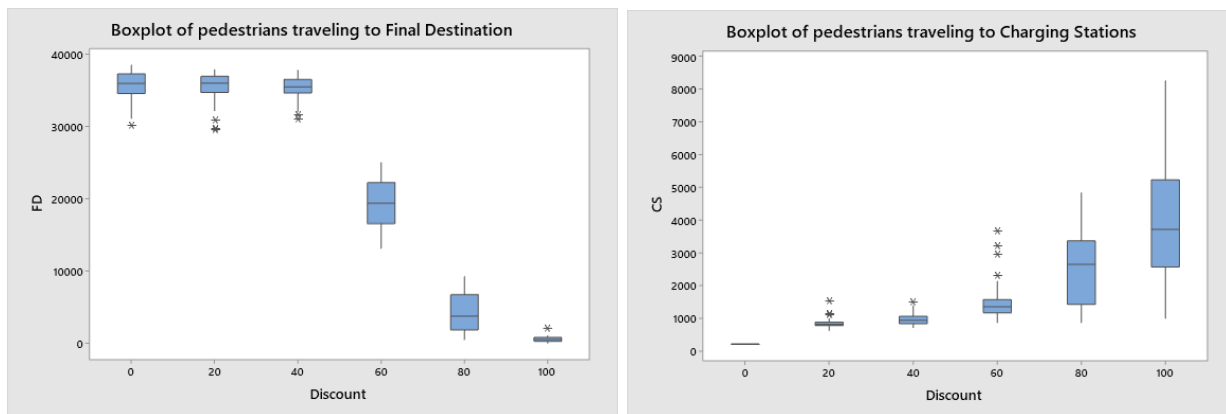


Figure 74: Boxplots of pedestrians who travel to their final destination or charging stations for varying discount %.

When varying the discount offered to agents to travel to the solar-powered charging station, a particular trend emerges. Observing the number of pedestrians who choose to travel to their final destination, a clear decrease is evident as the discount increases. Notably, when the discount reaches 100%, all iterations fall within the (0, 1000) bucket, indicating that nearly all agents opt to travel to the nearest charging station instead of their final destination.

On the other hand, when analyzing the number of pedestrians traveling to the nearest charging station, it becomes apparent that without any discount, all iterations remain in the first bucket of (0, 1000), consistent with previous cases. However, as a discount is introduced, the number steadily increases, reaching its highest peak of nearly 9000 pedestrians when a 100% discount is offered. It is important to highlight that this number does not reach the nearly 40.000 observed for the final destination. This discrepancy is attributed to the limited number of charging docks; while many users may choose to travel to the nearest charging station, some are forced to revert to their final destination when no docks are available at the station.

Having previously stated the methodology and procedure for conducting a Tukey test, the results of the test applied to pedestrian travel are as follows:

## Analysis of Variance

### Method

Null hypothesis All means are equal  
 Alternative hypothesis Not all means are equal  
 Significance level  $\alpha = 0.05$

Source	DF	Adj SS	Adj MS	F-Value	P-Value
Discount	5	66053534699	13210706940	2884.55	0.000
Error	294	1346466568	4579818		
Total	299	67400001267			

### Grouping Information Using the Tukey Method and 95% Confidence

Discount	N	Mean	Grouping
0	50	35554	A
20	50	35449	A
10	50	35423	A
40	50	35337	A
30	50	34984	A
50	50	24877	B
60	50	18914	C
70	50	13365	D
90	50	4721	E
80	50	4711	E
100	50	534.9	F

Means that do not share a letter are significantly different.

Figures 74: Tukey test results for pedestrians traveling to final destination

## Analysis of Variance

### Method

Null hypothesis All means are equal  
 Alternative hypothesis Not all means are equal  
 Significance level  $\alpha = 0.05$

Source	DF	Adj SS	Adj MS	F-Value	P-Value
Discount	5	491671473	98334295	123.30	0.000
Error	294	234470862	797520		
Total	299	726142335			

### Grouping Information Using the Tukey Method and 95% Confidence

Discount	N	Mean	Grouping
100	50	4079	A
90	50	3007	B
80	50	2532	B
70	50	1745.5	C
60	50	1502.1	C D
50	50	1111.5	D E
40	50	976.7	E F
30	50	937.3	E F
20	50	850.5	E F
10	50	581.9	F G
0	50	217.32	G

Means that do not share a letter are significantly different.

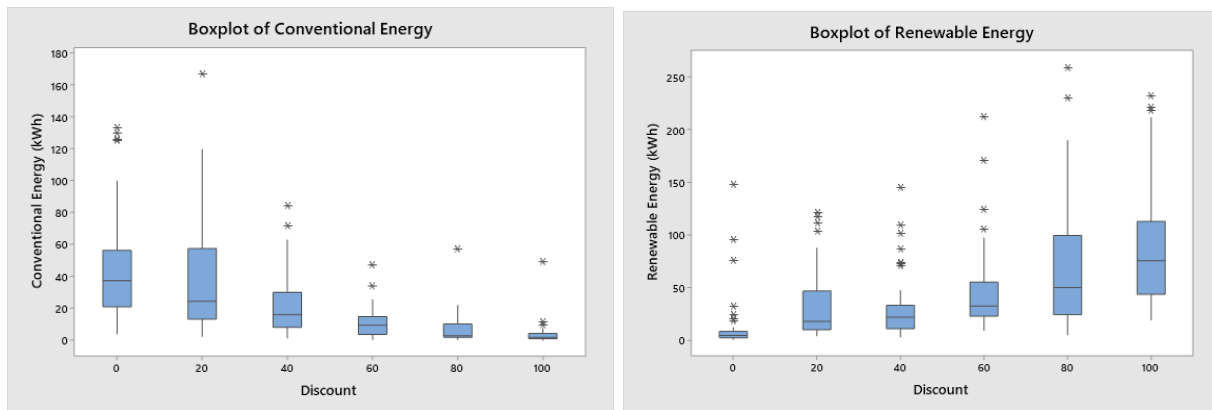
Figures 76: Tukey test results for pedestrians traveling to solar powered charging stations

The statistical analysis shows that significant changes in the mean value begin to appear after a 40% discount on the journey. Each additional discount beyond this threshold has a notable impact, demonstrating the effectiveness of larger discounts in influencing pedestrian behavior and optimizing system performance. However, the grouping varies significantly across the two reference variables. This occurs because some pedestrians may intend to travel to a charging station but cannot do so due to a lack of available charging docks upon arrival. For decision-making, the reference variable “pedestrians traveling to CS” provides a

more accurate measure, as offering discounts to attract more users would be ineffective if the system lacks the resources to accommodate them.

### 9.1.5.2 Conventional and Renewable Energy Consumption

Observing the amount of conventional energy consumed, a clear decrease is evident as the discount increases. By the time the discount reaches 100%, all iterations fall within the first bucket of (0, 10 kWh), indicating minimal reliance on conventional energy. On the other hand, analyzing renewable energy consumption reveals an increase as the discount rises. At the maximum discount of 100%, renewable energy consumption peaks at over 200 kWh, reflecting a significant shift toward sustainable energy use. These findings are consistent with earlier results, reinforcing the observation that incentivizing agents to utilize charging stations not only reduces conventional energy usage but also maximizes renewable energy consumption, enhancing the system's overall sustainability.



Figures 77: Boxplot of energy consumption for different discounts offered

A one-way ANOVA test was conducted for each variable analyzed in the histograms above to statistically validate the patterns observed in the graphical analysis. The results of the Tukey test are presented in Figures 77-78. These statistical tests confirm the initial hypotheses derived from the graphical analysis: after 40% discount is where there is a statistically significant increase in renewable energy usage and a decrease in the need for conventional energy.

#### Method

Null hypothesis All means are equal  
 Alternative hypothesis Not all means are equal  
 Significance level  $\alpha = 0.05$

Equal variances were assumed for the analysis.

#### Analysis of Variance

Source	DF	Adj SS	Adj MS	F-Value	P-Value
Discount	5	82554	16510.7	29.74	0.000
Error	294	163229	555.2		
Total	299	245783			

### Grouping Information Using the Tukey Method and 95% Confidence

Discount	N	Mean	Grouping
0	50	46.12	A
20	50	41.18	A
40	50	22.47	B
60	50	10.90	B C
80	50	6.65	C
100	50	3.485	C

Means that do not share a letter are significantly different.

Figures 78: Tukey test results for conventional energy

#### Method

Null hypothesis All means are equal  
 Alternative hypothesis Not all means are equal  
 Significance level  $\alpha = 0.05$

Equal variances were assumed for the analysis.

#### Analysis of Variance

Source	DF	Adj SS	Adj MS	F-Value	P-Value
Discount	5	199265	39853	21.80	0.000
Error	294	537392	1828		
Total	299	736657			

### Grouping Information Using the Tukey Method and 95% Confidence

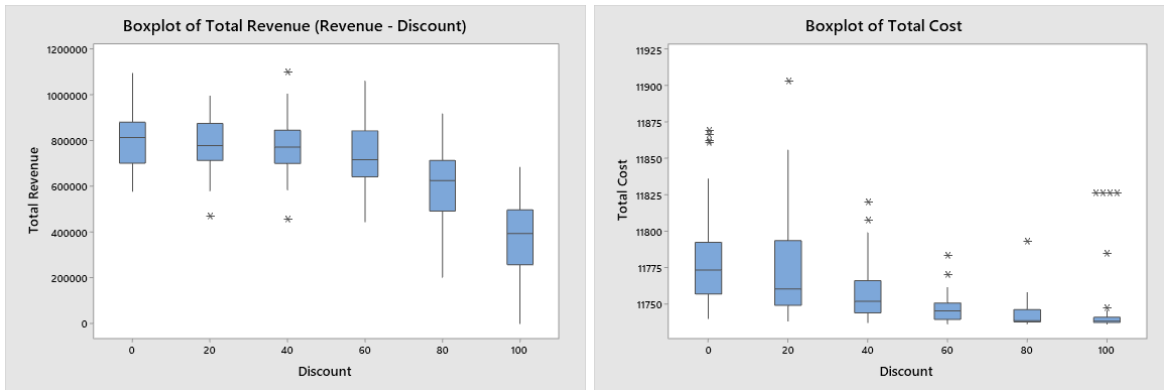
Discount	N	Mean	Grouping
100	50	88.48	A
80	50	70.49	A B
60	50	46.33	B C
20	50	31.38	C D
40	50	31.18	C D
0	50	12.08	D

Means that do not share a letter are significantly different.

Figures 79: Tukey test results for renewable energy

#### 9.1.5.3 Economic viability

To evaluate the feasibility of offering a discount to influence user behavior, it is necessary not only to determine the discount required to drive this change but also to evaluate whether the proposed discount would result in economic benefits for the service provider. Therefore, profitability was calculated by considering the revenue generated from rentals, subtracting the costs of conventional energy consumed and the discount offered, and adding the income from electricity sold back to the grid when solar-powered charging stations are not actively charging scooters. The results of this analysis are presented in the following histogram.



Figures 80: Boxplot of Total revenues (including discount) and costs

The histogram reveals significant insights like at 0% discount, the revenue distribution peaks at higher values, particularly around 900,000, emphasizing that maintaining full pricing maximizes profitability due to the absence of discount costs. As discounts increase to 20-40%, the revenue shifts slightly lower but remains concentrated within the 750,000–900,000 range, indicating this as a potential sweet spot for balancing user incentives and economic returns. However, at higher discount levels (80-100%), revenue declines sharply, with the majority falling within the 450,000–750,000 range. This trend highlights the diminishing returns of excessive discounts, whereas the cost of incentivizing users outweighs the revenue generated. While moderate discounts encourage user behavior without severely impacting profitability, higher discounts lead to significant revenue decline.

Discount	Average of Total Revenue	Average of Total Cost	Average Profits
0	€ 792,130.40	€ 11,782.12	€ 780,348.28
20	€ 785,227.73	€ 11,777.18	€ 773,450.55
40	€ 775,743.62	€ 11,758.47	€ 763,985.15
60	€ 725,466.89	€ 11,746.90	€ 713,719.98
80	€ 602,692.15	€ 11,742.65	€ 590,949.50
100	€ 377,078.54	€ 11,746.69	€ 365,331.85

Table 4: Average profit with different discount rates

## 9.2 Interpretation of Results

Chapter 9.1 provides a comprehensive analysis and interpretation of the experimental results obtained from implementing solar-powered charging stations for electric scooters in urban areas. The results emphasize the economic and environmental benefits of this innovative infrastructure, highlighting its potential to address the demand for sustainable urban transport solutions while offering a cost-effective alternative to conventional energy sources. The experiments explored various configurations, such as optimal station placement, dock capacities, and pricing strategies, generating valuable insights into designing an efficient and user-friendly system.

The analysis first demonstrated that while randomly allocating solar-powered charging stations did result in some usage and some reduction in conventional energy consumption, there was insufficient statistical evidence to conclude that it could meaningfully reduce the number of pedestrians opting to travel directly to their final destination. On the other hand, strategically allocating stations using metaheuristic methods, such as the Ant Colony Optimization algorithm, significantly improved performance metrics. Compared to random allocation, strategic placement increased station utilization by approximately 30%, and energy savings rose by over 20%. Importantly, this optimization required no additional infrastructure costs, showcasing the value of simulation planning.

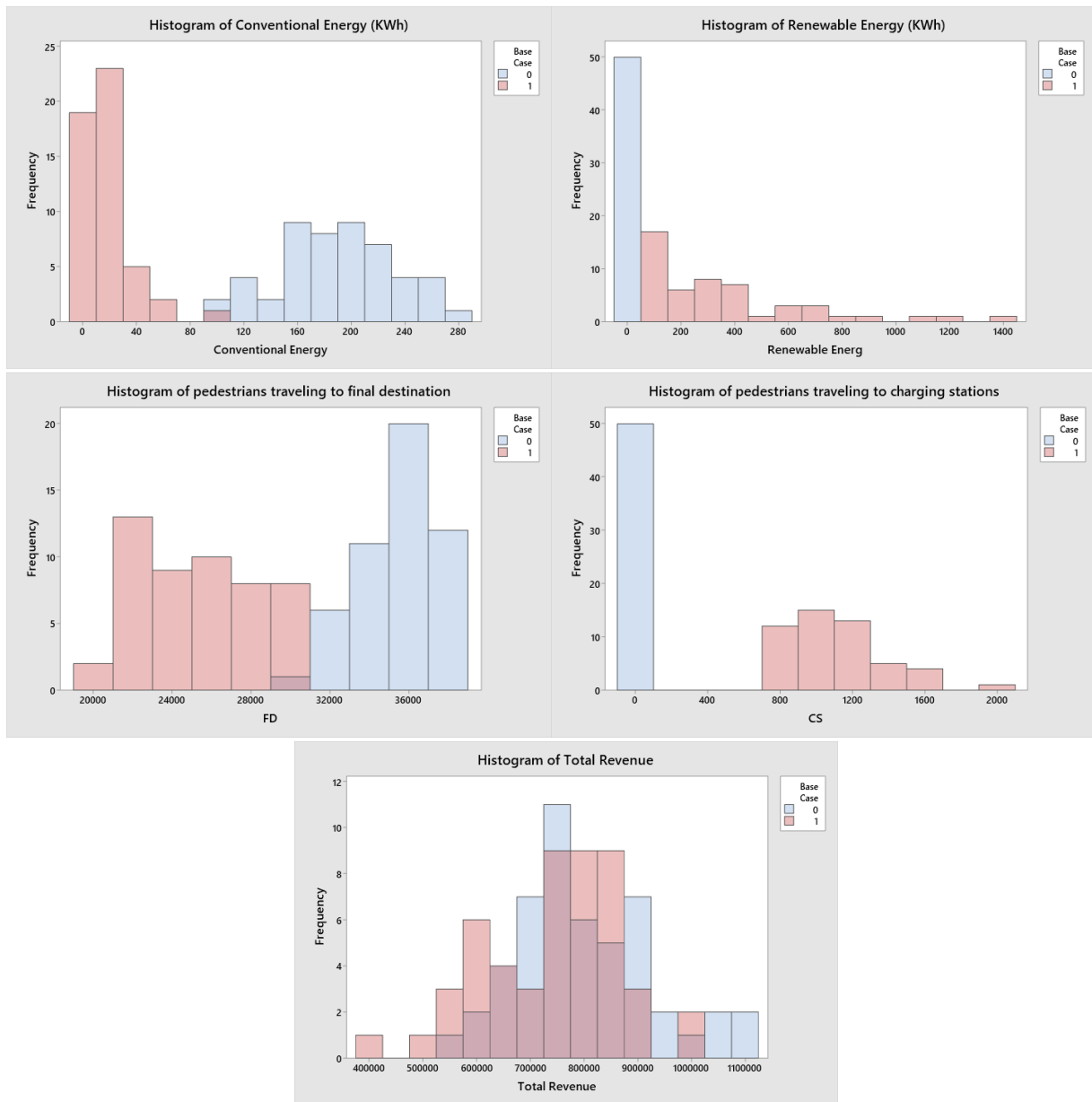
Furthermore, the relationship between population density and the number of charging stations/docks was analyzed to maximize system usage while minimizing costs. The findings are summarized in the following table:

		Optimal N. of Charging Stations	Optimal N. of Charging stations per km <sup>2</sup>	Optimal N of charging docks
Population density (ped / km <sup>2</sup> )	100	12	6	4
	50	9	4	4
	33	12	4	4

*Table 5: Summary of results from experiment 9.1.3 and 9.1.4*

Pricing incentives were analyzed to understand their impact on user adoption, energy consumption, and profitability. While the most profitable approach is to avoid discounts, offering a 40% discount on scooter rentals was found to increase the number of pedestrians traveling to charging stations by 77%. At this discount level, profitability remained stable, with revenue around \$750,000, a 51.7% reduction in conventional energy use, and a 257% increase in renewable energy consumption.

The final step involved in the framework described in Section 9.1 is taking the final configuration for the implementation of solar powered charging station, which includes 9-12 charging stations, 4 docks per station, and a 40% discount and comparing it with the current "as-is" case of electric scooter rental services. From the results shown in figure 80 where it's possible to observe that there are significant differences across all reference variables, except for total revenue and profitability which at first glance it is not possible to discern if there is a statistically significant difference.



Figures 81: Histogram of reference variables of base case vs. final case 2 - the scenario with base case corresponds to when the variable “base case” is set to 0, while the scenario the final configuration is represented with a 1.

Base Case	Average of Total Revenue	Average of Total Cost	Profitability
0	€ 801,429.48	€ 5,532.90	€ 795,896.58
1	€ 744,046.78	€ 11,754.25	€ 732,292.53

Table 6: Average profit with different discount rates

Following the methodology already established to analyze if the results of this test are statistically significant the following hypothesis are defined:

$H_0$  = There is no significant difference between the final configuration case and the base case for the reference variables being tested.

$H_1$  = There is a significant difference between the two cases.

Once the assumptions are validated the specific hypothesis are stated: taking the mean of the final configuration case ( $\mu_S$ ) and the mean of the base case ( $\mu_{S'}$ );

$$H_0 \Rightarrow \mu_S = \mu_{S'} \qquad H_1 \Rightarrow \mu_S \neq \mu_{S'}$$

The data is then entered into the Minitab software and the two sample t-tests are run.

### 9.2.1 Pedestrian behaviour

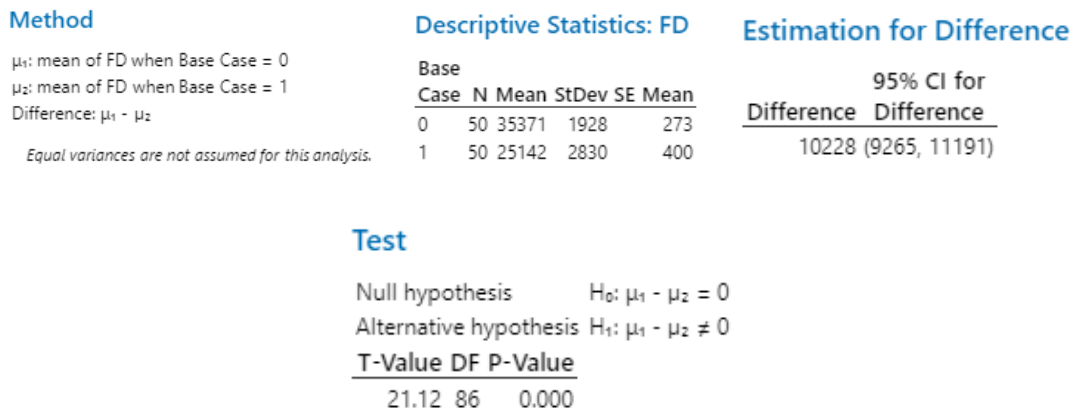


Figure 82: Two sample t-test for Pedestrians traveling to final destination

For pedestrians traveling to their final destination, the two-sample t-test returned a p-value of 0, which indicates that there is just sufficient statistical evidence to reject the null hypothesis and concludes that there is a significant difference between the mean of the two samples. This outcome implies that the observed difference is due to the implementation of the final configuration. Additionally, pedestrians traveling to charging stations was not analyzed since in the case where there are no charging stations the results are always zero, therefore the means always differ.

## 9.2.2 Conventional and Renewable Energy Consumption

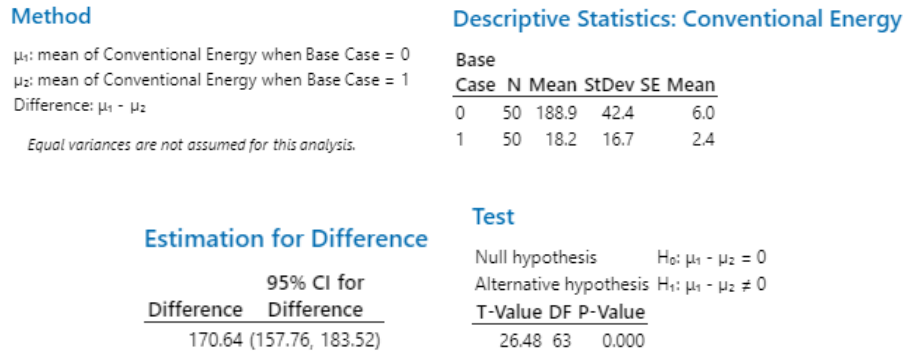


Figure 83: Welch's t-test for Conventional Energy Usage

For conventional energy use, Welch's t-test returned a p-value of 0, indicating strong statistical evidence to reject the null hypothesis. This result suggests that there is a significant difference between the means of the two samples. Furthermore, since the 95% confidence interval for the difference does not contain 0, it confirms that the observed difference is both statistically significant and meaningful. This finding implies that the implementation of the final configuration has a definitive impact of the reduction of conventional energy used.

Renewable energy usage is not analyzed as for the case in which no solar panels are introduced the amount of renewable energy used is always zero.

## 9.2.3 Economic viability

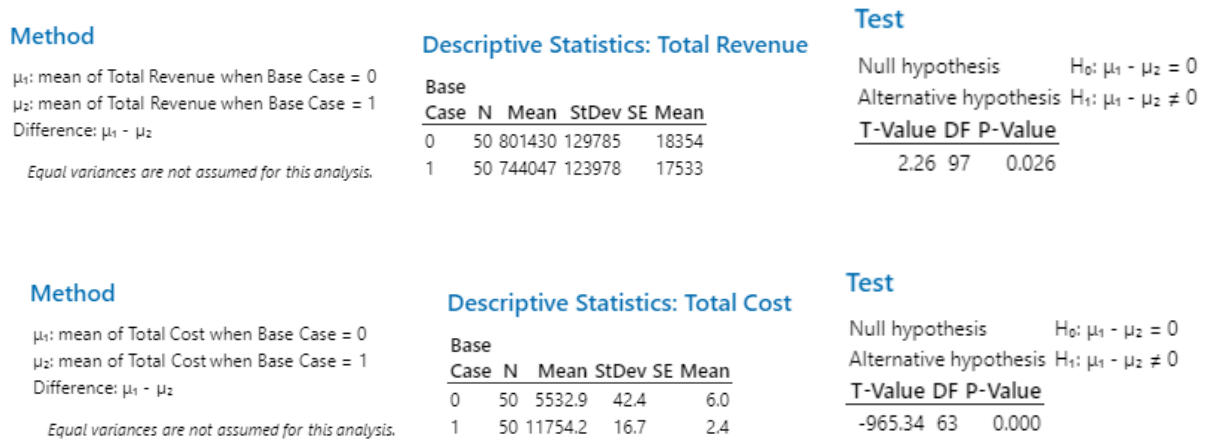


Figure 84: Two sample t-test for total cost and revenue

For both revenue and costs, the tests return a p-value of less than 0.05, indicating sufficient statistical evidence that implementing the final configuration with a 40% discount will impact profitability. While the

additional revenue from selling electricity back to the grid helps offset the reduced margins from discounted rides, there will still be a 7.9% decline in profit margin.

In conclusion, from an environmental perspective, the optimized solution results in approximately a 90% reduction in conventional energy usage, accompanied by an average renewable energy consumption of 356 kWh. Furthermore, there is about a 30% decrease in the number of pedestrians traveling directly to their final destination, as more users choose to utilize the solar-powered charging stations instead at a cost of 7.9% reduction in profit margins.

Ultimately, the interpretation of these results supports the conclusion that solar-powered charging stations represent a viable and forward-looking solution for enhancing micro-mobility in urban areas. In particular, strategic station placement using metaheuristics, optimizing the density of stations and docks, and implementing targeted discounts are this thesis' main recommendations. The key lies in understanding which are the sustainability goals that companies want to achieve.

The outcomes also pave the way for further research, particularly in refining optimization techniques, integrating larger urban datasets, and exploring additional incentives to promote user adoption to reduce the impact in profit margins. This chapter demonstrates how economic practicality and environmental consciousness can converge to create a greener, more efficient future in urban mobility.

## 10. Conclusions and Recommendations

This thesis aimed to address the key challenges of urban mobility by assessing the economic feasibility and sustainability of integrating solar-powered charging stations into electric scooter rental services. As urbanization drives the demand for greener transport solutions, this research focused on developing an AnyLogic simulation model to evaluate different strategies for implementing solar-powered charging stations. The goal was to determine whether solar energy could effectively reduce conventional energy consumption, lower operational costs, and enhance the profitability of e-scooter services.

By leveraging a simulation-based approach in AnyLogic, it was possible to test multiple scenarios without the financial risks of real-world pilot programs. The model optimized the placement and configuration of charging stations, assessed their influence on user adoption, and quantified both economic and environmental outcomes. Beyond answering the research question, this study developed a flexible and scalable simulation model that companies can use to evaluate charging station deployment strategies before implementation, ensuring informed decision-making and maximizing sustainability and profitability.

### 10.1 Challenges, Debugging and Limitations

Recreating a dynamic and intricate system within the constraints of Java and AnyLogic presented several challenges. Two primary obstacles encountered during the modeling process were sequentiality and the concatenation effect.

The sequentiality challenge primarily involved the necessity for certain operations to occur in a specific order within the AnyLogic model to produce the correct output. For example, agents had to first select a

scooter, then calculate the time required to walk to the scooter, assess whether it was within a reasonable distance, and finally proceed to the delay block and the walking state. While this sequence may appear logically sound when described, AnyLogic's default behavior, where transitions between blocks occur with zero-time delay, could result in insufficient computation time. This could cause the walking time to remain uncalculated when the agent entered the delay block, leading to an error in the simulation run. To address this issue, a delay block with a 1 millisecond delay was inserted, allowing the computation to catch up. Although this solution may not seem intuitive to someone unfamiliar with the model, it was deemed effective, as the cumulative added time did not exceed 10 milliseconds during trips typically ranging from 15 to 45 minutes, making the impact negligible.

The second challenge involved managing the complex web of agent interactions, particularly in referencing agents across different levels. With four agents interacting within the main agent, one of the primary difficulties was ensuring proper reference to agents, such as charging stations, pedestrians, or chargers, after the pick-up process. This is because in the pick-up block one agent is inserted within the agent of higher level. To resolve this, auxiliary variables, such as "pickUpBy" and "parkedIn," were introduced to enable communication and to pick up certain variables from lower-level agents.

Debugging the model also proved to be challenging, especially in relation to sequentiality issues. The parallel execution of multiple processes sometimes resulted in situations where one message needed to be sent before another to maintain the correct sequence. However, the Java interface did not explicitly indicate the cause of such issues, simply reporting an execution error. As a result, debugging required a manual and iterative process. Fortunately, the `traceln` function in Java allowed for real-time visualization of variable outputs during simulation, enabling the identification of bugs through a trial-and-error approach. Although the final model runs efficiently and produces valid, real-world representative data, future researchers are encouraged to carefully consider these challenges when building upon this work.

When considering the main limitations of the work presented in this thesis, several key points must be highlighted:

**Computational Limitations:** The model was designed with a high level of generalization to accommodate various cities, each with unique characteristics such as size, population densities, scooter distribution, placement algorithms, and more. However, to fully exploit the potential of this model, greater computational power is necessary than was available during the writing of this thesis. Specifically, running the model over multiple years could provide valuable insights, particularly in evaluating the costs associated with maintenance and the purchase of new scooters. Additionally, further investigation is encouraged into scenarios where charging stations are equipped with varying numbers of charging docks, as well as examining the effects of incorporating more than the 15 charging stations considered in this thesis.

**Weather Patterns:** The decision to base all simulations on a single weather dataset from one city, while useful for deriving preliminary results and maintaining the scope of this work, introduces limitations. Significant differences in outcomes may arise when comparing weather conditions in a city like Torino, with its relatively sunny climate, to those in a less sunny city. Therefore, this thesis encourages future research to assess how these results may vary across different cities, considering local weather patterns.

**Traffic and Competition:** The assumptions regarding travel time and competition were simplified as ideal conditions to align with the scope of this thesis. However, in the real-world economics of the rental scooter industry, competition is fierce. Once a first mover adopts solar-powered charging stations, it is likely that competing companies will quickly implement similar solutions. Consequently, the results obtained in this study are optimistic and represent ideal conditions. In a real-world scenario, it is expected that revenue would be significantly lower than the values generated by the model due to increased competition and market saturation.

**Fixed Scooter-to-Population Ratio:** This assumption assumes that the simulation will be established at a city with pre-existing scooter infrastructure and a number of scooters that is enough to maintain a smooth operation without shortage or excess of scooters. This may not fully capture variations in real-world demand, seasonal fluctuations, or changes in user behavior over time.

**Charger behaviour:** The model assumes that chargers will continue searching for scooters with less than 30% battery until either no low-charge scooters remain, or the van reaches full capacity. However, this may not always be the most efficient strategy. For example, a charger with seven scooters may have to travel across the entire map to collect one last scooter, which might not be practical. In reality, a charger may decide to proceed with charging before reaching full capacity to optimize time and efficiency. Future research could refine charger behavior by incorporating more dynamic decision-making based on travel distance, time constraints, and operational efficiency.

**Choosing charging station logic:** The *chooseCS* function was developed to choose the closest charging station to the pedestrian's final destination. However, this logic has its limitations, there could be a case where the closest CS may be beyond the final destination, i.e. there may be a CS 300m before the final destination and a CS 200m after the final destination. The function would choose the latter; however, the total journey time will be higher for the traveler, and this may not accurately describe real-world behaviours. This was done to balance computational time and complexity.

**Pre-existing infrastructure:** To develop this model it was assumed that the city that was being evaluated for the implementation of charging stations already had a pre-existing fleet of e-scooters and therefore this cost was not considered. This limits the applicability of the model and if readers wish to evaluate a city in which e-scooters are not yet present should take this into consideration.

## 10.2 Final Conclusions and Recommendations

This thesis sets out to address the growing challenges posed by urbanization, particularly the need for sustainable and efficient urban mobility solutions. By leveraging the potential of solar-powered charging stations for electric scooters, it aimed to provide both an environmentally sustainable and economically viable alternative to conventional urban transport systems. The simulation-based methodology employed in this study allowed for a robust analysis of the interactions between users, infrastructure, and environmental variables, shedding light on how renewable energy solutions may advance urban micro-mobility.

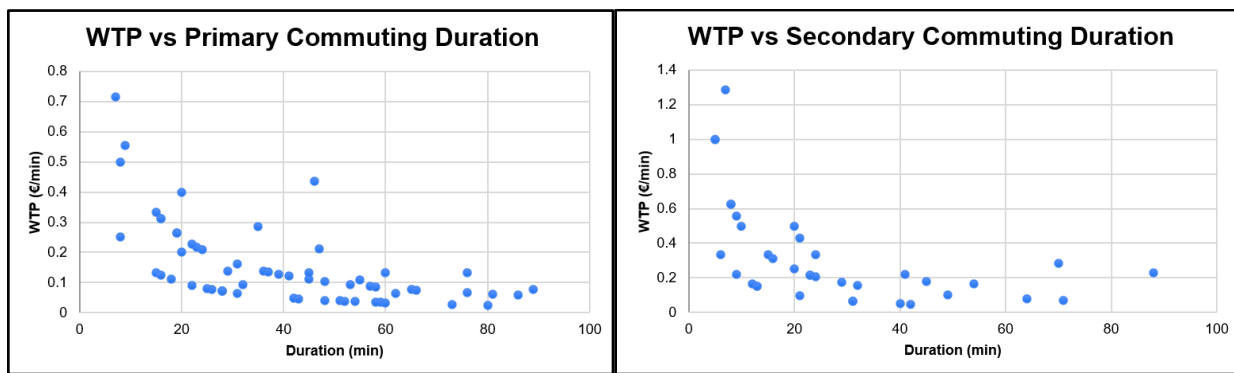
From an academic perspective, this thesis contributes significantly to the interdisciplinary literature on urban sustainability and renewable energy integration. It bridges gaps in the literature by combining user behavior analysis, simulation modeling, and renewable energy applications. The main contributions are:

1. Behavior Modeling: This study explored how users interact with fixed infrastructure, offering insights into travel behavior and deviations under incentives.
2. Optimized Infrastructure Placement: The application of the Ant Colony Optimization metaheuristic provides a new approach to the strategic deployment of solar-powered charging stations, ensuring high utility and cost-effectiveness.
3. Economic and Environmental Analysis: By quantifying both energy sustainability and profitability metrics, this work evaluates urban micro-mobility solutions that can incentivize businesses to go green without having to sacrifice profits or having to go against stakeholder's interests.

In practice, these findings provide actionable insights for stakeholders in the electric scooter rental industry. This thesis recommends implementing strategically placed charging stations with four docks and offering a 40% discount to encourage users to choose charging stations over driving directly to their final destination. This approach enables a significant reduction in conventional energy consumption with only a minimal decrease in profitability. However, companies looking to balance sustainability with financial performance could adjust the discount rate or implement dynamic pricing to mitigate the impact on profitability while still promoting environmentally friendly behavior.

Future research could address the limitations of this work by integrating real-time solar data, broader parameter variations, and longitudinal studies of user behavior. Additionally, incorporating emerging technologies like AI-driven dynamic pricing and real-time fleet management could enhance the practical applicability of the findings.

Interestingly during the analysis of the survey results, when plotting the calculated WTP against trip duration, a clear downward trend emerges. This suggests that participants' willingness to pay per minute decreases as trip duration increases, likely due to the overall cost becoming limiting for longer travel times. This trend implies the existence of an absolute limit to what participants are willing to pay, regardless of travel duration. While understanding this metric requires in-depth analysis, given its fundamental role in consumer decision-making, the scope of this thesis does not permit the exploration of its implications. Nevertheless, this observation is highlighted as a potential area for future researchers to investigate further.



Figures 85 and 86: Scatter charts of WTP and duration

In conclusion this thesis highlights the transformative potential of solar-powered charging stations for urban mobility. By combining environmental consciousness with an economic mindset, the study offers a roadmap for scaling sustainable micro-mobility solutions in cities worldwide. As urban areas continue to grow and the demand for efficient transport intensifies, these findings provide a crucial steppingstone for decision-makers, paving the way toward greener, more inclusive urban futures.

# BIBLIOGRAPHY

- Ai, Y., Li, Z., Gan, M., Zhang, Y., Yu, D., Chen, W., & Ju, Y. (2019). *A deep learning approach on short-term spatiotemporal distribution forecasting of dockless bike-sharing system*. <https://link.springer.com/article/10.1007/s00521-018-3470-9>
- Amazon.com. (n.d.). *42V 2A Scooter Charger with 6 in 1 Plugs for 36V Pocket Mod, Sports Mod, Razor, Gotrax, Jetson, Voyage, Ninebot, Lithium Battery Device, Electric Scooter Charger*. <https://www.amazon.com/42V-2A-36V-Lithium-Device/dp/B0D9FMY5HK>
- Amazon.com. (n.d.). *4000W Pure Sine Wave Inverter 12V DC to 120V AC Converter for Truck, Home, RV, Peak 8000W Off-Grid Solar Power Inverter with 4 AC Outlets, Dual 3.4A USB Ports, Remote Controller with Screen*. <https://www.amazon.com/EGSCATEE-Inverter-Converter-Indicator-Inverters/dp/B0BJF4GLKC>
- Amazon.com. (n.d.). *SOLPERK Solar Panel 2PCS Solar Panels 100 watt 12 volt, 200W Solar panel High Efficiency Monocrystalline PV Module Power Charger Solar Panel for boat car RV Motorcycle Marine*. <https://www.amazon.com/-/us/fotovoltaico-monocristalino-eficiencia-cargadoralimentaci%C3%B3n/dp/B0D53KHDRM>
- Andrew F. Seila. (1992). *Spreadsheet simulation*. *Proceedings / Winter Simulation Conference*.
- Bai, S., & Jiao, J. (2020). Exploring the usage characteristics of e-scooters in U.S. cities. *Sustainable Cities and Society*, 60, 102143. <https://doi.org/10.1016/j.scs.2020.102143>
- Banks, J. (1998). *Handbook of simulation: Principles, methodology, advances, applications, and practice*. John Wiley & Sons.
- Banks, J., Carson, J. S., Nelson, B. L., & Nicol, D. M. (1984). *Discrete-event system simulation*.
- Barabonkov, D., D'Alonzo, S., Pierre, J., Kondor, D., Zhang, X., Tien, M.A., 2020. *Simulating and Evaluating Rebalancing Strategies for Dockless Bike-Sharing Systems*. <https://arxiv.org/abs/2004.11565>
- Barslund, R. (2024, August 23). *What electric scooter models do Bird & Lime use?* ERideHero. <https://eridehero.com/what-scooters-do-bird-lime-use/>
- Boin, R., Möller, T., Pokotilo, V., Ricotti, A., & Sandri, N. (2023, March 27). *Infrastructure technologies: Challenges and solutions for smart mobility in urban areas*. McKinsey & Company. <https://www.mckinsey.com/industries/travel-logistics-and-infrastructure/our-insights/infrastructure-technologies-challenges-and-solutions-for-smart-mobility-in-urban-areas>
- Box, G. E. P., Hunter, W. G., & Hunter, J. S. (2005). *Statistics for experimenters (2nd ed.)*. John Wiley & Sons.
- Breidert, C., Hahsler, M., & Reutterer, T. (2006). *A review of methods for measuring willingness-to-pay*. *Innovative Marketing*, 2(4). [http://www.reutterer.com/papers/breidert&hahsler&reutterer\\_2006.pdf](http://www.reutterer.com/papers/breidert&hahsler&reutterer_2006.pdf)
- Calvo-Jurado, C., Ceballos-Martínez, J. M., García-Merino, J. C., Muñoz-Solano, M., & Sánchez-Herrera, F. J. (2024). *Optimal location of electric vehicle charging stations using proximity diagrams*. *Sustainable Cities and Society*, 113, 105719. <https://doi.org/10.1016/j.scs.2024.105719>
- Caspi, O., Smart, M., & Noland, R. B. (2020). *Spatial associations of dockless shared e-scooter usage*. *Transportation Research Part D: Transport and Environment*. <https://doi.org/10.1016/j.trd.2020.102396>
- Center for Law, Energy & the Environment. (2024). *City public and curbside EV charging strategies: Policy brief*. University of California, Berkeley. <https://clee.berkeley.edu>
- Che, Y., Chen, J., & Hong, J. (2020). *Safety implications of e-scooters: Evidence from observed data in California*. *Transportation Research Record*. <https://www.tandfonline.com/doi/full/10.1080/15568318.2020.1718252>
- Chen, Z., van Lierop, D., & Ettema, D. (2020). *Dockless bike-sharing systems: What are the implications?* <https://www.tandfonline.com/doi/full/10.1080/01441647.2019.1710306>
- Choi, B. K., & Kang, D. (2013). *Modeling and simulation of discrete event systems*. John Wiley & Sons.

- Curl, A., & Fitt, H. (2020). *Same same, but different? Cycling and e-scooter in a rapidly changing urban transport landscape*. *New Zealand Geographer*.  
<https://onlinelibrary.wiley.com/doi/10.1111/nzg.12271>
- De Zan, A. (2022). *Procedimientos abreviados con Minitab para análisis de más o dos muestras*. Blackboard. <https://learn-us-east-1-prod-fleet01xrhs.content.blackboardcdn.com>
- De Zan, A. (2022). *Procedimientos agregados con Minitab para modelos de regresión lineal simple*. Blackboard. <https://learn-us-east-1-prod-fleet01xrhs.content.blackboardcdn.com>
- Dhillon, N. K., Rojas-Rueda, D., & de Nazelle, A. (2020). *Road safety and urban air quality implications of shared mobility using e-scooters*. *Environmental Research Letters*. <https://doi.org/10.1088/1748-9326/ab9f8b>
- Doll, C., Mejia-Dorantes, L., Shaykutdinov, T., & Freckmann, P. (2014). *Success factors for public transport: The role of green communities*. *Transportation Research Board 93rd Annual Meeting*.  
<https://trid.trb.org/view.aspx?id=1289168>
- Dorigo, M., & Stützle, T. (2003). *The ant colony optimization metaheuristic: Algorithms, applications, and advances*. *International series in operations research & management science*. [https://doi.org/10.1007/0-306-48056-5\\_9](https://doi.org/10.1007/0-306-48056-5_9)
- Emissions – Global Energy & CO2 Status Report 2019 – Analysis - IEA. (2019). *International Energy Agency*. <https://www.iea.org/reports/global-energy-co2-status-report-2019/emissions>
- European Commission. (n.d.). *Photovoltaic Geographical Information System (PVGIS)*. *EU Science Hub*.  
[https://joint-research-centre.ec.europa.eu/photovoltaic-geographical-information-system-pvgis/pvgis-tools/daily-radiation\\_en](https://joint-research-centre.ec.europa.eu/photovoltaic-geographical-information-system-pvgis/pvgis-tools/daily-radiation_en)
- Fang, K., Agrawal, A. W., Steele, J., Hunter, J. J., & Hooper, A. M. (2018). *Where do riders park dockless, shared electric scooters?* *Mineta Transportation Institute*.
- Fig. 1. Heat map of the traffic accidents. (2015). *ResearchGate*. [https://www.researchgate.net/figure/Heat-map-of-the-traffic-accidents\\_fig1\\_271771639](https://www.researchgate.net/figure/Heat-map-of-the-traffic-accidents_fig1_271771639)
- Formolli, M., Croce, S., Vettorato, D., Paparella, R., Scognamiglio, A., Mainini, A. G., & Lobaccaro, G. (2022).
- Franco, J. F., Rider, M. J., & Romero, R. (2015). *A Mixed-Integer linear programming model for the electric vehicle charging coordination problem in unbalanced electrical distribution systems*. *IEEE Transactions on Smart Grid*, 6(5), 2200–2210. <https://doi.org/10.1109/tsg.2015.2394489>
- Foss, N. J., & Saebi, T. (2018). *Business models and value creation: How entrepreneurial firms foster value creation*. *Academy of Management Perspectives*, 32(3), 23-39.  
<https://doi.org/10.5465/amp.2016.0175>
- Gössling, S. (2020). *Integrating e-scooters in urban transportation: Problems, policies, and the prospect of system change*.  
[https://journals.hww.com/journalacs/abstract/2020/07000/electric\\_scooter\\_injury\\_in\\_southern\\_california.2\\_2.aspx](https://journals.hww.com/journalacs/abstract/2020/07000/electric_scooter_injury_in_southern_california.2_2.aspx)
- Hollingsworth, J., Copeland, B., & Johnson, J. X. (2019). *Are e-scooters polluters? The environmental impacts of shared dockless electric scooters*. *Environmental Research Letters*.  
<https://doi.org/10.1088/1748-9326/ab2da8>
- Hua, M., Chen, J., Chen, X., Gan, Z., Wang, P., Zhao, D., 2020. *Forecasting usage and bike distribution of dockless bike-sharing using journey data*. *IET Intell*. <https://doi.org/10.1049/iet-its.2020.0305>.
- Iglewicz, B. & Hoaglin, D.C. (1993). *How to detect and handle outliers*. *Milwaukee: ASQ*. Loftus, G.R. & Loftus, E.F. (1988). *Essence of Statistics (2nd Edition)*. *New York: McGraw Hill*.
- IRENA. (2016). *Renewable energy in cities*. *International Renewable Energy Agency, Abu Dhabi*.  
[www.irena.org](http://www.irena.org)
- IRENA. (2020). *Rise of renewables in cities: Energy solutions for the urban future*. *International Renewable Energy Agency, Abu Dhabi*. [www.irena.org](http://www.irena.org)

- Jiao, J., & Bai, S. (2020). Understanding e-scooter ridership patterns and urban features. *Journal of Transport Geography*. <https://doi.org/10.1016/j.jtrangeo.2020.102802>
- Kleijnen, J. P. (2015). *Design and analysis of simulation experiments*. Springer.
- Klingstam, P., & Gullander, P. (1999). Overview of simulation tools for computer-aided production engineering. *Computers in Industry*, 38(2), 173–186. [https://doi.org/10.1016/s0166-3615\(98\)00117-1](https://doi.org/10.1016/s0166-3615(98)00117-1)
- Law, A. (2006). *Simulation Modeling and Analysis with Expertfit Software*. McGraw-Hill Science/Engineering/Math.
- Lazarus, J., Pourquier, J.C., Feng, F., Hammel, H., Shaheen, S., 2020. Micromobility evolution and expansion: understanding how docked and dockless bikesharing models complement and compete—a case study of San Francisco. *J. Transport*. <https://doi.org/10.1016/j.jtrangeo.2019.102620>.
- Luo, X., Qin, Z., & Zhang, Y. (2019). Life cycle assessment of docked and dockless shared mobility systems: Impacts of rebalancing on greenhouse gas emissions. *Sustainability*. <https://doi.org/10.3390/su11061679>
- Macal, C. M., & North, M. J. (2007). Agent-based modeling and simulation: Desktop ABMS. *Winter Simulation Conference*, 95–106. <https://doi.org/10.5555/1351542.1351564>
- Ma, X., Ji, Y., Yuan, Y., Van Oort, N., Jin, Y., & Hoogendoorn, S. (2020). A comparison in travel patterns and determinants of user demand between docked and dockless bikesharing systems using multi-sourced data. <https://doi.org/10.1016/j.tra.2020.06.022>
- McKenzie, G., 2019. Spatiotemporal comparative analysis of scooter-share and bike-share usage patterns in Washington, D.C. *J.* <https://www.sciencedirect.com/science/article/abs/pii/S0966692319302741?via%3Dihub>
- OECD. (2011). *OECD environmental outlook to 2050*. <https://doi.org/10.1787/9789264122246-en>
- Overview of policy relating to e-scooters in European countries. (2020). *EU Urban Mobility Observatory*. [https://urban-mobility-observatory.transport.ec.europa.eu/resources/case-studies/overview-policy-relating-e-scooters-european-countries\\_en](https://urban-mobility-observatory.transport.ec.europa.eu/resources/case-studies/overview-policy-relating-e-scooters-european-countries_en)
- Pan, L., Cai, Q., Fang, Z., Tang, P., & Huang, L. (2019). A deep reinforcement learning framework for rebalancing dockless bike sharing systems. <https://ojs.aaai.org/index.php/AAAI/article/view/3940>
- Pinheiro, Y. (2023, May 26). Zeus introduces solar e-scooter charging stations in Germany. *Zag Daily*. <https://zagdaily.com/tech/zeus-introduces-solar-e-scooter-charging-station-in-germany/>
- QERY, Consumer electricity prices for households in Europe. (2024, October). *QERY*. Retrieved November 5, 2024, from <https://qery.no/consumer-energy-prices-in-europe/#:~:text=The%20average%20electricity%20price%20for,to%20the%20latest%20Eurostat%20data>
- Rose, J., Schellong, D., Schaetzberger, C., & Hill, J. (2020). How e-scooters can win a place in urban transport. *BCG*. <https://www.bcg.com/publications/2020/e-scooters-can-win-place-in-urban-transport>
- Salian, N. (2022, April 18). DEWA EV Green Chargers provide 8,800+ MWh of electricity to date. *Gulf Business*. <https://gulfbusiness.com/dewa-ev-green-chargers-provide-8800-mwh-of-electricity-to-date/>
- Sargent, R. G. (2012). Verification and validation of simulation models. *Journal of Simulation*, 7(1), 12–24. <https://doi.org/10.1057/jos.2012.20>
- Severengiz, S., Uysal, M., Keles, Ö., & Bilgen, S. (2020). Life cycle sustainability assessment of shared e-scooters. *Sustainable Production and Consumption*. <https://doi.org/10.1016/j.spc.2020.05.001>
- Sikka, N., Vila, C., Stratton, M., Ghassemi, M., & Pourmand, A. (2019). Sharing the sidewalk: A case of e-scooter related pedestrian injury. *The American Journal of Emergency Medicine* <https://doi.org/10.1016/j.ajem.2019.06.017>
- SolarPower Europe. (2023). *EU market outlook for solar power 2023-2027*. <https://www.solarpowereurope.org/insights/outlooks/eu-market-outlook-for-solar-power-2023-2027/detail>

- *Solar energy in urban planning: Lesson learned and recommendations from six Italian case studies.* *Applied Sciences*, 12(6), 2950. <https://doi.org/10.3390/app12062950>
- Trivedi, T. K., Liu, C., Antonio, A. L. M., Wheaton, N., Kreger, V., Yap, A., & Schriger, D. (2019). *Injuries associated with standing electric scooter use.* <https://doi.org/10.1001/jamanetworkopen.2018.7381>
- Vazifeh, M. M., Zhang, H., Santi, P., & Ratti, C. (2019). *Optimizing the deployment of electric vehicle charging stations using pervasive mobility data.* *Transportation Research Part a Policy and Practice*, 121, 75–91. <https://doi.org/10.1016/j.tra.2019.01.002>
- *What is the Google Map walking speed? Is this a constant value or does it change depending on slope? - Google Maps Community.* (2021). <https://support.google.com/maps/thread/92124954/what-is-the-google-map-walking-speed-is-this-a-constant-value-or-does-it-change-depending-on-slope?hl=en>
- Wang, Y., Wu, J., Chen, K., & Liu, P. (2021). *Are shared electric scooters energy efficient?* *Communications in Transportation Research*, 1, 100022. <https://doi.org/10.1016/j.commtr.2021.100022>
- Xu, C., Ji, J., & Liu, P. (2018). *The station-free sharing bike demand forecasting with a deep learning approach and large-scale datasets.* <https://doi.org/10.1016/j.trc.2018.07.013>
- Yang, H., Ma, Q., Wang, Z., Cai, Q., Xie, K., & Yang, D. (2020). *Safety of micro-mobility: Analysis of e-scooter crashes by mining news reports.* *Accident Analysis & Prevention.* <https://doi.org/10.1016/j.aap.2020.105608>
- Yan, Q., Lin, H., Li, J., Ai, X., Shi, M., Zhang, M., & Gejirifu, D. (2022). *Many-objective charging optimization for electric vehicles considering demand response and multi-uncertainties based on Markov chain and information gap decision theory.* *Sustainable Cities and Society*, 78, 103652. <https://doi.org/10.1016/j.scs.2021.103652>
- Yin, C., & McKay, A. (2018). *Introduction to modeling and simulation techniques.* College of Engineering, China Agricultural University, Beijing, China. <https://eprints.whiterose.ac.uk/135646/>
- Younes, H., Zou, Z., Wu, J., & Baiocchi, G. (2020). *Comparing the temporal determinants of dockless scooter-share and station-based bike-share in Washington, D.C.* <https://doi.org/10.1016/j.tra.2020.02.021>
- Zhu, R., Zhang, X., Kondor, D., Santi, P., & Ratti, C. (2020). *Understanding spatio-temporal heterogeneity of bike-sharing and scooter-sharing mobility.* *Comput. Environ. Urban Syst.* <https://doi.org/10.1016/j.compenvurbsys.2020.101483>

# APPENDIX

## A.0 Computer Specifications

Device name DESKTOP-C0FK8FD  
Processor Intel(R) Core(TM) i7-8565U CPU @ 1.80GHz 1.99 GHz  
Installed RAM 16.0 GB (15.8 GB usable)  
System type 64-bit operating system, x64-based processor

## A.1 Survey

# Urban Mobility and Sustainability: Exploring Commuter Preferences and Innovative Solutions

Dear Participant,

Thank you for taking part in this survey! The purpose of this questionnaire is to gather information about commuting and travel habits in cities. The data you provide will help us create a realistic simulation model of city life, where agents will represent people like yourself, commuting to work, school, or running daily activities. Your input is vital in shaping the behavior of these agents in a virtual environment, allowing us to analyze and optimize transportation systems and urban planning.

This survey will take a maximum of 10 minutes to answer, please answer the following questions based on your personal commuting experiences. Your responses will remain anonymous and will be used solely for research purposes.

---

\* Indicates required question

1. Do you regularly commute to any of the following places? (Select primary \* commuting route) *Mark only one oval.*

- Work
- School/University
- Daily activities (e.g. grocery shopping, gym, etc..)
- I don't have regular commutes

## Commuting

2. How many days per week do you usually commute or engage in activities? \*

*Mark only one oval.*

- 1 day
- 2-3 days
- 4-5 days
- 6-7 days

3. At what time do you most frequently begin your commute or activity? \*

\_\_\_\_\_

*Example: 8:30 AM*

4. At what time do you most frequently return from your commute or activity? \*

\_\_\_\_\_

*Example: 8:30 AM*

5. How long does your commute or activity usually take? (one way) \*

*Mark only one oval.*

- <15 minutes
- 15-30 minutes
- 30-45 minutes
- 45-60 minutes
- + 60 minutes

6. Do your commute or activity times vary between weekdays and weekends? \*

Mark only one oval.

- Yes, I commute at different times
- No, my commute times are the same
- I don't commute on weekends

7. How much do you currently spend on your commute per day (**one way**)? \*

Mark only one oval.

- < €2
- €2 -€5
- €5 - €10 €10
- €15 more
- than €15

#### Commuting

8. Do you have any other regular commuting routes? (Select secondary commuting \* route)

Mark only one oval.

- Work
- School/University
- Daily activities (e.g. grocery shopping, gym, etc..)
- I  don't have any other commuting routes *Skip to question 15*

#### Commuting

9. How many days per week do you usually commute or engage in secondary \* activities?

Mark only one oval.

- 1 day
- 2-3 days
- 4-5 days
- 6-7 days

10. At what time do you most frequently begin your secondary commute or activity? \*

---

*Example: 8:30 AM*

11. At what time do you most frequently return from your secondary commute or activity? \*

---

*Example: 8:30 AM*

12. How long does your secondary commute or activity usually take? (one way) \*

*Mark only one oval.*

- <15 minutes
- 15-30 minutes
- 30-45 minutes
- 45-60 minutes
- + 60 minutes

13. Do your second commute or activity times vary between weekdays and \* weekends?

*Mark only one oval.*

- Yes, I commute at different times
- No, my commute times are the same
- I don't commute on weekends

14. How much do you currently spend on your secondary commute per day (**one** \_\_\_\_\_\*  
**way**)?

*Mark only one oval.*

- < €2
- €2 -€5
- €5 - €10 €10
- €15 more
- than €15

### Electric Scooters

In this section, we will focus on electric scooters, which are becoming a popular mode of transport in many cities. We aim to understand your experience with scooters, if any, and your preferences for using them as part of your commute. Your answers will help us better simulate how scooters can serve as a viable transportation option in a city.

15. Have you ever used an electric scooter for commuting or other purposes? \*

*Mark only one oval.*

- Yes
- No

16. Do you use an electric scooter as regular part of your commute or travel routine? \*

*Mark only one oval.*

- Yes, it's my primary mode of transport
- Yes, but only sometimes
- No, but I would consider it as my main mode of commuting
- No, but I would use it as an occasional mode of transport
- No, and I don't plan to use it

Choosing a scooter

17. When choosing an electric scooter, what is the **maximum amount of time** you <sup>\*</sup> would be willing to walk to pick one up before considering other transportation options?

*Mark only one oval.*

- < 2 minutes
- 2-5 minutes
- 5-10 minutes
- + 10 minutes

18. If you arrive at the location of the scooter you were planning to pick up, but <sup>\*</sup> someone else has taken it, what would you do?

*Mark only one oval.*

- I  would search for another scooter nearby *Skip to question 19*
- I would switch to another mode of transportation (e.g., bus, walking, ride-sharing)
- It  depends on how far the next available scooter is *Skip to question 19*

Choosing a scooter

19. How far would you be willing to walk to find another available scooter? <sup>\*</sup>

*Mark only one oval.*

- <2 minutes
- 2-5 minutes
- 5-10 minutes
- +10 minutes

### Solar powered charging docks

We're exploring the idea of implementing solar-powered charging stations for electric scooters. This solution aims to reduce reliance on traditional electricity sources, offering an environmentally friendly option that lowers carbon emissions and promotes sustainability in urban transportation. By charging scooters using clean energy, we could significantly reduce the environmental impact of daily commutes.

20. If solar-powered charging stations for scooters were available, would you be \* willing to deviate from your final destination to drop off the scooter at a charging station?

*Mark only one oval.*

- Yes
- No
- It depends

21. How much of a discount on your ride would make you consider deviating to leave \* the scooter at a solar charging station? *Mark only one oval.*

0   1   2   3   4   5   6   7   8   9   10

---

0%            100% discount

# Google Forms

## A.2 Survey Results

Primary					
Ci = Clase i	fai	pi = P(XCi)	fei = N*pi	(fa-fe) <sup>2</sup>	(fa-fe) <sup>2</sup> /fe
0	3	0.07799	7.56503	20.8394989	2.754714641
4	19	0.25382	24.62054	31.59046989	1.283094111
8	46	0.31101	30.16797	250.6531739	8.308586024
12	10	0.22213	21.54661	133.3242025	6.187711315
16	16	0.1001	9.7097	39.56787409	4.07508719
20	3	0.02893	2.80621	0.037554564	0.013382663

Secondary					
Ci = Clase i	fai	pi = P(XCi)	fei = N*pi	(fa-fe) <sup>2</sup>	(fa-fe) <sup>2</sup> /fe
0	0	0.00103	0.09991	0.009982008	0.09991
4	0	0.02194	2.12818	4.529150112	2.12818
8	4	0.11089	10.75633	45.64799507	4.2438262
12	17	0.27363	26.54211	91.05186325	3.43046816
16	60	0.35233	34.17601	666.8784595	19.51305783
20	16	0.20086	19.48342	12.1342149	0.622796968

Table A.1: Chi - Square test calculation for Weibull fit distribution

WTP					
Ci = Clase i	fai	pi = P(XCi)	fei = N*pi	(fa-fe) <sup>2</sup>	(fa-fe) <sup>2</sup> /fe
0-0.05	12	0.13766	13.35302	1.83066312	0.13709731
0.05-0.15	39	0.31866	30.91002	65.4477764	2.117364415
0.15-0.25	19	0.22399	21.72703	7.436692621	0.34227838
0.25-0.35	13	0.13765	13.35205	0.123939203	0.00928241
0.35-0.45	3	0.08033	7.79201	22.96335984	2.947039318
0.45-0.55	3	0.04559	4.42223	2.022738173	0.4574023
0.55-0.65	4	0.02544	2.46768	2.348004582	0.951502862
0.65-0.75	1	0.01402	1.35994	0.129556804	0.095266559
0.75-0.85	0	0.00766	0.74302	0.55207872	0.74302
0.85-0.95	0	0.00416	0.40352	0.16282839	0.40352
0.95-1.05	2	0.00225	0.21825	3.174633063	8.821926
1.05-1.15	0	0.0012	0.1164	0.01354896	0.1164
1.15-1.25	0	0.00065	0.06305	0.003975303	0.06305
1.25-1.35	1	0.00035	0.03395	0.933252603	0.33485

Table A.2: Chi - Square test calculation for Gamma fit distribution

### A.3 Operational Model - UI

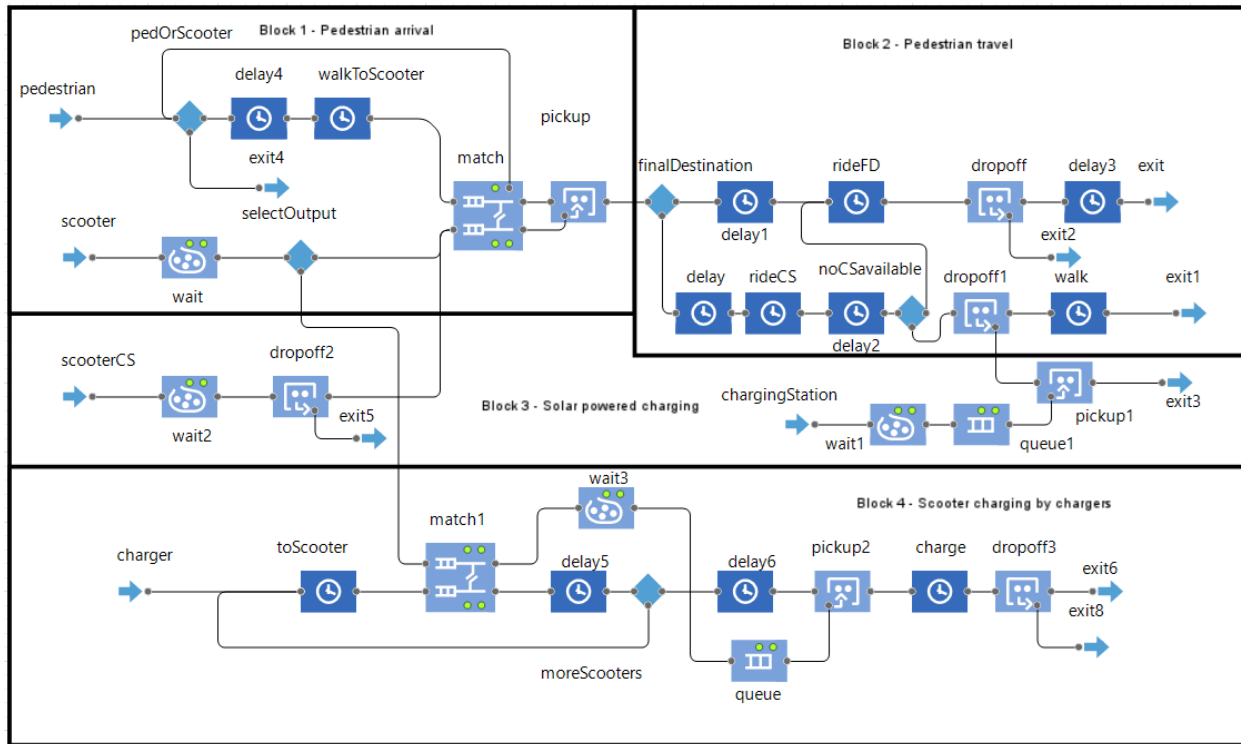


Figure A.1: Main Agent

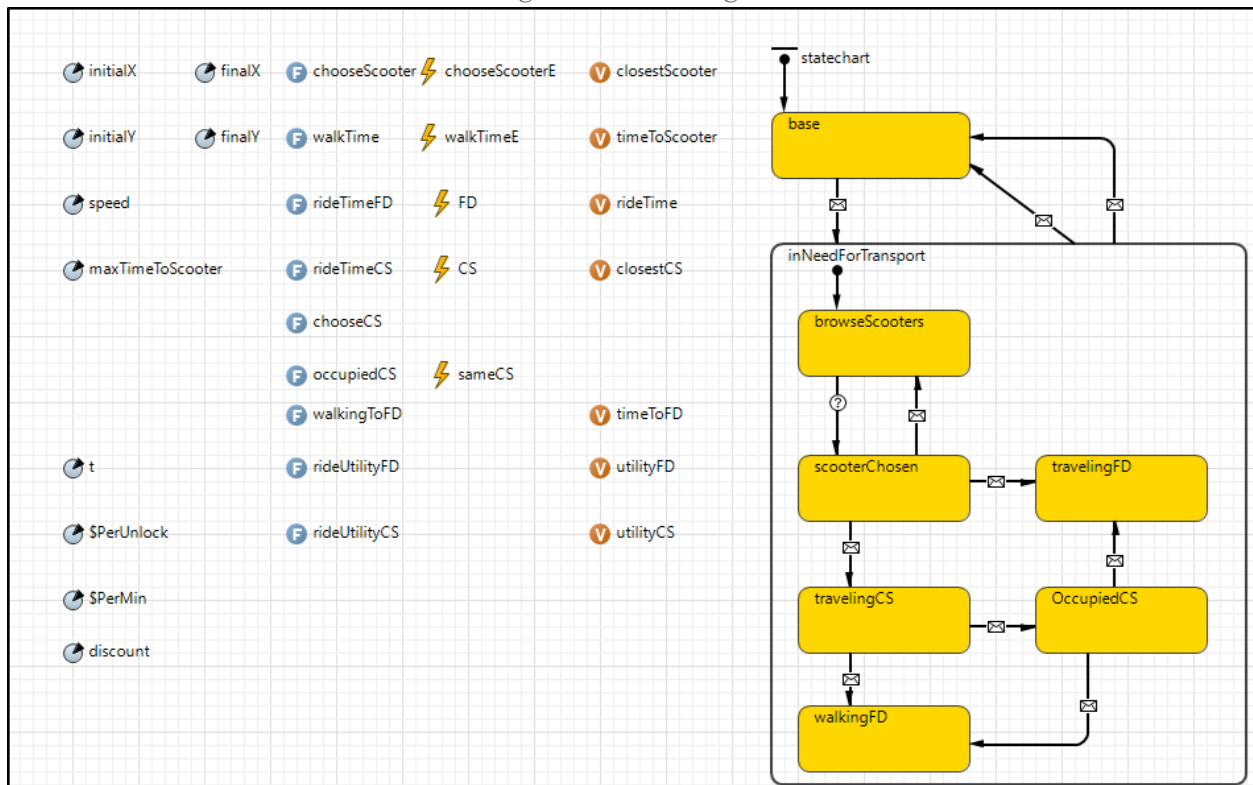


Figure A.2: Pedestrian Agent

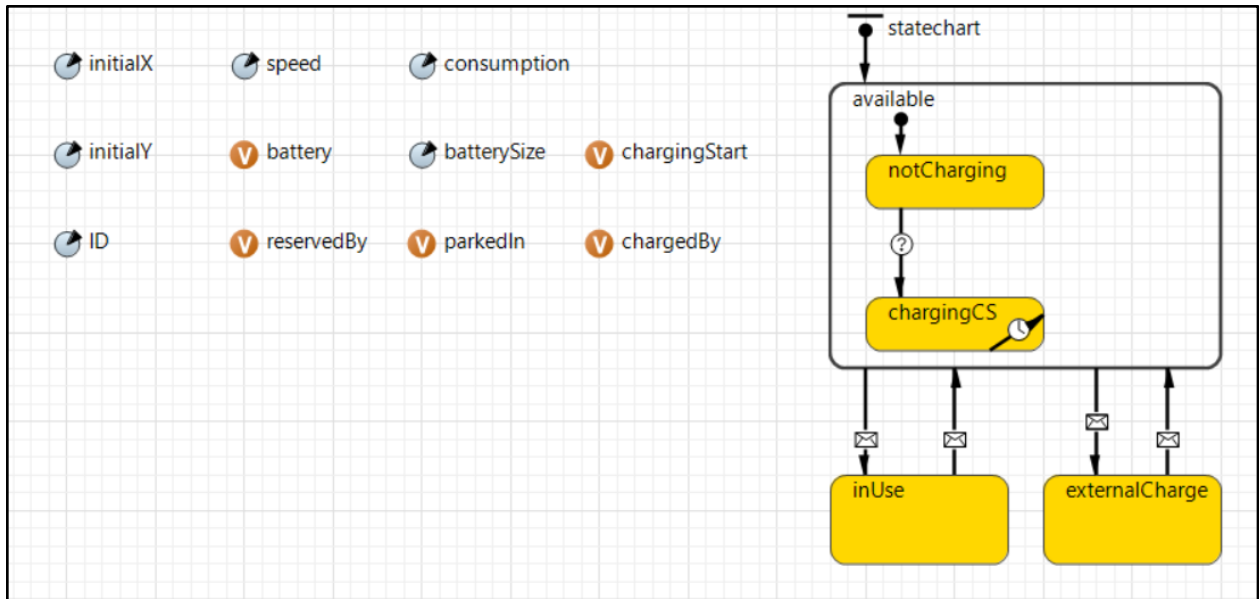


Figure A. 3: Scooter Agent

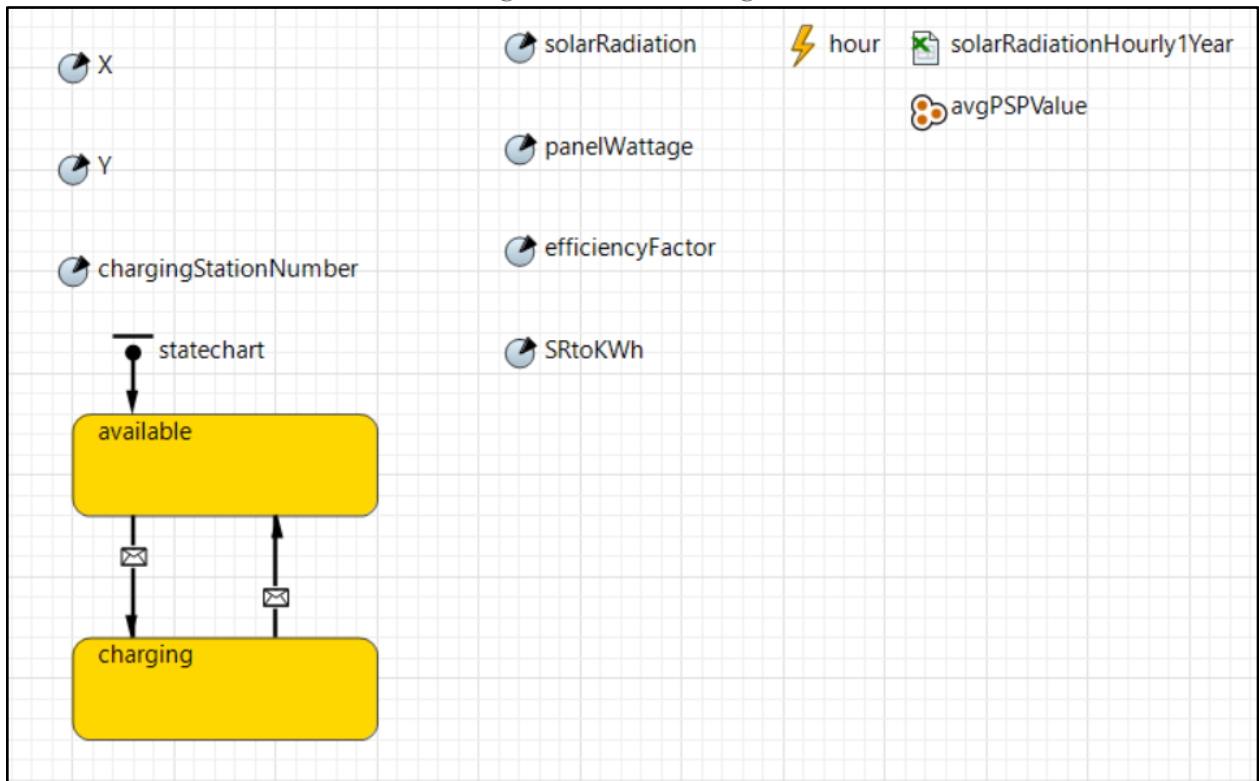


Figure A4: Charging Station Agent

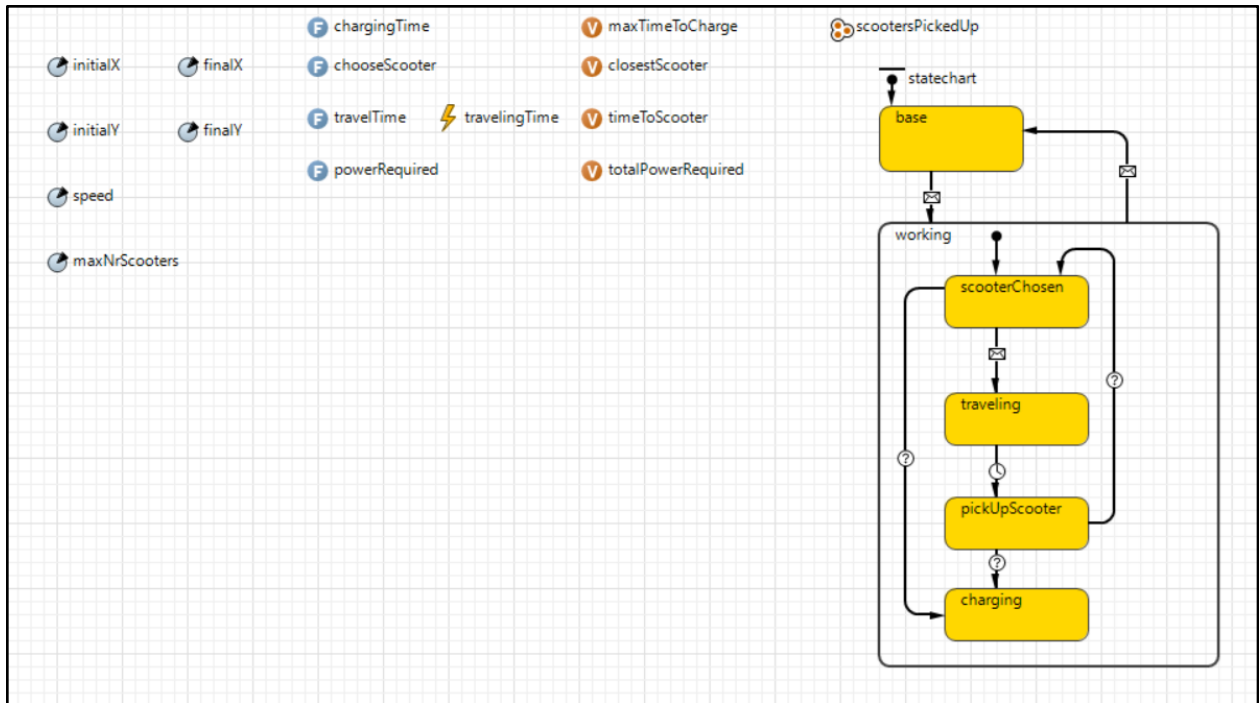


Figure A.5 :Charger Agent

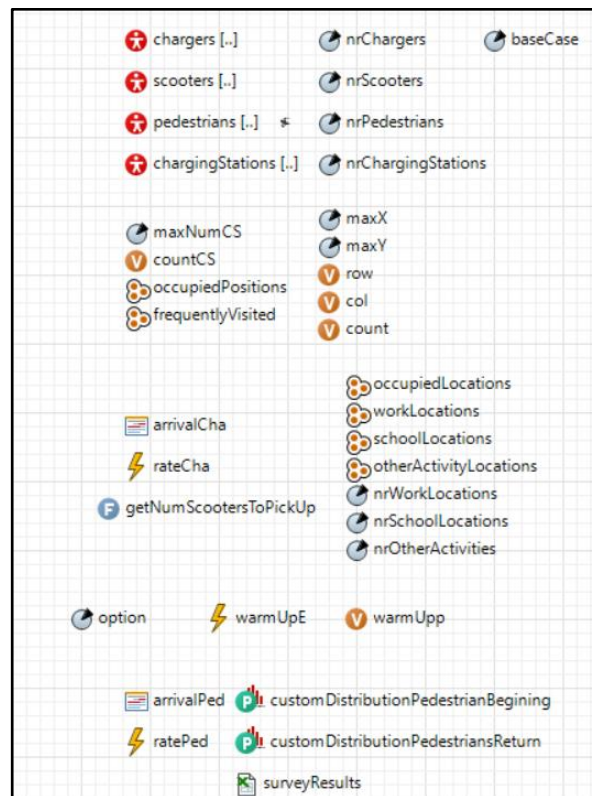


Figure A.6: All Auxiliary Parameters

## A.4 Operational Model - Main Codes and Logics

---

### A.4.1 Code for generating frequented locations

```
// Generate random locations for work
for (int i = 0; i < nrWorkLocations; i++) {
    double workX, workY;
    // Ensure unique coordinates
    do {
        if (randomTrue(0.5)) {
            workX = uniform(0, maxX);
            workY = 100 * ((int) (Math.random() * (maxY / 100))); // y is a
multiple of 100
        } else {
            workY = uniform(0, maxY);
            workX = 100 * ((int) (Math.random() * (maxX / 100))); // x is a
multiple of 100
        }
    } while (occupiedLocations.contains(workX + "," + workY));
    // Add to the list and mark position as occupied
    workLocations.add(workX + "," + workY);
    occupiedLocations.add(workX + "," + workY);
}
// Generate random locations for school
for (int i = 0; i < nrSchoolLocations; i++) {
    double schoolX, schoolY;
    do {
        if (randomTrue(0.5)) {
            schoolX = uniform(0, maxX);
            schoolY = 100 * ((int) (Math.random() * (maxY / 100)));
        } else {
            schoolY = uniform(0, maxY);
            schoolX = 100 * ((int) (Math.random() * (maxX / 100)));
        }
    } while (occupiedLocations.contains(schoolX + "," + schoolY));
    schoolLocations.add(schoolX + "," + schoolY);
    occupiedLocations.add(schoolX + "," + schoolY);
}
// Generate random locations for other activities
for (int i = 0; i < nrOtherActivities; i++) {
    double otherX, otherY;
    do {
        if (randomTrue(0.5)) {
            otherX = uniform(0, maxX);
            otherY = 100 * ((int) (Math.random() * (maxY / 100)));
        } else {
            otherY = uniform(0, maxY);
            otherX = 100 * ((int) (Math.random() * (maxX / 100)));
        }
    } while (occupiedLocations.contains(otherX + "," + otherY));
    otherActivityLocations.add(otherX + "," + otherY);
    occupiedLocations.add(otherX + "," + otherY);
}
```

---

---

## A.4.2 Code for assigning destination to pedestrians when leaving the “base” state

```
// Generate initial coordinates
int initialDestinationType = (int) Math.round(triangular(1, 2, 4)); //
Triangular distribution returning 1, 2, 3, or 4
switch (initialDestinationType) {
    case 1: // Other activities
        int i = (int) Math.round(uniform(0, main.nrOtherActivities-1)); //
Random index for other activities
        String initialOtherActivity = main.otherActivityLocations.get(i); //
Retrieve coordinate as string
        initialX = Double.parseDouble(initialOtherActivity.substring(0,
initialOtherActivity.indexOf(',')));
        initialY =
Double.parseDouble(initialOtherActivity.substring(initialOtherActivity.indexO
f(',') + 1));
        break;
    case 2: // Work
        int i2 = (int) Math.round(uniform(0, main.nrWorkLocations-1)); //
Random index for work locations
        String initialWork = main.workLocations.get(i2); // Retrieve
coordinate as string
        initialX = Double.parseDouble(initialWork.substring(0,
initialWork.indexOf(',')));
        initialY =
Double.parseDouble(initialWork.substring(initialWork.indexOf(',') + 1));
        break;
    case 3: // School
        int i3 = (int) Math.round(uniform(0, main.nrSchoolLocations-1)); //
Random index for school locations
        String initialSchool = main.schoolLocations.get(i3); // Retrieve
coordinate as string
        initialX = Double.parseDouble(initialSchool.substring(0,
initialSchool.indexOf(',')));
        initialY =
Double.parseDouble(initialSchool.substring(initialSchool.indexOf(',') + 1));
        break;
    case 4: // Completely random
        if (randomTrue(0.5)) {
            initialX = uniform(0, main.maxX);
            initialY = round(uniform(0, main.maxY) * 100) / 100;
        } else {
            initialY = uniform(0, main.maxY);
            initialX = round(uniform(0, main.maxX) * 100) / 100;
        }
        break;
}
// Generate final coordinates
int finalDestinationType = (int) Math.round(triangular(1, 2, 4)); //
Triangular distribution returning 1, 2, 3, or 4
switch (finalDestinationType) {
    case 1: // Other activities
        int i1 = (int) Math.round(uniform(0, main.nrOtherActivities-1)); //
Random index for other activities
```

```

        String finalOtherActivity = main.otherActivityLocations.get(i1); //
Retrieve coordinate as string
        finalX = Double.parseDouble(finalOtherActivity.substring(0,
finalOtherActivity.indexOf(',') ));
        finalY =
Double.parseDouble(finalOtherActivity.substring(finalOtherActivity.indexOf(',')
+ 1));
        break;
    case 2: // Work
        int i2Final = (int) Math.round(uniform(0, main.nrWorkLocations-1));
// Random index for work locations
        String finalWork = main.workLocations.get(i2Final); // Retrieve
coordinate as string
        finalX = Double.parseDouble(finalWork.substring(0,
finalWork.indexOf(',') ));
        finalY = Double.parseDouble(finalWork.substring(finalWork.indexOf(',')
+ 1));
        break;
    case 3: // School
        int i3Final = (int) Math.round(uniform(0, main.nrSchoolLocations-1));
// Random index for school locations
        String finalSchool = main.schoolLocations.get(i3Final); // Retrieve
coordinate as string
        finalX = Double.parseDouble(finalSchool.substring(0,
finalSchool.indexOf(',') ));
        finalY =
Double.parseDouble(finalSchool.substring(finalSchool.indexOf(',') + 1));
        break;
    case 4: // Completely random
        if (randomTrue(0.5)) {
            finalX = uniform(0, main.maxX);
            finalY = round(uniform(0, main.maxY) * 100) / 100;
        } else {
            finalY = uniform(0, main.maxY);
            finalX = round(uniform(0, main.maxX) * 100) / 100;
        }
        break;
}

```

---

---

### A.4.3 Code for generating randomly placed charging stations and docks

```
if(option == 0){
// To avoid placing two stations at the same spot, use a set to store occupied
positions
for (int i = 0; i < nrChargingStations; i++) {
    double stationX, stationY;
    // Generate random X and Y as multiples of 100, ensure they are not occupied
by another station
    do {
        stationX = 100 * ((int) (Math.random() * 11));
        stationY = 100 * ((int) (Math.random() * 11));
    } while (occupiedPositions.contains(stationX + "," + stationY));
    // Mark this position as occupied
    occupiedPositions.add(stationX + "," + stationY);
    // Assign the same coordinates to all docks in this charging station
    for (chargingStation s : chargingStations) {
        // Check if the charging station belongs to the current group
        if (s.chargingStationNumber >= i * maxNumCS && s.chargingStationNumber
< (i + 1) * maxNumCS) {
            s.X = stationX;
            s.Y = stationY;
        }
    }
}
}
```

---

---

#### A.4.4 Code for generating optimally placed charging stations and docks

```
if (option == 1){
// Step 1: Count occurrences of each location in frequentlyVisited
int freqCount = frequentlyVisited.size(); // Total number of locations
String[] uniqueLocations = new String[freqCount]; // To store unique locations
int[] locationCounts = new int[freqCount];
int uniqueIndex = 0;
for (String location : frequentlyVisited) {
    boolean found = false;
    for (int i = 0; i < uniqueIndex; i++) {
        if (uniqueLocations[i].equals(location)) {
            locationCounts[i]++;
            found = true;
            break;
        }
    }
    if (!found) {
        uniqueLocations[uniqueIndex] = location;
        locationCounts[uniqueIndex] = 1;
        uniqueIndex++;
    }
}
// Step 2: Sort uniqueLocations by their counts in descending order
for (int i = 0; i < uniqueIndex - 1; i++) {
    for (int j = i + 1; j < uniqueIndex; j++) {
        if (locationCounts[i] < locationCounts[j]) {
            int tempCount = locationCounts[i];
            locationCounts[i] = locationCounts[j];
            locationCounts[j] = tempCount;
            String tempLocation = uniqueLocations[i];
            uniqueLocations[i] = uniqueLocations[j];
            uniqueLocations[j] = tempLocation;
        }
    }
}
// Step 3: Assign charging stations to the most frequently visited locations
int stationIndex = 0; // Index for charging stations
for (int i = 0; i < uniqueIndex && stationIndex < nrChargingStations; i++) {
    String location = uniqueLocations[i];
    String[] coordinates = location.replace("(", "").replace(")",
    "").split(",");
    double stationX = Double.parseDouble(coordinates[0]);
    double stationY = Double.parseDouble(coordinates[1]);
    for (chargingStation s : chargingStations) {
        if (s.chargingStationNumber >= stationIndex * maxNumCS &&
            s.chargingStationNumber < (stationIndex + 1) * maxNumCS) {
            s.X = stationX;
            s.Y = stationY;
        }
    }
}
```

```
    }  
}
```

---

#### A.4.5 Code for assigning destination to chargers when leaving the “base” state

```
//Generate initial X and Y  
if(randomTrue(0.5) == true){  
    initialX = uniform(0,main.maxX);  
    initialY = round(uniform(0,main.maxY)*100)/100;  
}  
else{  
    initialY = uniform(0,main.maxY);  
    initialX = round(uniform(0,main.maxX)*100)/100;  
}  
//generate final X and Y  
// Pick a random index from the positionList  
int randomIndex = (int) (Math.random() * main.occupiedPositions.size());  
String position = main.occupiedPositions.get(randomIndex);  
// Split the "X,Y" string into two parts (X and Y)  
String[] coordinates = position.split(",");  
// Convert the split strings into doubles  
double stationX = Double.parseDouble(coordinates[0]);  
double stationY = Double.parseDouble(coordinates[1]);  
// Set finalX and finalY of the charger to the chosen position  
finalX = stationX;  
finalY = stationY;
```

---

### 9.1.1 Zero resource case vs. Solar-powered charging station without incentive case

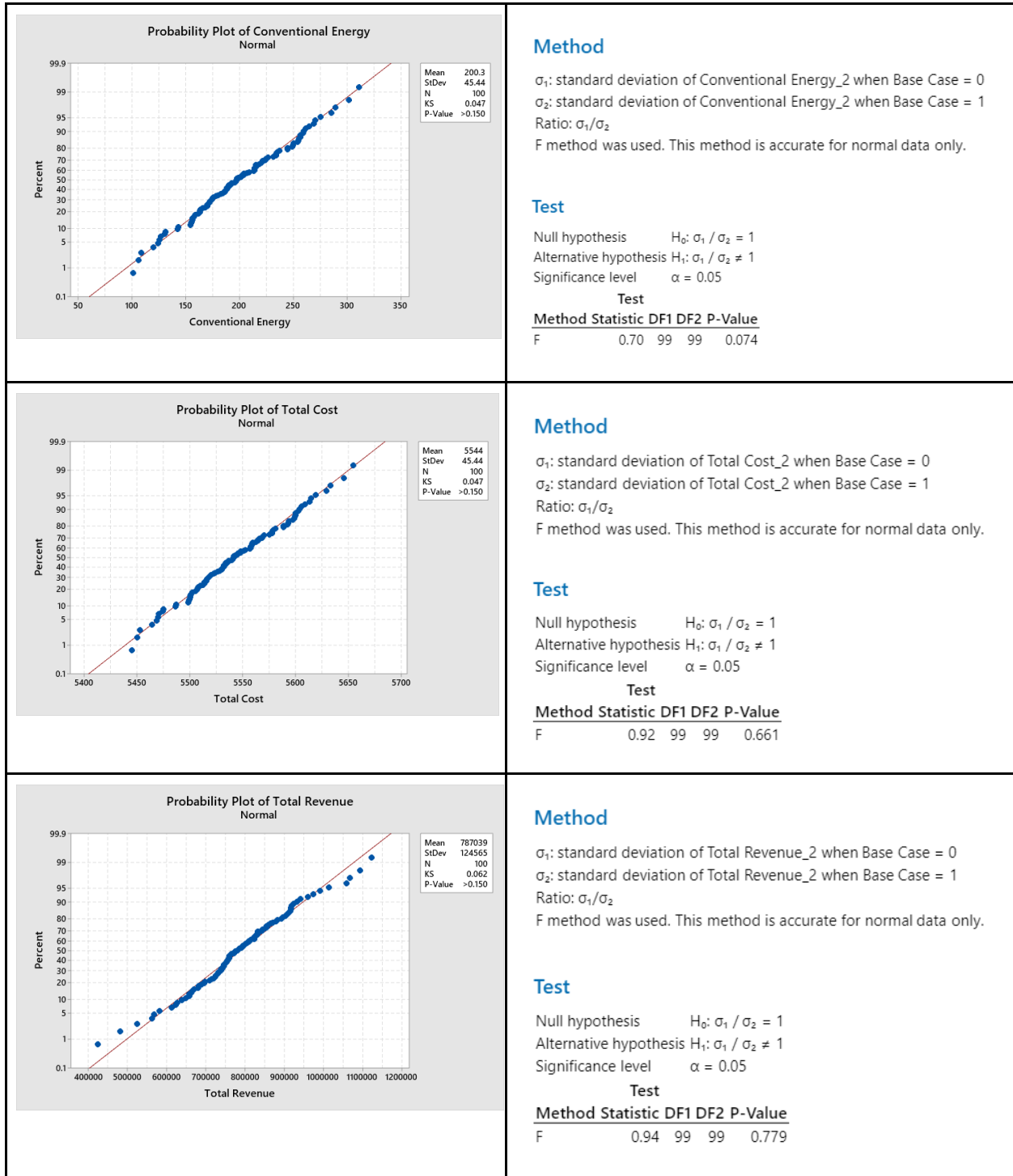


Figure A.7: Kolmogorov-Smirnov normality test and F-test variance test for reference variables

## 9.1.2 Solar-powered charging station allocation: Random vs Metaheuristic

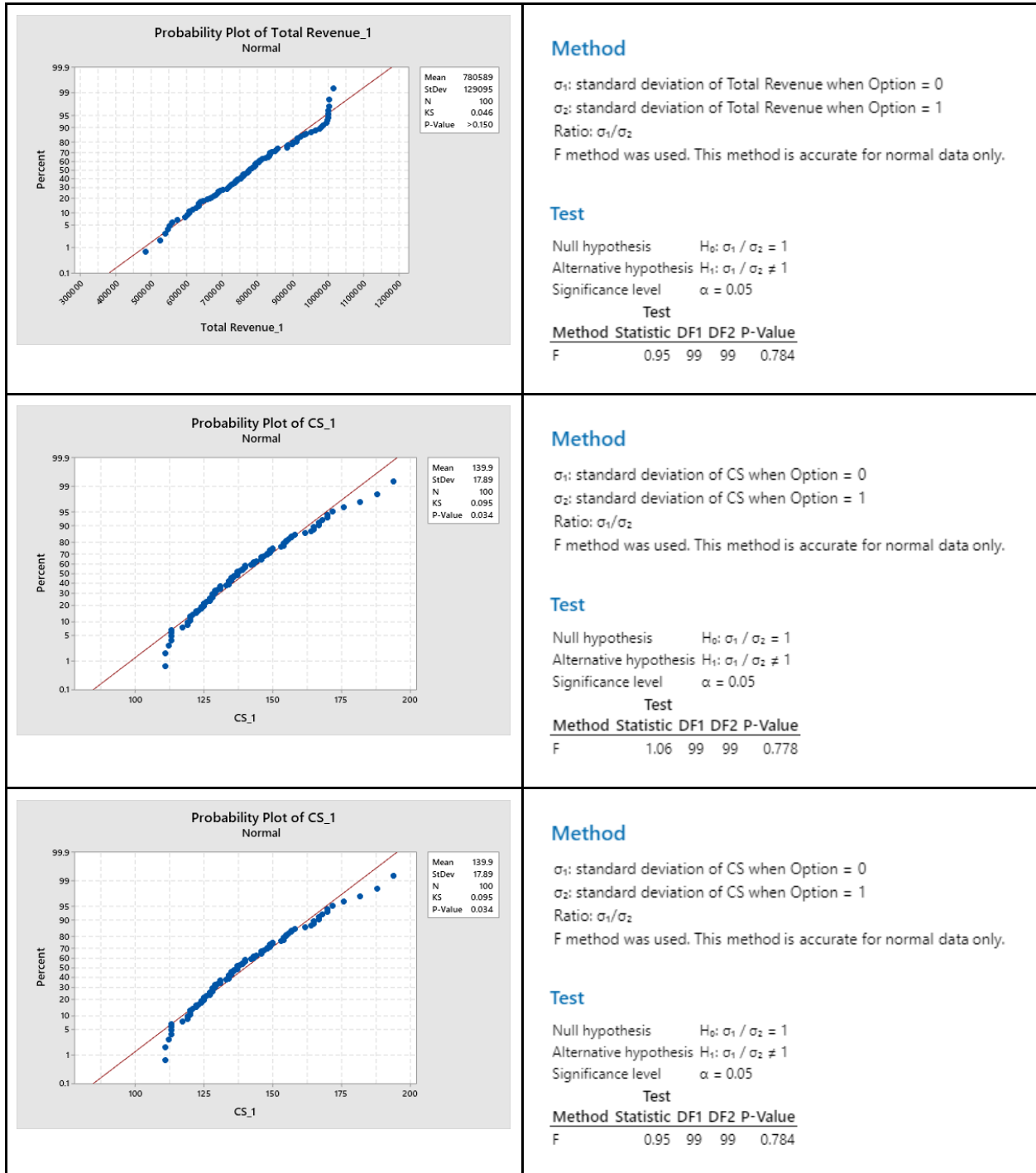


Figure A.8: Kolmogorov-Smirnov normality test and F-test variance test for reference variables

